Geol Survey

In Situ Strength Characteristics
of Coal Mine Floor Strata in Illinois

by
Yoginder P. Chugh
Southern Illinois University at Carbondale
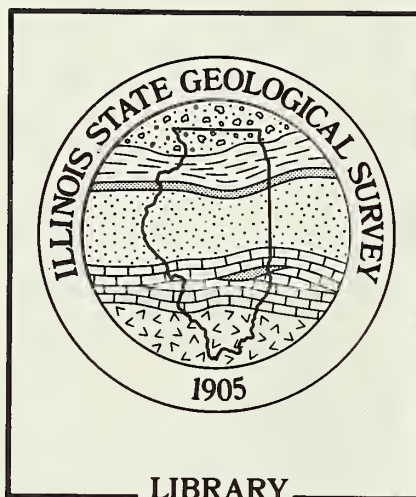
IMSRP

Illinois Mine Subsidence Research Program

cooperating agencies

ILLINOIS STATE GEOLOGICAL SURVEY
Illinois Department of Energy and Natural Resources

BUREAU OF MINES
United States Department of the Interior

The **Illinois Mine Subsidence Research Program** (IMSRP) was established in 1985 to investigate methods and develop guidelines for underground mining operations that aim to maximize coal extraction yet preserve the productivity of prime farmland. The research program was initiated by the Illinois Coal Association and the Illinois Farm Bureau.

The Illinois State Geological Survey, a division of the Illinois Department of Energy and Natural Resources, is directing the IMSRP. Participating research institutions include Southern Illinois University at Carbondale, the University of Illinois at Urbana-Champaign, Northern Illinois University, and the Illinois State Geological Survey. A five-year Memorandum of Agreement, signed by the State of Illinois and the Bureau of Mines, U.S. Department of the Interior, ensures collaboration, cooperation, and financial support through 1991. Major funding is also provided by the Illinois Coal Development Board.

This publication is one in a series printed and distributed by the Illinois State Geological Survey as a service to the IMSRP. The views and conclusions contained in the document are those of the author(s) and should not be interpreted as necessarily representing the official policies or recommendations of the Illinois State Geological Survey. The manuscript has been reviewed and approved for publication by selected peer reviewers, company representatives, and members of the Illinois Mine Subsidence Research Program Technical Committee.

In Situ Strength Characteristics
of Coal Mine Floor Strata in Illinois

by
Yoginder P. Chugh
Southern Illinois University at Carbondale

Illinois Mine Subsidence Research Program

777-157			
REPORT DOCUMENTATION PAGE	1. REPORT NO.	2.	3. Recipient's Accession No.
4. Title and Subtitle. In-Situ Strength Characteristics of Coal Mine Floor Strata in Illinois			5. Report Date. September, 1986
			6.
7. Author(s) Yoginder P. Chugh			8. Performing Organization Rept. No.
9. Performing Organization Name and Address Department of Mining Engineering Southern Illinois University Carbondale, IL 62901			10. Project/Task/Work Unit No.
			11. Contract(C) or Grant(G) No. (C) JO256002 (G).
12. Sponsoring Organization Name and Address. Bureau of Mines Columbia Plaza 2401 E Street, N.W. Washington, D.C. 20241			13. Type of Report & Period Covered Final Oct. 15, 1985-July 22, 1986
			14.

15. Supplementary Notes.

16. Abstract (Limit 200 words).
This report presents data on bearing capacity and in-place shear strength characteristics of immediate floor strata. Plate load tests were conducted under as-mined and saturated-wet conditions. Borehole shear tests were conducted to determine cohesive strength, angle of internal friction, and failure envelope for floor strata at different depths. An attempt was made to correlate the above data with laboratory determined strength-deformation characteristics and engineering index properties of floor strata from ongoing studies. The results indicate the nature of floor strata at the two mines to be very similar. Statistically significant correlations were observed for two sets of variables: 1) ultimate bearing capacity and deformation modulus, and 2) natural moisture content of floor in the 0-12 in/depth range below the coal seam and ultimate bearing capacity. Attempts to correlate ultimate bearing capacity and cohesive strength of immediate floor strata determined from borehole tests and confined compression tests were generally unsuccessful.

17. Document Analysis. a. Descriptors

Strength-deformation characteristics of immediate floor strata, design of coal pillars under weak floor conditions, correlation between in-situ and laboratory-determined properties.

b. Identifiers/Open-Ended Terms.

Ultimate bearing capacity, borehole shear tests, rock borehole shear tester, unconfined shear strength, angle of internal friction

c. COSATI Field/Group.

18. Availability Statement	19. Security Class (This Report) unclassified	21. No. of Pages
	20. Security Class (This Page) unclassified	22. Price

FOREWORD

This report was prepared by Southern Illinois University at Carbondale, Illinois under Bureau of Mines Contract J0256002. The contract was initiated under the Mining Technology Program. It was administered under the technical direction of the Twin Cities Research Center with Mr. Ted Triplett acting as Technical Project Officer. Ms. Sandra Schlesier was the Contract Administrator, Denver, Colorado, for the Bureau of Mines. This report is a summary of the work recently completed as a part of this contract during the period October, 1985 to September 22, 1986. This report was submitted by the authors on September 22, 1986. This report does not contain any copyrighted or proprietary material or patentable information.

On behalf of the College of Engineering and Technology and the Department of Mining Engineering at Southern Illinois University at Carbondale (SIUC), the author would like to convey sincere thanks to the following organizations and/or individuals who were particularly helpful in the performance of the studies reported here.

* Mr. T. Triplett and Mr. L. Powell of the Twin Cities Mining Research Center for their technical assistance and helpful comments.

* Administration and staff of the coal companies participating in the study. Without their sincere interest and significant cooperation this study would not have been possible. Particular thanks are due to Misters E. H. Roberts, John Prudent, Richard

CONTENTS

ILLUSTRATIONS

TABLES

UNITS OF MEASURE-ABBREVIATIONS USED
IN THIS REPORT

deg	degrees
g	gram
hr	hours
in	inch
in^2	square inch
in^3/min	cubic inch per minute
lbs	pounds
lbs/in^2	pounds per square inch
μ	microinch
psig	pounds per square in (gauge)
pct	percent
sec	seconds
t	tons
t/ft^2	tons per square foot
V	volts

INSITU STRENGTH OF COAL MINE FLOOR STRATA
IN ILLINOIS

by

Yoginder P. Chugh[1]

ABSTRACT

Design of mine openings and pillars in coal seams underlain by weak floor strata, such as in Illinois, requires consideration of the interaction of weak floor with immediate roof strata and coal pillars. This requires a knowledge of the in-place strength-deformation characteristics of immediate floor strata. This report presents data on ultimate bearing capacity and in-place shear strength characteristics of immediate floor strata. Plate bearing tests and borehole shear tests were conducted at five sites each in two underground coal mines in Illinois; one mining the No. 6 coal seam and the other the No. 5 coal seam. Plate load tests were conducted under as-mined and saturated-wet conditions with square plates 6-18 in size. Borehole shear tests were conducted with a rock borehole shear tester to develop a failure envelope and determine the cohesive strength and angle of internal friction for immediate floor strata at different depths. An attempt was made to correlate the above data with laboratory determined strength-deformation characteristics and engineering index properties from ongoing studies under a contract from the State of Illinois. The results indicate the nature of the immediate floor strata at the two mines to be very similar. Statistically significant correlations were observed for two sets of variables: 1) ultimate bearing capacity and deformation modulus, and 2) natural moisture content of floor in the 0-12 in range and ultimate bearing capacilty. Attempts to correlate ultimate bearing capacity and cohesive strength of the immediate floor strata determined from borehole shear tests and confined compression tests were generally unsuccessful.

[1] Professor, Department of Mining Engineering
Southern Illinois University, Carbondale, Illinois 62901

Chapter 1

INTRODUCTION

1.1 Background and Statement of the Problem

Roof-pillar-floor interaction must be considered in assessing the stability of mine workings and surface subsidence in mining stratified deposits. The nature and severity of ground displacements depends significantly upon this interaction. More specifically, surface subsidence resulting from pillar or roof failures is expected to be significantly different from that resulting from pillars punching into a weak floor. A review of the open literature reveals a limited number of studies on the effects of weak floor interaction on mine stability and surface subsidence.

Actively mined coal seams in Illinois (No.6 and No.5) are generally underlain by weak (100-500 psi compressive strength) and relatively thick (2-7 ft) underclays. Therefore, a consideration of floor interaction with roof and pillar elements is extremely important. This requires the determination of in-place strength-deformation characteristics of the immediate floor strata associated with coal seams. These may be determined in the field or estimated from similar or index properties determined in the laboratory on cores obtained during exploratory drilling.

Laboratory characterization of immediate floor strata associated with coal seams was recently initiated under the Mine Subsidence Research Program (MSRP) in Illinois. Under a separate contract from the Bureau of Mines (J0256002), a study was initiated to determine the in-place strength-deformation characteristics of immediate floor strata in the same mines and at the same sites where cores of floor

strata were taken for laboratory characterization. In this manner

correlation studies between laboratory determined engineering index

properties and strength-deformation characteristics and in-place

strength-deformation characteristics could be conducted. A final

report on the "Laboratory Characterization of Immediate Floor Strata

Associated with Coal Seams in Illinois" was submitted to the State of

Illinois in May, 1986. This final report summarizes the results of

studies to determine the in-place strength-deformation characteristics

of immediate floor strata and attempted correlations between

laboratory and field determined properties.

1.2 Specific Objectives

The objectives of the research were to 1) measure the ultimate

bearing capacity (UBC) and shear strength of immediate floor strata

below the Illinois No.6 and No.5 coal seams in two underground mines,

and 2) make a comparison of these properties with laboratory

determined values from ongoing studies. The results of this and other

similar studies will eventually be utilized to develop pillar design

equations under weak floor conditions.

1.3 Overall Approach

The research was subdivided into four elements: 1) review of

related literature, 2) measurement of UBC of immediate floor strata

and shear strength of immediate floor strata in the field, 3)

laboratory studies on cores, and 4) data analysis. A brief discussion

of each element is given below.

Pertinent literature on the design of pillars for weak floor

conditions was reviewed. Important strength properties and variables

affecting design were identified based on this review. Available data

on the strength properties of immediate floor strata were reviewed and
compiled in the data base developed for the State of Illinois under
the MSRP.

Measurement techniques for determining the UBC were reviewed and
limitations of previous tests and test procedures were identified.
Plate bearing tests and borehole shear tests were utilized to measure
the UBC and shear strength of immediate floor strata in the field.
Plate bearing tests were generally conducted with three (3) different
sizes of plates (6 in, 8 in, and 12 in square plates) at a particular
site, depending upon the UBC of the floor strata. A limited number of
tests with 18 in square plates did not lead to floor failure at any of
the sites tested. These tests were conducted under as-mined and
water-saturated conditions.

Boreholes were drilled to recover cores of immediate floor strata
for laboratory strength-deformation studies. The boreholes were
drilled in the floor with air through the weak underclay and at least
2-3 ft into the competent bed below it. They were also utilized to
determine cohesive strength (S_o) and the angle of internal friction
(ϕ) at various depths using a portable Rock Borehole Shear Tester
(RBST). Borehole shear tests were conducted at several different
normal stresses within 6-8 in of a specified depth to delineate Mohr's
failure envelope for a stratum in that range. The procedures utilized
for these tests were those recommended by the Bureau of Mines (Haramy,
1981). All plate bearing test data were analyzed for ultimate bearing
capacity and deformation moduli, and the effect of plate size on these
parameters. Borehole shear test data at each site were plotted to
obtain failure envelopes. The data were analyzed to provide

unconfined shear strength (S_o) and angle of internal friction (ϕ), and where appropriate, an equation of the linear failure envelope. Similar studies were also conducted for the immediate roof strata and coal seam at one site in each mine. Laboratory studies on cores of immediate floor strata included the engineering index properties and strength-deformation properties under unconfined and confined compressive stress. These studies have been described in detail elsewhere (Chugh, 1986). A limited number of laboratory tests on the immediate roof, floor and coal were also undertaken at the sites where plate bearing tests and borehole shear tests were conducted. Specifically, unconfined compressive strength tests were conducted to obtain strength and elastic deformation moduli values. Moisture gain measurements on powdered samples of the immediate floor strata under varying moisture conditions were also undertaken.

S_o and ϕ values obtained from borehole shear tests were compared with those obtained from confined compression tests in the laboratory. Strength-deformation characteristics determined from field studies were then compared with those obtained from laboratory studies on cores to develop suitable criteria for estimating in-place strength properties of immediate floor.

The aforementioned studies were conducted at two underground mines in Illinois; one mining the Herrin (No.6) coal seam and the other the Springfield (No.5) coal seam. Characteristics of these mines are discussed in Chapter 3.

Chapter 2

REVIEW OF PERTINENT LITERATURE

2.1 Introduction

The object of the present study is to explore the possibility of arriving at reasonable strength-deformation characteristics of mine floors under the pillars by simple laboratory and field tests which can be used ultimately in the design of pillars and openings. Behavior of coal pillars on weak underclay floor closely resembles that of shallow strip or square foundations on cohesive soil or rock. Bearing capacity of shallow foundations on soils has been extensively studied in the soil mechanics literature. Therefore, available research on this subject was reviewed to ascertain the influence of different factors on the bearing capacity of shallow foundations so that the more significant ones could be identified. Experimental studies conducted in mines by previous investigators were also reviewed to delineate relevant bearing capacity and rock mass deformability factors and to formulate appropriate experimental and analytical procedures for this study. A brief review of the relevant technical literature is presented here.

2.2 Theoretical Determination of Bearing Capacity

The UBC of a soil or weak strata is defined as its ability to carry a load without plastic failure. Figure 2.1 represents the formulation of the problem of bearing capacity for a shallow foundation which can be solved based on the theory of plasticity. The basic solution given by Prandtl (1921) and Reissener (1924) for a rigid plastic material with a linear failure envelope postulates that the failure region consists of three zones: I, II, and III. Zone I is the active Rankine
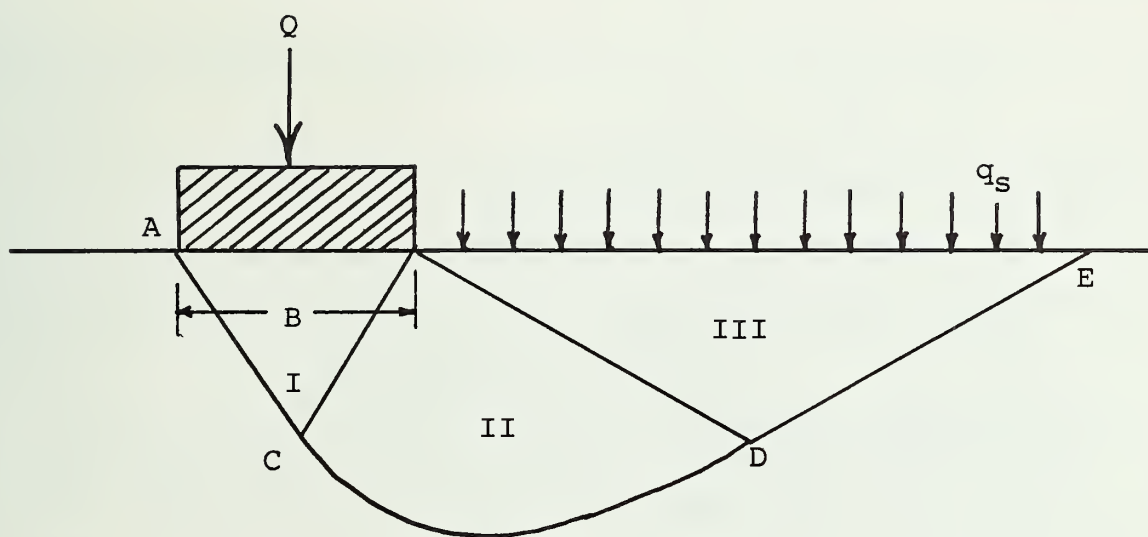
FIGURE 2.1 Bearing capacity analysis of shallow foundations.

zone which pushes the radial Prandtl zone II laterally and forces the passive Rankine zone III in the upward direction. The failure boundary ACDE consists of lines AC and DE at 45° ± $\phi/2$ to the horizontal. The curved portion CD is a logarithmic spiral for $\gamma B/q_s$ = 0 and degenerates into a circle for $\phi = 0$.

Where,

γ = unit wt. of soil

q_s = surcharge stress due to weight of soil above the foundation

B = width of foundation

ϕ = angle of internal friction.

For a general case the curved portion lies between these two limits.

Buisman (1940) and Terzaghi (1943) defined the UBC to consist of three components based on the above formulation.

1. Bearing capacity of a weightless material with cohesion and friction and no surcharge, $\gamma = 0$, $q_s = 0$, $S_o \neq 0$, $\phi \neq 0$

2. Resistance to failure due to evenly distributed surcharge, $\gamma = 0$, $q_s \neq 0$, $S_o = 0$, $\phi \neq 0$

3. Bearing capacity of a cohesionless material with weight and friction, $\gamma \neq 0$, $\phi \neq 0$, $S_o = 0$

Superimposing the three components, which is not precisely correct, they arrived at the following equation:

$$q_o = S_o N_c + q_s N_q + 1/2 \; \gamma B N_\gamma \qquad (2.1)$$

where q_o = ultimate bearing capacity of a shallow strip foundation.

S_o = cohesion of soil

N_c, N_q, N_γ = dimensionless bearing capacity factors

The bearing capacity factors, shown in Figure 2.2 can also be calculated from the following equations.

$$N_q = e^{\pi \tan\phi} \tan^2(\pi/4 + \phi/2) \qquad (2.2)$$

$$N_c = (Nq - 1) \cot\phi; \text{ for } \phi = 0, N_c = 5.14 \qquad (2.3)$$

$$N_\gamma = 2 (Nq + 1) \tan \phi \qquad (2.4)$$

The value of N_γ above can be approximated within an error of 10% for $15° < \phi < 45°$ and within 5% for $20° < \phi < 40°$ according to Vesic (1973).

Vesic (1973) pointed out that the superposition as used by Terzaghi (Eq. 2.1) was not strictly correct since it led to an error of 17% to 20% for ϕ of 30° to 40°. However, it was accepted as reasonable for lack of a more accurate mathematical model.

Bearing capacity failure in soils can take place either as general shear, local shear or punching shear failure (Figure 2.3). In the case of general shear, a continuous failure surface is developed and the material is displaced upwards and outwards from beneath the foundation. If a continuous slip surface does not develop to the surface, the failure mode is referred to as local shear. If the foundation can punch into the weak material without the formation of a continuous failure surface, the failure is known as punching shear failure. Load-deformation characteristics for each failure mode are also shown in Figure 2.3.

Several factors have been identified which affect the ultimate bearing capacity, and some of the more relevant ones are described below.
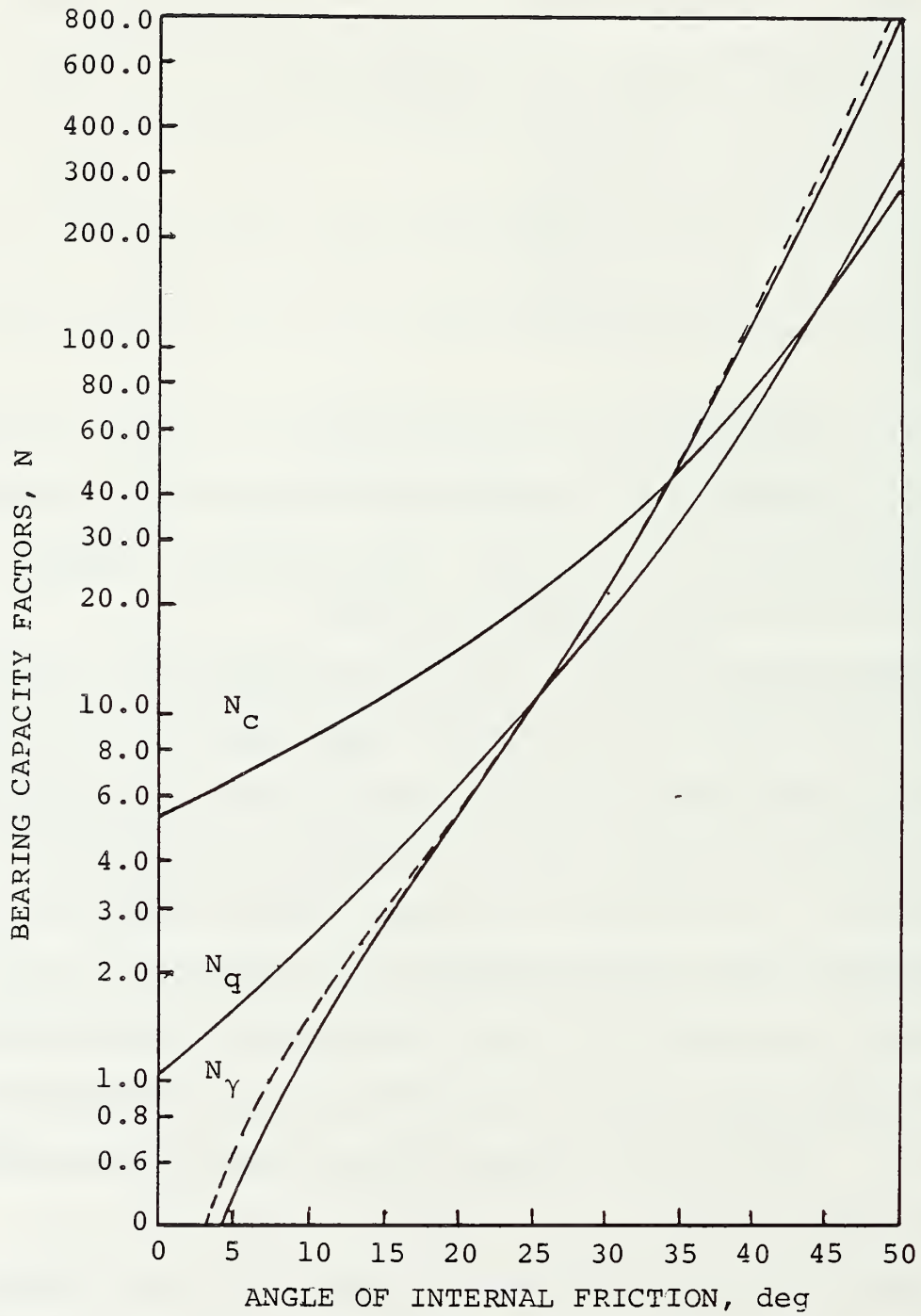
FIGURE 2.2 The bearing capacity factors
(after Prandtl, 1921; Reissner,
1924; Vesic, 1970)
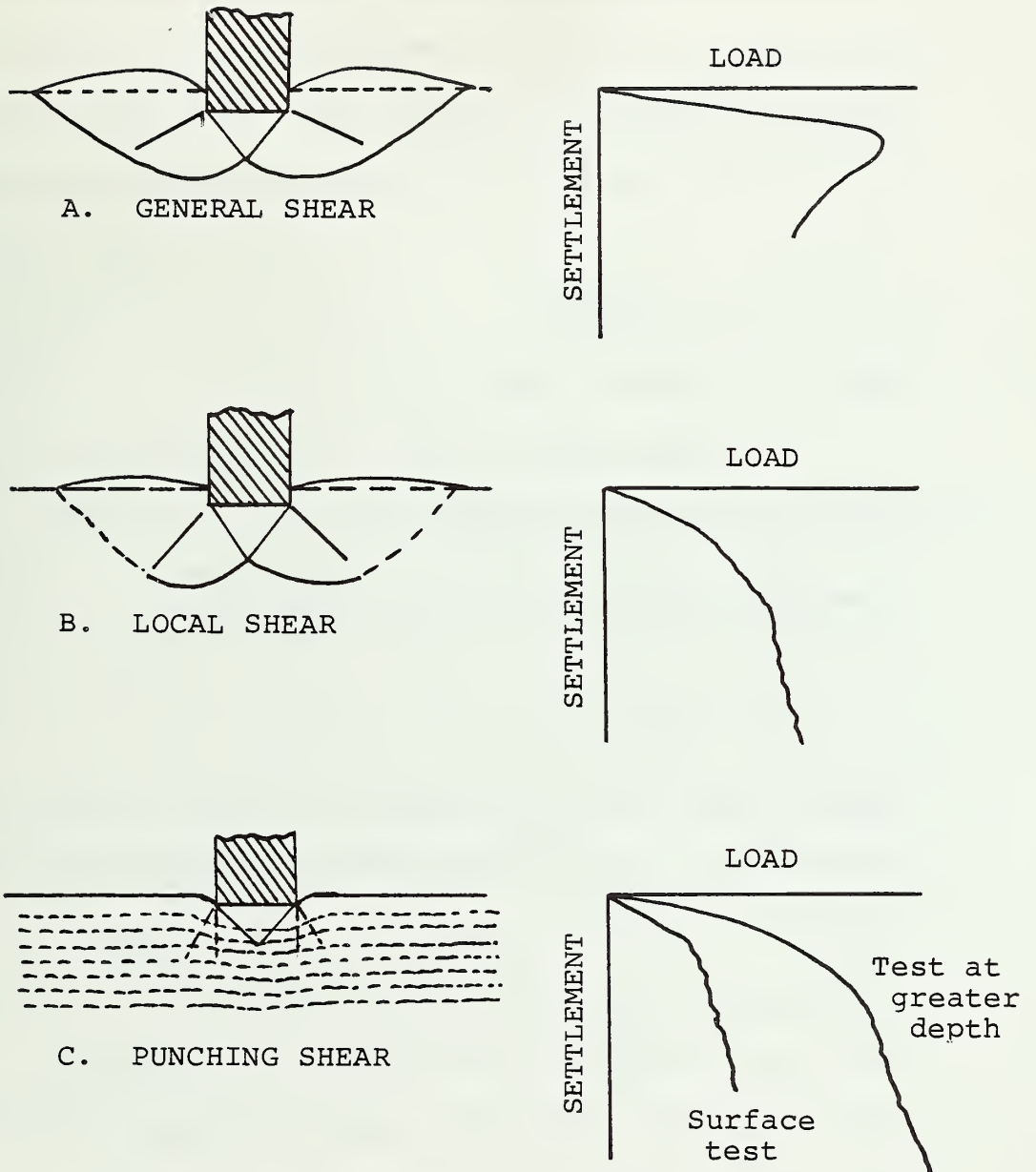
FIGURE 2.3 Modes of bearing capacity failure
(after Vesic, 1963).

Soil Compressibility

Eq. 2.1 represents the bearing capacity failure in the general shear mode for rigid-plastic soil behavior. For compressible soils the failure mode is more likely to be a local or punching type shear failure with a lower value of bearing capacity. To evaluate the effect of compressibility of soils, Vesic (1963, 1965) proposed a rigidity index, I_γ, which can be calculated from the equation:

$$I_\gamma = \frac{G}{S_o + q \tan\phi} , \qquad (2.5)$$

where I_γ = rigidity index

         G = shear modulus of soil.

The value of I_γ can be reduced to $I_{\gamma\gamma} = \delta_v I_\gamma$ to compensate for the volumetric strain, Δ, in the plastic zone where:

$$\delta_v = \frac{1}{1 + I_\gamma \Delta} . \qquad (2.6)$$

The critical value of the rigidity index for any angle ϕ below which bearing capacity must be reduced because of compressibility effects is given by the equation:

$$(I_\gamma)_{crit} = 1/2 \exp[(3.30-0.45 \, B/L)\cot(45°-\phi/2)], \qquad (2.7)$$

where B and L are the width and length of the foundation, respectively. For soils with I_γ less than $(I_\gamma)_{crit}$, the bearing capacity may be reduced by introducing compressibility factors δ_{qc}, δ_{cc} and $\delta_{\gamma c}$ in Eq. 2.1. These factors are given by the following equations (Vesic, 1970):

$$\delta_{qc} = \exp\{[(-4.40+.6B/L)\tan\phi]$$ (2.8)

$$+[(3.07\sin\phi)(\log_{10}2I_\gamma)/(1+\sin\phi)]\}$$

$$\delta_{cc} = 0.32 + 0.12 \ B/L + 0.60 \ \log_{10}I_\gamma \quad \text{and,}$$ (2.9)

$$\delta_{\gamma c} = \delta_{qc} \ .$$ (2.10)

The general bearing capacity equation, taking into account the compressibility of soils, may then be written as:

$$q_o = S_o N_c \delta_c + q_s N_q \delta_q + 1/2 \ \gamma \ B \ N_\gamma \delta_{\gamma c}$$ (2.11)

The value of bearing capacity for very compressible soils may be reduced to 30-40% of that for rigid soils.

Foundation Shape and Size

Eq. 2.1 is suitable for long rectangular foundations. Mathematical solutions for other shapes are difficult to obtain. Hence, semi-empirical approaches have been used to evaluate the effects of foundation shape on bearing capacity. On the basis of comparative loading tests with foundations of different shapes, including long rectangles, equation 2.1 has been modified as follows to account for the foundation shape:

$$q_o = S_o N_c E_c + q_s N_q E_q + 1/2 \ \gamma B N_\gamma E_\gamma,$$ (2.12)

where E_c, E_q, E_γ are shape factors whose values depend on ϕ and are given in Table 2.1.

TABLE 2.1 - Shape Factors for Shallow Foundations (De Beer,
1967, Vesic, 1970)

Shape of Foundation Base	E_c	E_q	E_γ
Strip	1.00	1.00	1.00
Rectangle	$1+B/L(N_q/N_c)$	$1+(B/L)\tan\phi$	$1 - 0.4B/L$
Circle or Square	$1+(N_q/N_c)$	$1 + \tan\phi$	0.60

Thus, for a square foundation, the bearing capacity increase may range from about 20% for $\phi = 0°$ to 120% for $\phi = 50°$, neglecting the effect of any surcharge.

Afrouz (1975) used circular, square, and rectangular plates to determine the UBC of underclay floors in coal mines. He could not find any definite effect of the shape of plates on bearing capacity but found that the ratio of the base periphery to its area (P/A) affected UBC and developed the following equation:

$$q_o = k + m \ (P/A)^n, \qquad\qquad (2.13)$$

where q_o = ultimate bearing capacity

k, m, n = constants of the empirical formula based on experimental studies

He observed an increase in UBC from about 870 to 1740 psi as the P/A ratio was increased from 0.20 to 0.35. Afrouz (1975) concluded that the UBC of floor strata should decrease with the increase in the size

of the foundation. The actual reduction of bearing capacity in his experiments was on the order of 5% to 20% for underclay and 16% to 35% for shale. The size of test plates varied between 4 in and 12 in for circular plates, 4.43 in to 10.65 in for square plates and 6.26 in x 3.13 in to 15.04 in x 7.52 in for rectangular plates.

De Beer (1963, 1965), Vesic (1964, 1965), and Kerisel (1967), found that in the case of shallow foundations the average shear strength mobilized along a slip line under the foundation decreased with foundation size. This was attributed to three independent reasons whose relative contribution would vary with soil type and the range of foundation size: (1) the curvature of the Mohr's envelope, (2) progressive rupture along the slip line, and (3) presence of zones or seams of weakness in soil deposits. De Beer (1965) showed that the change primarily occurred in the values of N_γ, which decreased significantly with an increase in foundation size. Figure 2.4 summarizes the decrease in values of N_γ based on several experimental studies.

Barry and Nair (1970), as a result of floor bearing tests in U.S. mines, concluded that the UBC tended to be independent of size when using rectangular or square plates. They used plate sizes between 6 in and 12 in only, and the floor rock was shale, not underclay.

Kimura, Kusakabi, and Satoh (1985) conducted bearing capacity tests in the laboratory using centrifuges and agreed that scale effects as predicted by De Beer (1965) and Vesic (1964, 1965) were valid.

Moisture

The presence of moisture has a weakening effect on the stability and strength of the mine floor. Jenkins (1958) found a decrease of 10% to
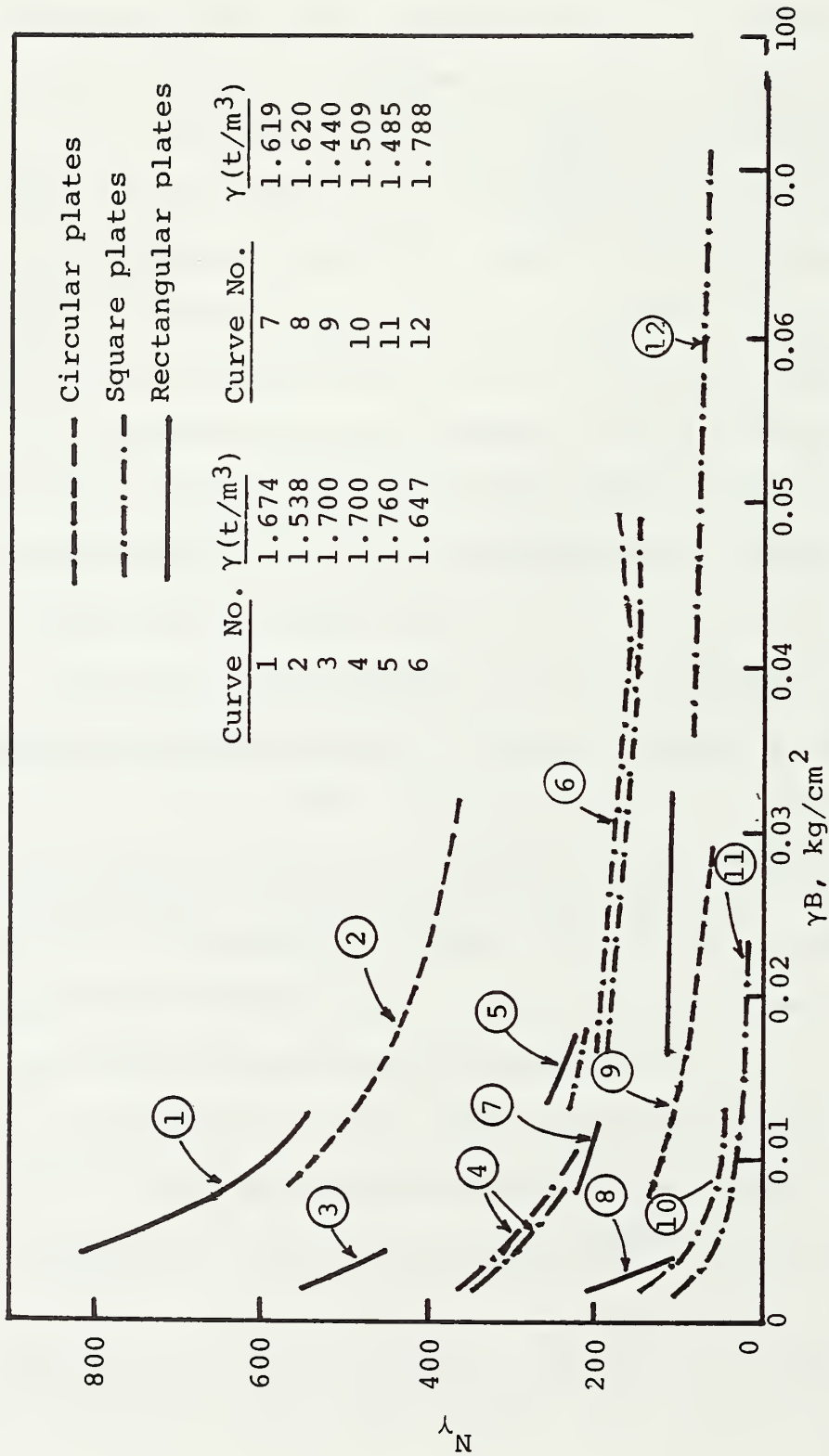
FIGURE 2.4. Effect of size on bearing capacity of shallow foundations. (After De Beer, 1965).

35% in the UBC of mine floor/underclays when wet. Afrouz (1975) also
reported similar reductions. The percentage saturation of floor at
the time of the test, total time the floor was affected by moisture,
quartz content of the floor rock and proximity of predeveloped cracks
in the vicinity of test plates were described as influencing factors
by Afrouz. Barry and Nair (1970) of the Bureau of Mines also
confirmed the weakening effect of the presence of moisture while
conducting bearing capacity tests in various mines in the USA.

Nonhomogeneous Soils

The effect of two-layer soil strata on UBC was first studied by
Kraft and Herfrich (1983), and they suggested that the bearing
capacity of a foundation is influenced by variation in the stress-
strain and strength characteristics of the soil with depth. It is
hypothesized that for a layered system where the soil modulus in the
top layer exceeds that in the underlying layer, the horizontal normal
stresses decrease and the maximum shear stress increases in the bottom
half of the upper layer as compared with the stresses for a
homogeneous mass. The decrease in the normal horizontal stress
reduces the strength and the increase in the shear stress requires
mobilization of a greater proportion of shear resistance. These two
effects contribute to reduce the bearing capacity of the upper layer.

Brown and Meyerhof (1969) proposed the following equation for the
determination of bearing capacity for foundations on a soft stratum
lying above a hard stratum, which is the case when the immediate floor
consists of underclays overlying a harder limestone or claystone
(Figure 2.5):

$$q_o = S_1 N_m ,$$ (2.14)
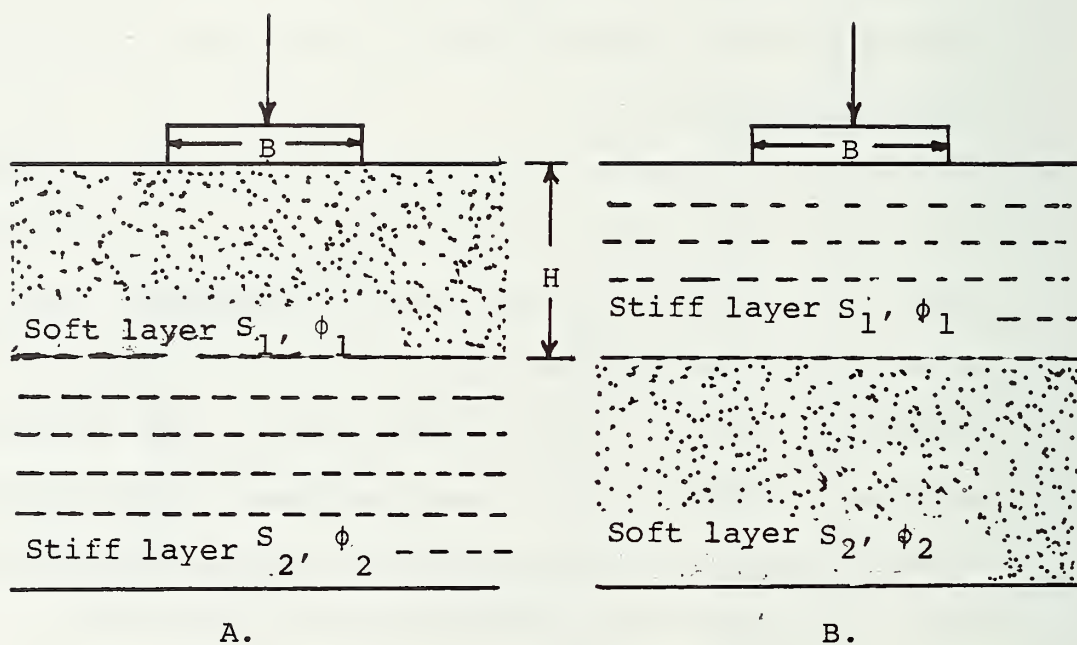
FIGURE 2.5   Bearing capacity analysis for two layered
soil media (after Brown and Meyerhof, 1969).

where S_1 = unconfined shear strength of the soft stratum

N_m = modified bearing capacity factor.

Vesic (1970) proposed the following equation for the determination of N_m:

$$N_m = \frac{KN_c^*(N_c^*+\beta-1)[(K+1)N_c^*+(1+K\beta)N_c^*+\beta-1]}{[K(K+1)N_c^*+K+\beta-1][(N_c^*+\beta)N_c^*+\beta-1]-(KN_c^*+\beta-1)(N_c^*+1)}, \quad (2.15)$$

where, K = ratio of the unconfined shear strength of the lower hard layer (S_2) to the upper weak layer (S_1)

$$N_c^* = E_c N_c; \; N_c^* = 6.17 \text{ for } \phi=0 \qquad (2.16)$$

E_c = shape factor (Table 2.1)

N_c = bearing capacity factor for the weak layer

$$\beta = \frac{BL}{[2(B+L)H]} \qquad (2.17)$$

B = width of foundation

L = length of foundation

H = thickness of the weak layer.

Speck (1981) found a good correlation between the natural water content and triaxial strength of underclays. He modified Vesic's Eq. 2.14 to include underclay water content:

$$q_o = (N_m)[2070 - (167)(uwc)](RF), \qquad (2.18)$$

where uwc is the natural moisture content of underclay and RF is the reduction factor. A value of 0.15 for RF is recommended.

Brown and Meyerhof (1969) suggested the following equation for calculating N_m for the case of a stiff clay layer overlying a soft clay layer assuming the punching type of shear failure.

$$N_m = 1/\beta + K \, E_c \, N_c. \qquad\qquad (2.19)$$

In this case, the effective strength of the upper layer is reduced and is attributed to progressive failure. The value of S_1 in Eq.2.14 must be suitably reduced to calculate the bearing capacity.

The above semi-empirical approaches for a two-layered system were developed primarily on the basis of experimental investigations. Most of them are applicable to vertical loading and cannot predict the effect of weak thin layers which may exist in the soil. Recently, Georgiadis, et al. (1985) have given a new numerical method called the "slip surface" method (originally due to Lauritzen and Schjente, 1976) which can be used to determine bearing capacity of more than two layers. The method computes a factor of safety against failure using an iterative procedure. This represents the reduction which should be applied to the strength properties of various soil layers in order to obtain equilibrium between the resisting and applied forces. The results are claimed to compare satisfactorily with the results of semi-empirical methods for the case of uniform and two-layered soils as well as with those of finite element analysis.

Adjacent Foundations

Graham, Raymond, and Suppiah (1984) observed that interaction between adjacent foundations permits higher total loads to be carried as compared to isolated foundations. This effect was found to increase the UBC by 150% in sand with $\phi = 35°$ when the centerline spacing of the foundation was twice the foundation widths. Experiments showed that the interaction effect was maximum when the spacing to width ratio was 1.7 and disappeared when it was four.

Studies carried out by Stuart (1962), Madel (1965) and West and Stuart (1965) indicated that the effects of adjacent foundations varied considerably with the angle ϕ. For low ϕ values, the effect was negligible but for high ϕ values it might be significant. These effects were considerably reduced as L/B approached one. Similarly, the increased compressibility of soils has the effect of reducing the interaction effects. There are practically no such effects for the case of punching shear failure.

Rate of Loading

Viscous and inertia effects may be mobilized in the soil mass depending upon the rate of loading. It has been observed that as the rate of loading increases from 10^{-4} in/sec (static loading) to 10 in/sec (impact loading), the failure mode of the foundation changes from the general shear mode to the punching shear mode. The bearing capacity of dense sands shows a slight drop with increased loading rate followed by a steady increase, which extends all the way up to the impact velocity ranges. Foundations on compacted clay also show a considerable increase in the UBC as the rate of loading changes from static to impact loading conditions. It is generally accepted that moderate rates of loading would have no significant effect on the bearing capacity. For moderately rapid loadings, the strength parameters S_o and ϕ may have to be modified for strain rate effects by introducing factors suggested by Whitman (1970).

2.3 Sensitivity Analyses of Bearing Capacity Equation

Assuming that the Buisman-Terzaghi (Eq. 2.1), Brown and Meyerhof (Eq. 2.14) and Vesic (Eq. 2.15) equations are reasonable models for the estimation of the ultimate bearing capacity in soils and rocks, it

is important to analyze the relative importance of different variables in the equations. Chugh and Chandrashekhar (1986) have conducted sensitivity studies of different variables with the following conclusions and observations.

Buisman-Terzaghi Equation

1) For $\phi = 0$ and small values of B (less than 60 ft), the cohesive component $S_o N_c$ contributes over 90% to the UBC. This may be the reason why size of the plate in plate bearing tests appears to have little or no effect on the UBC of homogeneous floor strata.

2) For $\phi = 0$ and values of B on the order of pillar sizes (60-80 ft) commonly utilized in Illinois basin mines, the contribution of the component $1/2\gamma.B.N_\gamma$ toward the UBC becomes significant. Some studies in soils indicate that N_γ may decrease with increasing values of plate size. Similar data for immediate floor strata associated with coal seams in Illinois are not available.

3) The UBC value is highly sensitive to the angle ϕ, since N_c, N_q, and N_γ values increase rapidly with increasing values of ϕ. N_γ values increase much more rapidly with ϕ than N_c values (Figure 2.2).

4) For $\phi = 30°$, $S_o = 100$ psi, $\gamma = 144$ pcf, and B = 60 ft, the contributions of the $S_o N_c$, $q_s N_q$, and $1/2$ $\gamma B N_\gamma$ to the UBC are 90.8%, 8.8%, and 0.4%, respectively.

5) Based on the above analyses and discussion, the important variables for the determination of the UBC are S_o and ϕ. An

estimate of γ may be used without incurring much error in the calculation of the UBC.

<u>Vesic Equation</u>

The modified bearing capacity factor, N_m (EQ. 2.15) basically represents the factor N_c in the Buisman-Terzaghi equation. The components due to surcharge ($q_s N_q$ and $1/2\gamma BN_\gamma$) must be accounted for in the calculation of the UBC of non-homogeneous floor strata.

1) N_m is more sensitive to the angle ϕ for a positive change in ϕ than for a negative change (Figure 2.6). For only +25% change in ϕ, N_m (and hence bearing capacity) will change by 100%. This is true irrespective of the B/H and S_2/S_1 ratios.

2) N_m is not very sensitive to changes in S_2/S_1 (Figure 2.7). A 100% change in S_2/S_1 for B/H = 30 increases N_m by only 2%. With increasing underclay thickness (B/H = 6) this increase in N_m becomes even smaller (0.98%). Very large thickness of underclay may even result in a slight decrease in the N_m value.

3) There is a linear increase in N_m with increasing B/H. The slope of this line is greater for higher S_2/S_1 ratios (Figure 2.8). Similar trends are observed at different values of ϕ, keeping S_2/S_1 constant. In this case, however, the slope is greater for lower values of ϕ. The changes in N_m are not as significant as in (1). Doubling B/H (reducing soft floor thickness by half) increases N_m by only 10%.
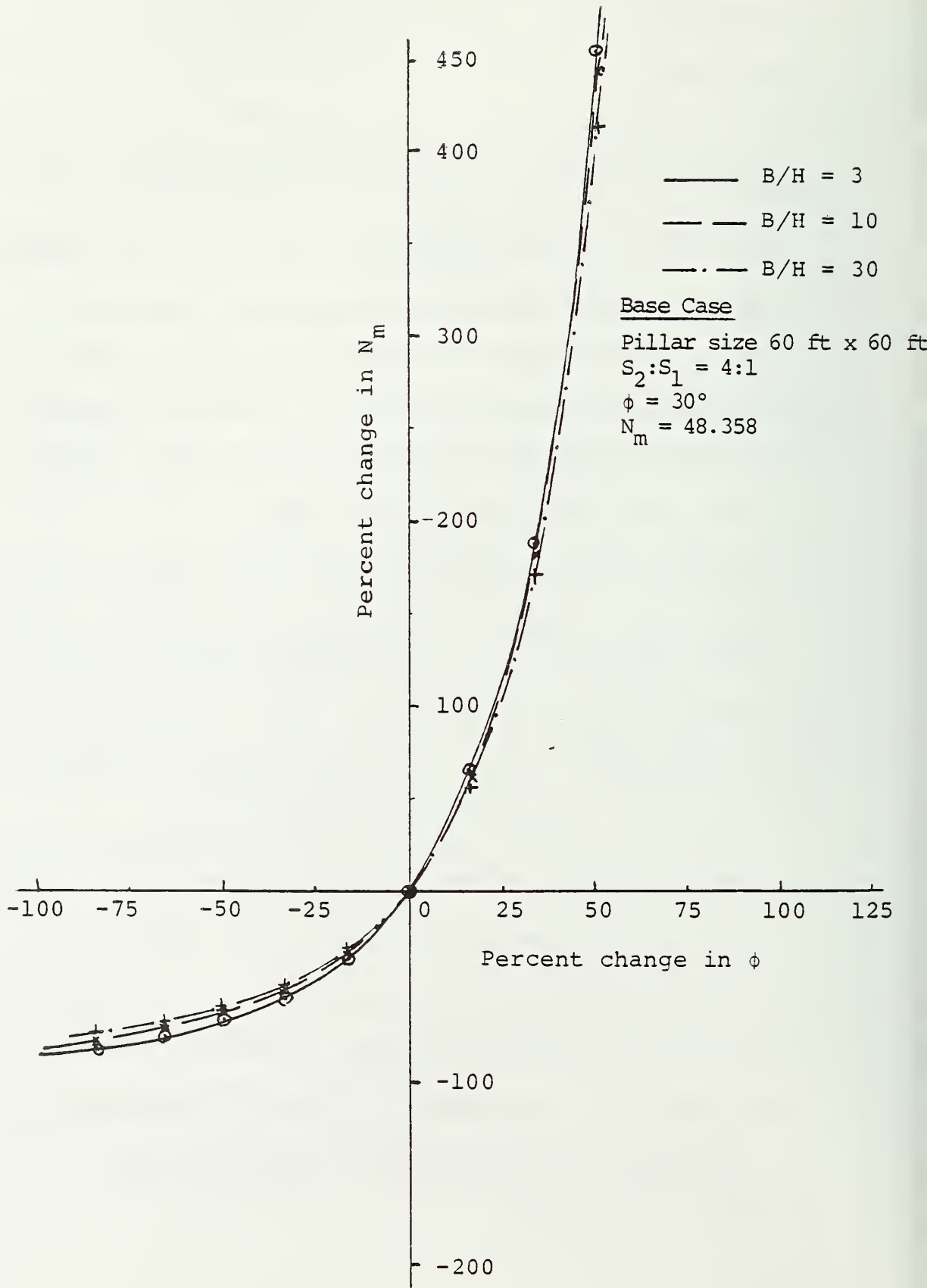
FIGURE 2.6 Sensitivity analysis of N_m with ϕ (Chugh and Chandrashekhar, 1986).
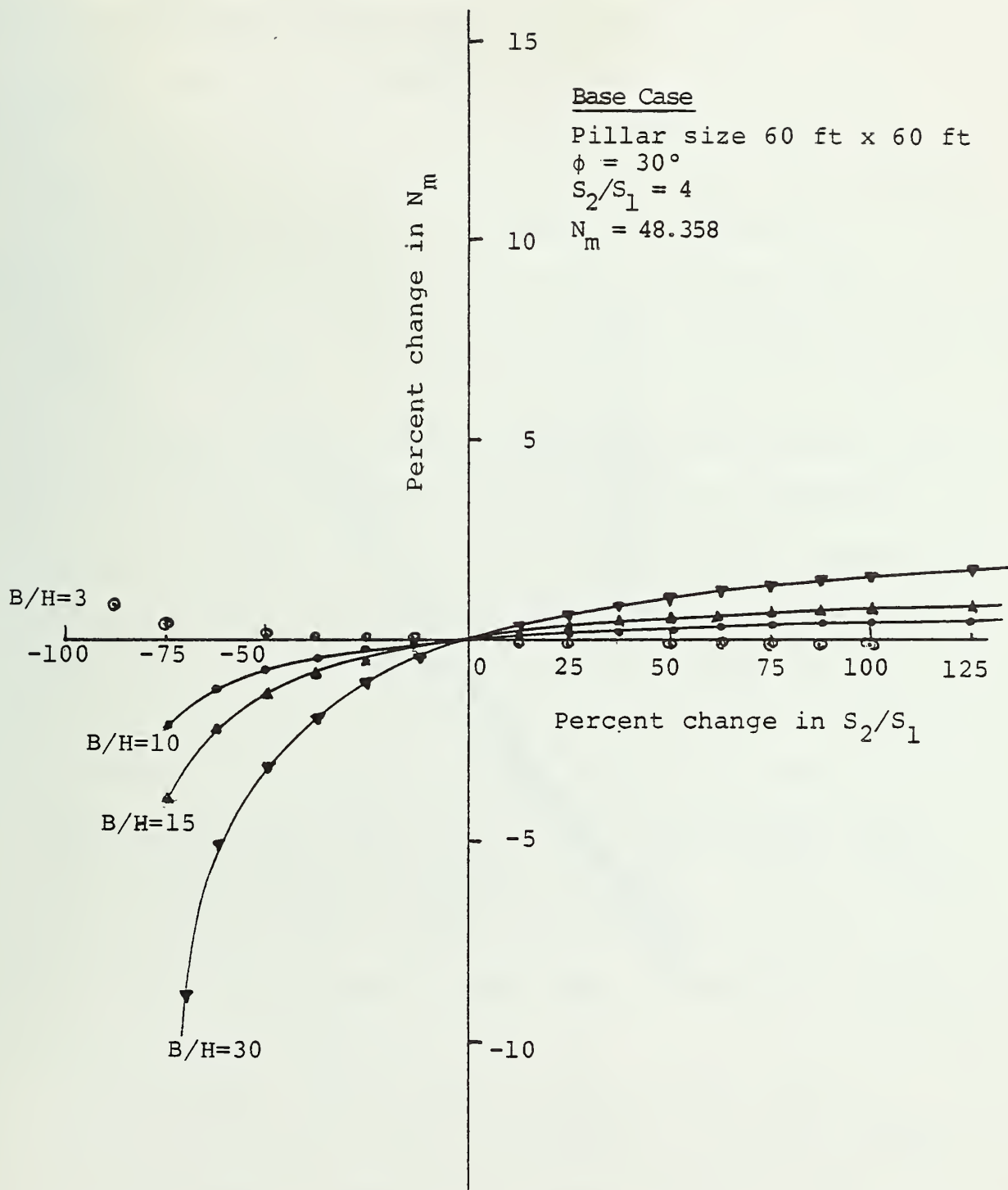
FIGURE 2.7 Sensitivity analysis of N_m with S_2/S_1 (Chugh and Chandrashekhar, 1986).
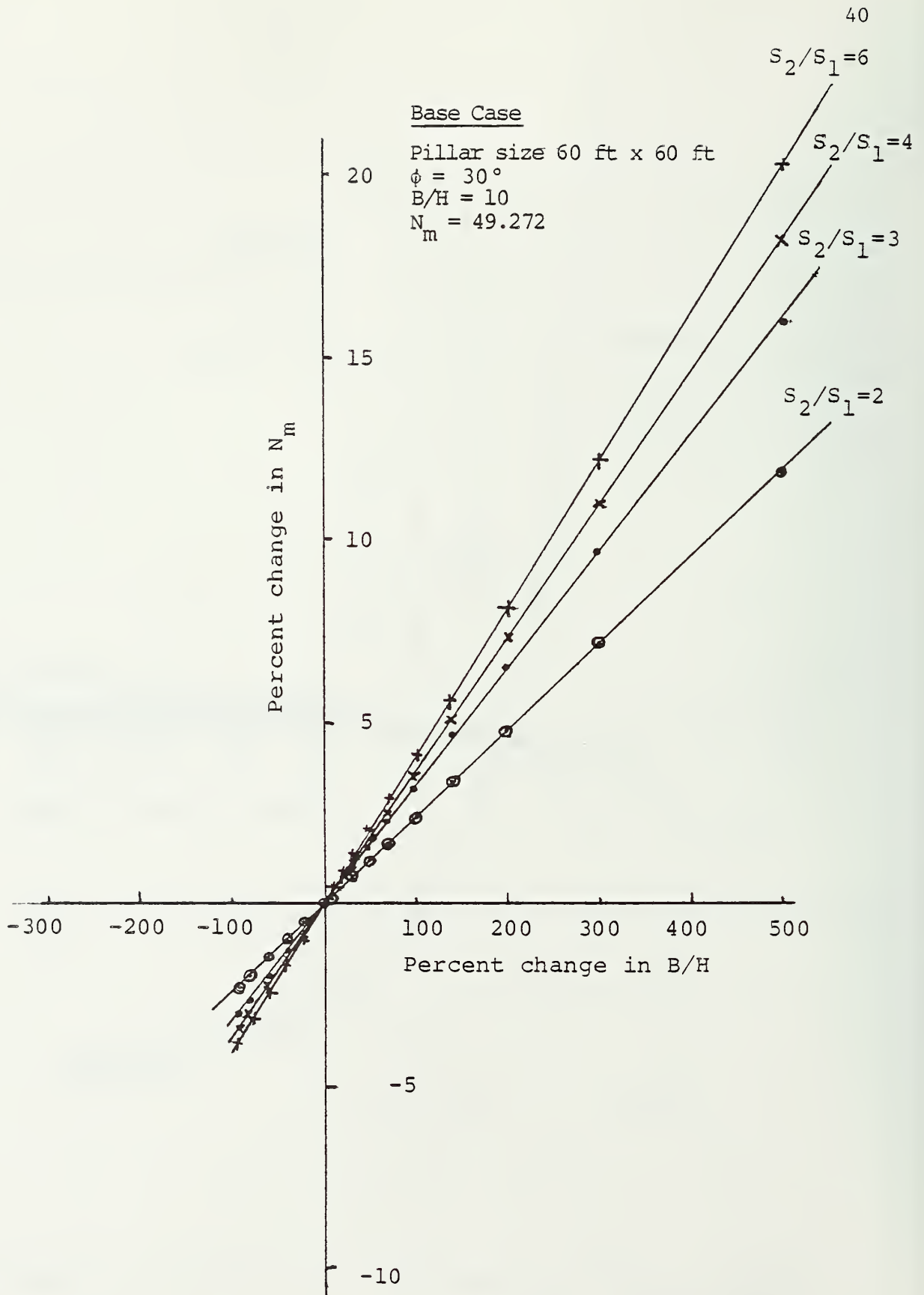
FIGURE 2.8 Sensitivity analysis of N_m with B/H (Chugh and Chandrashekhar, 1986).

2.4 Field Determination of the Ultimate Bearing Capacity

UBC tests for soil have been extensively utilized by civil engineers for foundation design. Standardized procedures by the American Society for Testing Materials (ASTM) have been developed for this purpose. Mining engineers have used the UBC of immediate roof and floor strata primarily for longwall support design; however, test procedures are not well defined. Barry and Nair (1970) have described equipment and procedures utilized by the Bureau of Mines for determination of the bearing capacity of roof and floor strata. Others have utilized similar or slightly modified equipment for this purpose.

ASTM procedure D1194-72 (1977) for conducting bearing capacity tests of soils by plate loading tests requires that the load increments should not exceed 1.0 t/ft^2 or 10% of the estimated UBC to ensure that the load is applied as a static load without impact, fluctuation, or eccentricity. A minimum of six load settlement measurements are recommended and should be made as soon as possible before and after the application of each load increment. Vesic (1963) suggested the failure criterion for determination of the UBC to be the point on the linear stress-deformation plot at which the slope of the curve becomes zero or a steady minimum or a point where the stress deformation curve on the log-log plot changes its slope suddenly. These criteria are shown in Figures 2.9 and 2.10.

Mine floors and roofs were tested by Barry and Nair (1970) to determine the minimum allowable bearing pressure that can be applied by the foot plates and canopies of a longwall support. A 100 t hydraulic jack in conjunction with an air operated hydraulic pump was
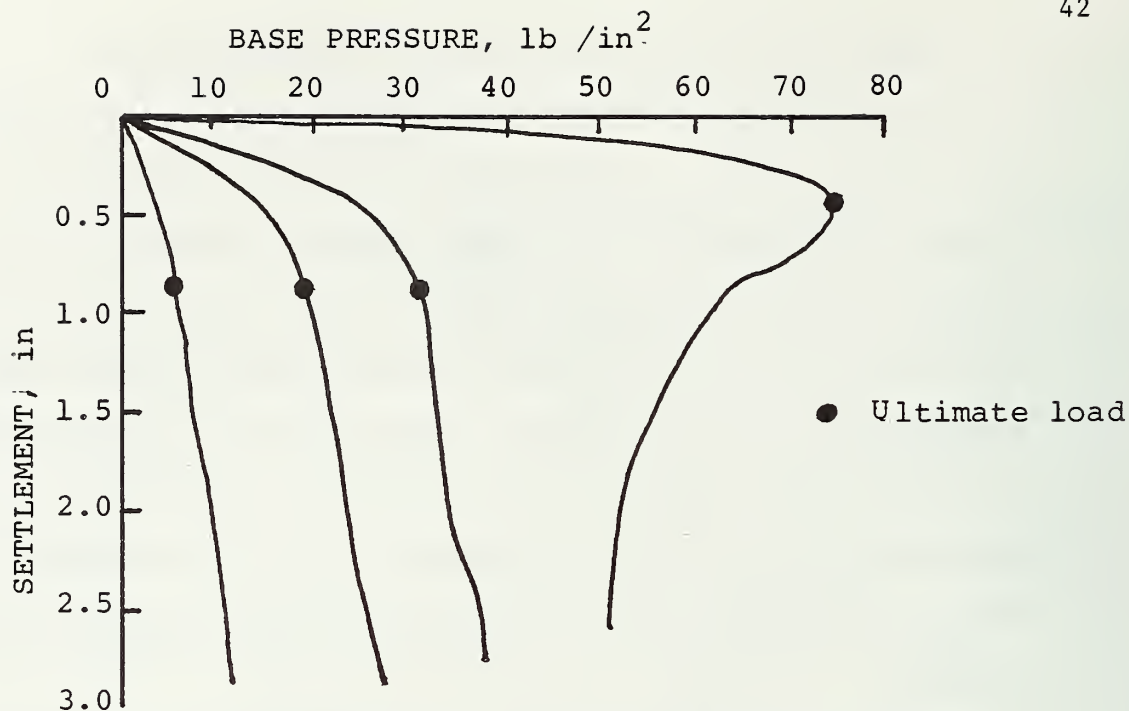
FIGURE 2.9 Vesic's criterion for determin-
ation of ultimate bearing capacity
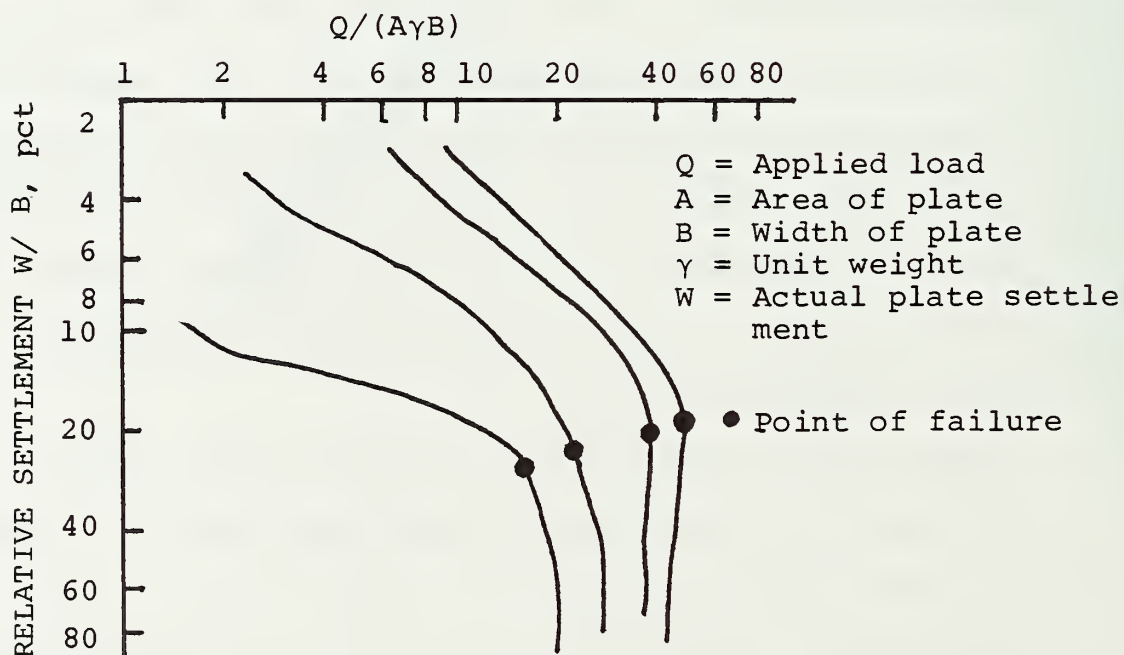
FIGURE 2.10 De Beer's criterion for deter-
mination of ultimate bearing
capacity.

used, and a settlement rate of 0.2 in per 5 min was maintained. To reduce the difference between the shape and sizes of the test plates and the foot plates and canopies of the longwall supports; test plates of 6 in x 6 in, 12 in x 12 in and 6 in x 18 in size with rounded edges were used. A typical square plate is shown in Figure 2.11 and specifications for selected plate sizes are given in Table 2.2.

Coates and Gyenge (1966) conducted bearing capacity tests in the walls of drifts to determine the deformation and strength properties of rock. Similar considerations for load applications were used so that time-dependent deformations could be obtained for each load increment. Deformation modulus for each load increment was also calculated and found to be a good measure of rock strength properties. Moderately good agreement was obtained between the strength properties as determined by plate load tests and laboratory tests. However, interpolation of results to large size foundations such as coal pillars did not give very accurate results. The authors also accepted the usefulness of plate load tests where little interpolation of results was required for prototype structure.

Dulaney (1960) tested the bearing capacity of mine floors in several states of the United States. He used square plates of 1.5 in to 12 in size and could not find any effect of plate size on the bearing capacity. The bearing capacity was found to be slightly higher than the unconfined compressive strength of wet samples which may therefore be taken as the in-situ strength of the mine floor for design purposes. However, where the floor contained more than 30% clay size minerals or montmorillonite was present, neither the wet compressive
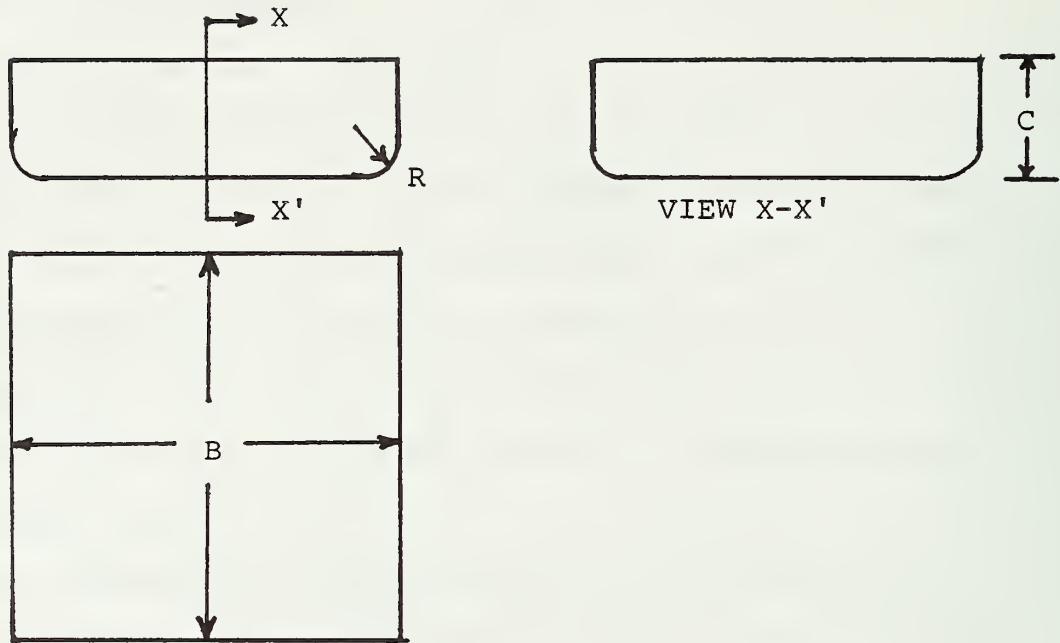
FIGURE 2.11 Bearing capacity plate dimensions.

TABLE 2.2 Plate dimensions.

Plate No.	B	C	R
1	6	2	3/8
2	8	2	3/8
3	12	2	3/8

strength of specimens nor in-place plate bearing strength could give a true measure of the in-situ strength.

Bandopadhay (1982) conducted floor bearing capacity tests at a mine in western Kentucky. The data was used as one of the strength properties of the underclay in a finite element model developed to analyze floor heave in a room and pillar panel. A scaling factor of two (2) was applied to the laboratory measured strength properties before they were used in the model, but the UBC was not scaled. Displacements computed from the analytical model compared well with those observed in the field.

Rockaway and Stephenson (1979) conducted seven bearing capacity tests for immediate floor strata of two mines in Illinois. They determined the following scaling factor to compute the operational strength of mine floors from laboratory unconfined compressive strength, C_o:

$$q_o = 3.08C_o \qquad (2.20)$$

Speck (1981) utilized bearing capacity determination to investigate floor heave problems. He developed a "Heave Factor" index, similar to the safety factor, which is defined as:

$$HF = UBC/\sigma_{avg}, \qquad (2.21)$$

where   HF = heave factor

UBC = ultimate bearing capacity of mine floor based on natural water content correlation with triaxial compressive strength (Eq. 2.18)

σ_{avg} = average pillar stress applied to mine floor.

An HF less than one indicates a potentially unstable mine floor while an HF equal to or greater than one indicates a potentially stable mine floor.

2.5 Limitations of Plate Loading Tests

The major problem in accepting the plate load test as a reliable method of determining the bearing capacity of mine floor under a pillar has been the difference in size of the test plates used and the coal pillar. Some investigators have observed that the bearing capacity decreases with the increase in the size of the test plate; others have observed no effect. Extrapolation of the results have been carried on a small scale, and no specific relationship has been determined to correlate the UBC variation with the size of the foundation. The exact effect of the rate of loading also has not been determined.

A plate load test involves layers up to a depth of about two diameters of the test plate; hence, a bearing capacity test reflects the strength and deformation properties of these upper layers only. However, under an actual pillar the layers involved would extend to a much greater depth, and the ordinary plate test may not adequately simulate the field condition. The number of layers involved will generally be more than two, but no simple analytical method exists for determining bearing capacity under such conditions. Finite element analysis can deal with soil profiles which contain a large number of layers, but the high cost of analysis and the difficulties associated with modeling the individual frictional layers restrict the wide use of the method for bearing capacity purposes.

Pillars in a room and pillar mining layout resemble closely-spaced foundations. The interaction of the pillars is likely to lead to increased bearing capacity, but the exact relationship between bearing capacity and width/spacing ratio of the pillars is unknown.

The ratio of the width of pillar to thickness of underclay in mines is usually more than one. The normal bearing capacity formulae assume that this ratio is 0.5 or less. The bearing capacity factors may consequently have to be modified according to the method proposed by Mandel and Salecon (1969). In this method, the coefficients F_c and F_γ are introduced in the bearing capacity factors to account for an increase in B/H ratio.

2.6 Determination of Deformability of Immediate Floor Strata by Surficial Loading

Figure 2.12 shows a test setup for studying the deformability of the roof and floor (ISRM, 1978). Depending upon the area to be tested in either roof or floor or both roof and floor, flat jacks are placed and boreholes are drilled for setting up multiple position borehole extensometers (MPBXs). Depending upon the lithology, MPBX anchors are set at specific points. Incremental and cyclic loading up to a maximum pressure of 1.2 to 1.5 times that imposed by the structure provide data for calculation of loading and unloading moduli. Plots of deformation vs time, pressure, or depth are used to determine creep, rebound, and permanent set characteristics of the rock mass. Plate load tests discussed earlier may also be effectively used for the purpose (Chugh, Caudle and Bandopadhay, 1984).
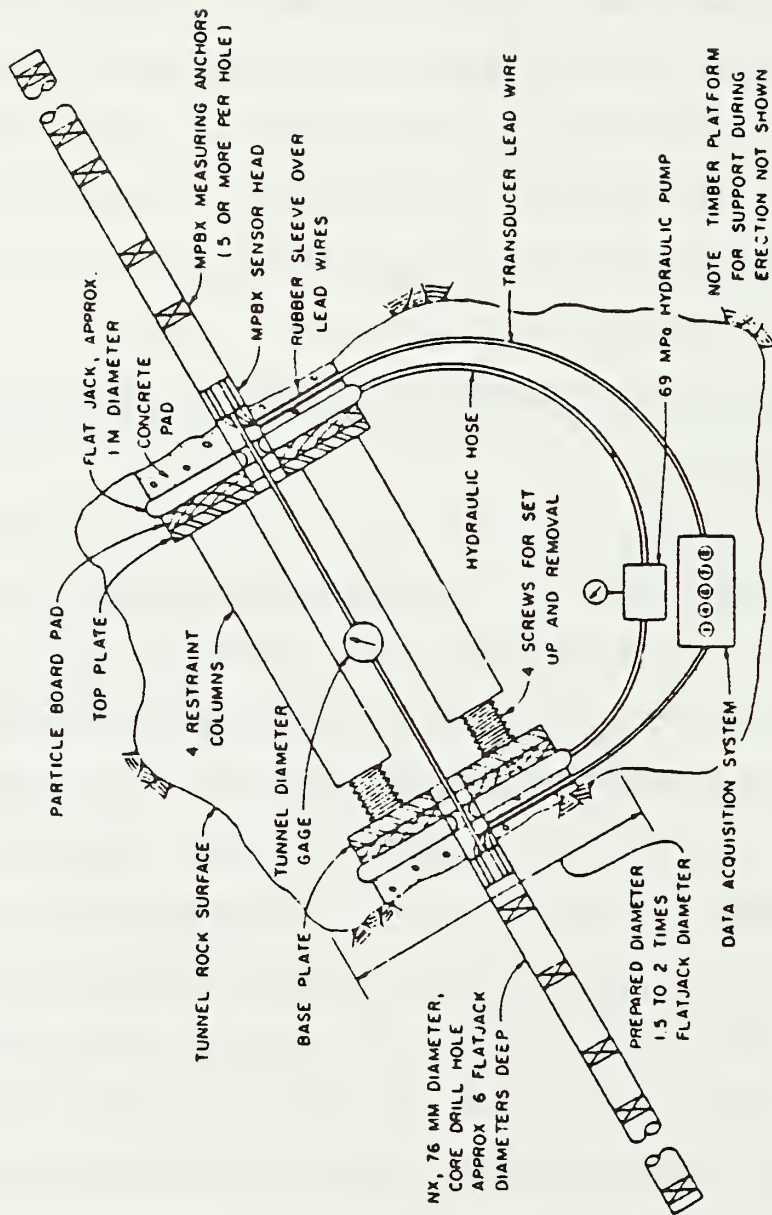
Figure 2.12 In-situ Deformability Measurement Technique (ISRM, 1978)

For loads applied with a circular flat jack with a hole in the center in elastic, homogeneous and isotropic medium, the displacement W_z, in the direction of the applied load, (Figure 2.13) can be calculated from the following equation based on the theory of elasticity:

$$W_z = \frac{2q(1-\mu^2)}{E}[a_2^2 + z^2)^{1/2}(a_1^2+z^2)^{1/2}]$$

$$+\frac{z\ q(1+\mu)}{E}\ [(a_1^2+z^2)^{-1/2}-(a_2^2+z^2)^{-1/2}], \qquad (2.22)$$

where z = distance from the loaded surface to the point where displacement is calculated or measured.

   q = applied pressure

   μ = Poisson's ratio

   E = deformation modulus

   a_2 = outer radius of the flat jack

   a_1 = inner radius of the flat jack or radius of hole.

For specific values of a_1, a_2, μ and z, for a particular case, the equation reduces to:

$$W_z = \frac{q}{E}(K_z). \qquad (2.23)$$

   where K_z is a constant.

If displacements W_{z1} and W_{z2} are measured at points z1 and z2, the indicated deformation modulus of the material between z1 and z2 may be calculated from the following equation:

$$E = q(\frac{K_{z1} - K_{z2}}{W_{z1} - W_{z2}}) \qquad (2.24)$$

Rock mass deformability at different depths may also be determined by using a plate load test at the bottom of a borehole (ISRM, 1978).
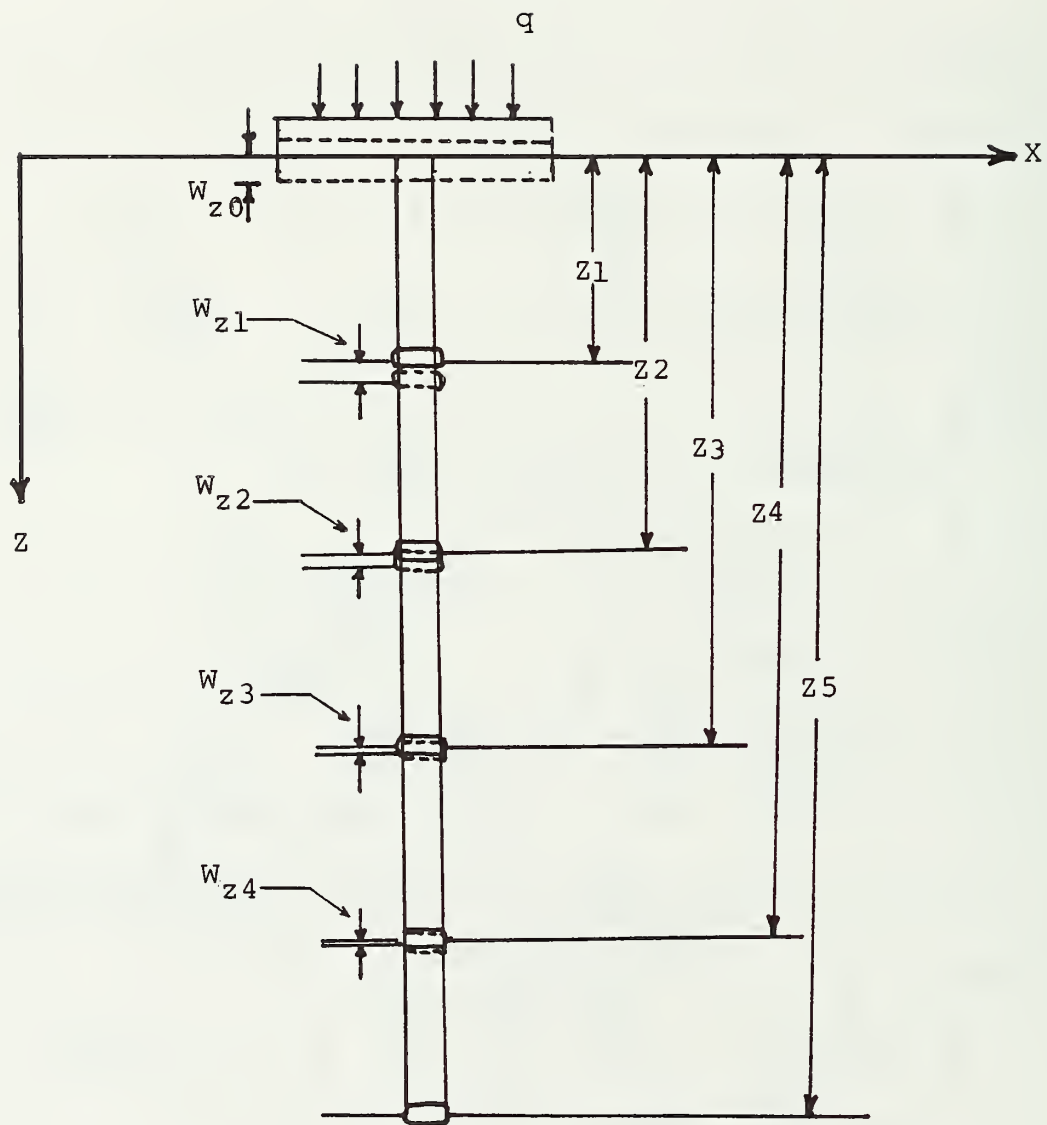
Figure 2.13. Variation of deformation with depth below a plate load test.

Elastic deformation moduli may be derived from graphs of bearing
pressure versus displacement and time-dependent creep properties may
be determined from graphs of displacement versus time. The
deformation modulus may then calculated from the following formula:

$$E = \frac{dq}{dW_z} \frac{\pi}{4} d \; (1-\mu^2) \; I_c \qquad\qquad (2.25)$$

where　　E　= deformation modulus

q　= applied pressure

W_z = plate settlement

d　= plate diameter

μ　= Poisson's ratio

I_c = depth correction factor (ISRM, 1978).

2.7　Insitu Determination of S_o and ϕ by Borehole Shear Tests

Application of rock mechanics to design of underground mines and
other structures in a rock mass has faced two major obstacles that
undermine the confidence level of the predicted designs. These
obstacles are 1) the difficulty in measuring in-situ stress, and 2)
problems in determining the rock mass strength in response to present
and anticipated stresses. While considerable effort has been directed
towards the determination of in-situ stress fields, the strength
properties of a rock mass are estimated mostly from laboratory tests
of core samples. Coring of soft to moderately hard rocks almost
inevitably introduces bias due to incomplete core recovery. At times
it is difficult, if not impossible, to obtain and prepare undamaged
test specimens for use in determining mechanical properties of rocks
which are very friable in nature. In-mine direct shear tests of
carved out blocks of rock are expensive and time consuming; and hence,

these tests are not very frequently done. To overcome these difficulties, an in-situ shear testing device, "The Rock Borehole Shear Tester" (RBST), was developed by Handy (1975) under a Bureau of Mines contract.

The RBST consists of a pair of shear plates which are expanded against the sidewall of an NX (3 in) size borehole under a known normal stress. Then the force required to shear the rock from under these plates is measured and converted to the shear stress of the rock for the normal load applied. The RBST can be used to take 12 to 20 shear strength readings per shift. This generates sufficient shear strength versus normal stress data to develop a Mohr-Coulomb failure envelope. In addition, C_o, T_o, S_o, and ϕ can be calculated or estimated (Haramy and DeMarco, 1983) from the following formulas:

$$C_o = \frac{2S_o \cos\phi}{1 + \sin\phi} \qquad (2.26)$$

$$T_o = \frac{2S_o}{\tan\phi + [(\tan\phi)^2 + 1]^{1/2}}. \qquad (2.27)$$

Principal stresses σ_1 and σ_3 in a direct shear test are related by the equation:

$$\sigma_1 = S_o + \sigma_3 \tan\phi. \qquad (2.28)$$

The RBST has been extensively tested by Panek (1979) and Handy (1976), and the required modifications have been made to adapt it for use in medium hard to hard rocks. Panek (1979) evaluated the modified RBST and observed: "The RBST is indicated to be an efficient, practical apparatus for relatively rapid testing of the strength of the rock mass in-situ. The results are consistent and reproducible.

Strength estimates formulated in terms of Mohr-Coulomb criterion appear to be lower by RBST than Triaxial Compressive Test (TCT) but the RBST results are believed to be more realistic values for design purposes."

The RBST features a small test area which is convenient and necessary to keep forces within manageable bounds and minimize elastic working of the shear plates. Though the small size of test area has the disadvantage of not directly giving averaged strength, statistical considerations indicate an advantage for analysis (Handy, 1976). Mohr circles generated from triaxial compressive strength tests have been found to generate erroneously high and low S_o values; whereas in the same testing time the RBST would generate multiple failure envelopes with corresponding values of both S_o and ϕ, for which the means, standard deviations, and confidence limits could be obtained. Experiments carried out by Handy, et al (1976) show that the RBST gives lower values of cohesion when compared to that given by laboratory confined or triaxial compression tests. Panek (1979) explains this by arguing that a RBST gives a test result in any type of material, whereas confined compression test data are inherently biased to the high side, since intact test specimens necessarily exclude the material from the weak end of the strength distribution, the most fractured, poorly cemented, and highly altered portions of in-situ rock mass. Even moisture content is higher in case of in-situ rock when compared to the drilled cores, which may account for lower values. Its use in evaluating strength characteristics of immediate floor strata was first attempted by Rockaway and Stephenson (1979) with relatively little success. They summarized their experiences as

follows: "Originally, the RBST data were intended to be used in support of a study of weak floor conditions, but initial difficulties in adapting the equipment for use in soft strata prevented this objective from being accomplished. The major difficulties encountered in the use of the RBST were related to non-reproducibility of the data obtained from in-situ testing."

Rockaway and Stephenson also discussed some of the factors affecting data scatter, including the size of the shear plates in relation to the fissure and fracture density in the underclay, the presence of limestone nodules in the underclay, and the calibration of the equipment and degree of accuracy of the gages.

2.8 Concluding Remarks

The foregoing literture review reveals that plate loading tests provide a simple means for determining the operational strength of immediate floor strata. It is uncertain, however, whether this value represents the UBC of floor strata underneath the pillars. The RBST provides a means to determine S_o and ϕ values for immediate floor strata at various depths which may be used in analytical models to estimate the UBC underneath pillars. Therefore, attempts must be made to correlate the UBC as determined by plate loading tests with S_o and ϕ values determined by the RBST and laboratory confined compression tests. Similar attempts must also be made to correlate the UBC with some of the engineering index properties of immediate floor strata, such as natural moisture content, clay content, and Atterberg limits.

Chapter 3

EXPERIMENTAL

3.1 Introduction

Ultimate bearing capacity tests and borehole shear tests were conducted at two underground mines in Illinois during this study to determine the in-situ strength and deformation characteristics of immediate floor strata. An automated microcomputer-based equipment setup for the determination of bearing capacity was designed and fabricated during the project. A Rock Borehole Shear Tester was purchased from Handy Corporation. This chapter describes the characteristics of the study mines, equipment, and experimental and data analysis procedures utilized in this study.

3.2 Mine Characteristics

Mine 1 is located in southern Illinois and extracts the Springfield (No. 5) seam at a depth varying from 800-900 ft using a room-and-pillar mining method. The seam is 5.5-6.5 ft thick and is underlain by underclay 1-2 ft in thickness. The underclay is underlain by grey silty shale which contains little or no carbonate. Floor heave in isolated areas is commonly observed at this mine in development as well as in retreat mining areas.

Mine 2 is also located in southern Illinois and extracts the Herrin (No. 6) coal seam at a depth of 700 ft using a room-and- pillar mining method. The seam is 6.5-8.5 ft thick and is underlain by relatively weak shale of variable thickness (2-7 ft). Below this are a thin weak layer of shale and a limestone layer. Floor heave is commonly encountered in retreat-mined areas.

3.3 Automated Bearing Capacity Equipment

Since a large number of bearing capacity tests were to be conducted during this study, an equipment setup as shown in Figure 3.1 was designed and fabricated by Kennard (1985). This setup is capable of providing a maximum load of 200,000 lbs with a maximum allowable deformation of 2 in. The overall setup consists of an automated loading and data aquisition system. An electric motor-driven hydraulic pump provides automated loading, and linear variable differential transformers (LVDT) are utilized to measure deformations. Load-deformation data are formatted and recorded continuously on a field data logger. The data from the logger are transferred to an IBM-PC[1] microcomputer for analysis. A more detailed discussion of the system components is given below.

Hydraulic Jack

An ENERPAC hydraulic jack (Model RC-1006) of 100t capacity was utilized in the setup. The jack has a cylinder rod diameter of 4.125 in and a bore diameter of 5.125 in. It can be operated at a maximum pressure of 10,000 psi and has a maximum travel of 6.625 in. The overall diameter of the jack is 6.875 in.

Hydraulic Power Source

An ENERPAC[1] electric motor drives a hydraulic pump (Model PEM-1541), with a capacity to deliver oil at a maximum pressure of 10,000 psi. The hydraulic pump is provided with a throttle valve to control the amount of oil flow to the hydraulic jack. Maximum flow

---

[1] Reference to specific brands, equipment, or trade names in this report is made to facilitate understanding and does not imply endorsement by Bureau of Mines.

ROOF

Roof Bearing Plate

Tubular Steel Post

COAL
RIB

COAL
RIB

Pressure
Transducer

Data Logger

Hydraulic
Pump

Hydraulic
Jack

LVDT

Floor Bearing Plate

Reference Bar

FLOOR
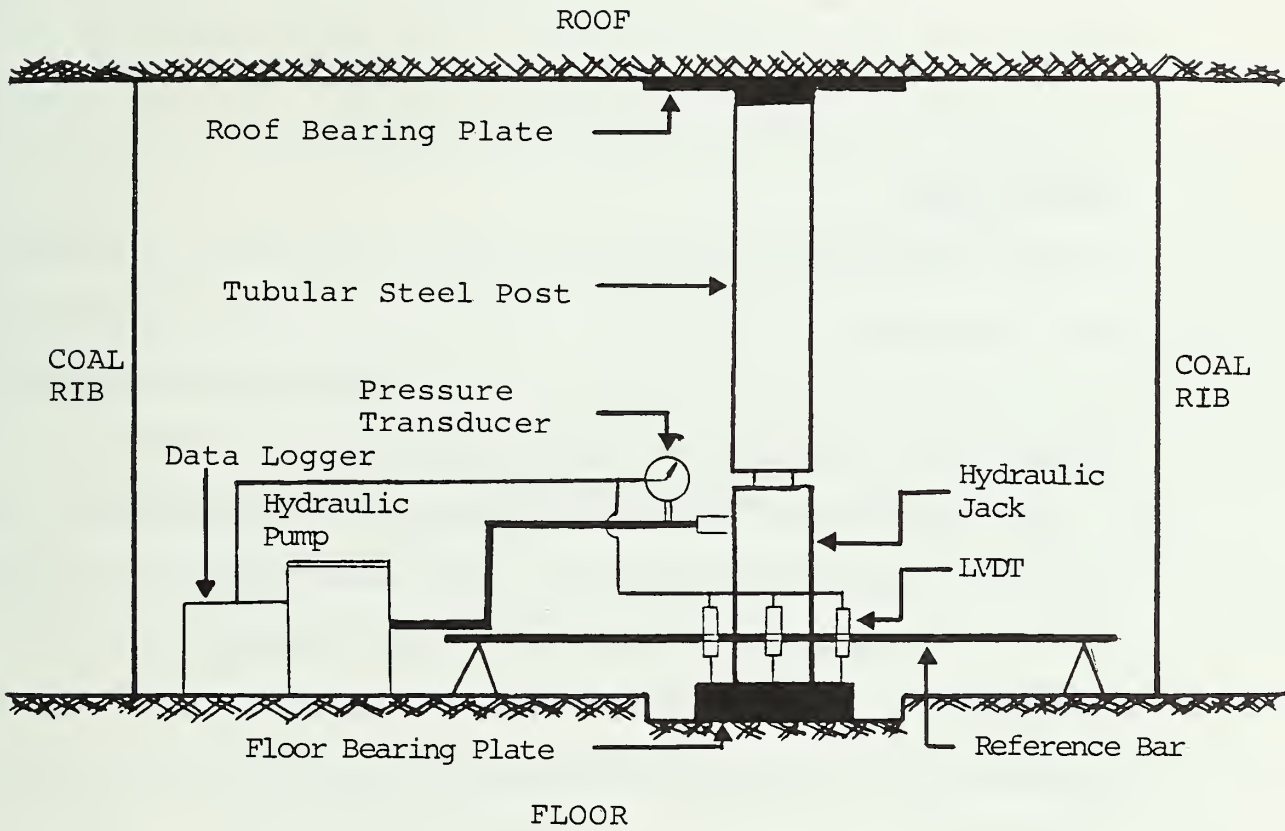
Figure 3.1. Bearing Capacity Measurement Setup.

rates for the pump are: 280 in^3/min at 0 psi, 250 in^3/min at 200 psi,

and 13 in^3/min at 10,000 psi. The system provides some control on the

rate of loading, but it is not precise. The loading rate can be

varied within the range of 200-500 psi/min, but the rate of

deformation is not directly controlled.

Hydraulic pressure applied to a bearing plate is measured with a

pressure transducer manufactured by SCHAEVITZ (Model #P703-0001). The

transducer has a range of 0-10,000 psi, linearity of 0.04%, and

repeatability of 0.01% in the full range output.

Bearing Plates

Rigid square plates of 6 in, 8 in, 12 in, 18 in, and 24 in in size

were fabricated and suitably heat treated for use in the study. A

typical plate is shown in Figure 2.8, and specifications for different

plates used in this study are shown in Table 2.2.

Tubular steel props, 6-8 in in diameter and of various heights, were

utilized to apply load to the bearing plate in the floor and immediate

roof. One or more steel plates, about 24 in in diameter and 1 in in

thickness, were placed between the tubular steel prop and the

immediate roof to distribute the load over a wider area and prevent it

from failing.

Deformation Measurement System

Three LVDTs set 90° apart on the bearing plate are utilized to

measure deformation of the immediate floor under the plate. The LVDTs

are excited by 12.0 V DC and have a maximum displacement range of ±

1.0 in. Output signal conditioning is included in the LVDTs unit

itself. The sensitivity and linearity of the LVDTs are 10.25 V/in and

0.11% of full range output, respectively. The resolution of the overall deformation monitoring system is 100 μin.

The LVDTs are mounted on the bearing plate from an angle-iron reference beam through suitable magnetic bases, as shown in Figure 3.1. The reference beam is designed to be of variable length so that its edges can rest on stable ground unaffected by the ground movements associated with the bearing capacity test.

An analysis was conducted to estimate the amount of error that may occur due to the LVDTs being installed at a slight inclination on the bearing plate rather than being perfectly vertical. The analysis showed that for 10° inclination, the errors would generally be less than 2-3 %.

Data Acquisition System

A Metrosonic microcomputer-based data logger (Model dl-721) with eight channels was utilized to monitor and store load-deformation data from the plate bearing tests. Load from the pressure transducer and deformations from the LVDT were monitored every 5 sec and were recorded in the data logger. In this manner the data collection is improved and the variation in the calculation of ultimate load bearing capacity is significantly reduced.

3.4 Site Preparation and Test Procedures

Ultimate bearing capacity tests were conducted at five (5) sites in each mine. Selection of sites was made in cooperation with mine management based on future mining plans and underclay thickness in different areas. Most of the sites selected had been mined less than 30 days. At each site, tests were conducted under as-mined and soaked-wet conditions. Wet conditions were achieved by soaking the

test site area for a period of 24 hr. Two or three different plate
sizes were utilized for conducting tests at each site and for each
condition. The following paragraphs describe the site preparation and
test procedures utilized.

The test site was selected in an area with a roof capable of bearing
a load of 100 t without developing major cracks or deforming
significantly. The selected test site was at least three to four
plate widths away from the pillar rib or roof support.

The area around the site was cleaned of all gob material and chipped
with a suitable hammer until the actual floor material was exposed.
Cleaning and chipping to a depth of 3-5 in was generally necessary to
achieve this. Chipping was continued until a relatively level surface
was prepared and all visible slickensides in the immediate floor were
removed.

A thin layer of quick setting plaster was spread on this leveled
area and the plate of designated size was placed on it and leveled
with as much accuracy as possible using a carpenter level. After the
plaster had dried and set, the hydraulic jack was centered on the
plate and tightened against the roof with tubular steel props and roof
bearing plates. LVDTs were mounted at 90° angles to each other on the
plate from the reference beam. A pressure transducer was connected in
the hydraulic line to measure the load applied to the plate.

The LVDTs and the pressure transducer were hooked to the data logger
which was programmed to collect and record readings from these
transducers. Initially, about 1000 lb of load was applied to the
plate to set the plate in place and check the data acquisition system.
The load was then removed from the plate. The load was then reapplied

at a uniform loading rate varying from 200-500 psi/min until failure occurred. The failure criterion was defined as the point where the plate could not sustain any further load and/or the rate of deformation increased significantly with a sustained load. The loading was continued beyond the failure point for 10-15 sec to study post-failure strength-deformation characteristics.

3.5 Data Analysis Procedures

Load-deformation-time history data recorded on the data logger in the field were transferred to an IBM-PC microcomputer in the department. The data were then transferred from the PC into the IBM main-frame computer and analyzed to obtain a stress-deformation plot. The ultimate bearing capacity was determined using the Vesic's criterion (1970) of failure. A computer program was written in Fortran IV language to compute slopes of the stress-deformation curve at stress intervals of 5% of the ultimate failure stress. The initial point of minimum steady slope was used to define the point of failure and ultimate bearing capacity, as shown in Figure 2.9.

Deformation moduli of the immediate floor strata were calculated at 50% and 90% of the ultimate bearing capacity (DM_{50}, DM_{90}) by using equation 2.22 and a Poisson's ratio of 0.35. Ultimate bearing capacities and deformation moduli under as-mined and soaked-wet conditions and for different plate sizes were analyzed to determine the effects of wetting and plate size. Linear regression analysis was utilized for conducting correlation studies. The significance of a determined correlation coefficient was based on the number of observations. A confidence level of 90% was used to determine if the correlation between variables was significant or not.

3.6 Borehole Shear Tests

Immediate floor strata cores are generally very difficult to obtain in Illinois basin coal mines because of the weak and friable nature of underclays. Even if they could be obtained, they would be very expensive and difficult to prepare for conducting laboratory tests. Therefore, borehole shear tests were conducted in this study to determine the failure characteristics of immediate floor strata (S_o and ϕ) at different depths under in-situ conditions using a Rock Borehole Shear Tester. Both these parameters are required for calculating the ultimate baring capacity of immediate floor strata for the design of coal pillars.

RBST equipment and procedures have been described elsewhere (Haramy, 1981), and it is not intended to discuss those here. Only the specifications of the RBST used in this study are presented in Table 3.1. A schematic of a RBST in a borehole is shown in Figure 3.2. The procedures described by Haramy were closely followed in conducting these tests. Pressure gages for monitoring normal and shear stresses were calibrated in the laboratory prior to taking equipment into the field.

During this study, borehole shear tests were conducted in 3 in diameter boreholes drilled with a diamond-tipped core barrel. Cores of immediate floor strata obtained during the drilling process were studied for engineering index properties and laboratory strength-deformation properties under unconfined and confined compressive stress. RBST tests were conducted at different depths at intervals of 12-18 in starting from the bottom of the borehole and moving toward the top. At each depth, four (4) shear tests were conducted at

Table 3.1   Specifications of a Rock Borehole Shear Tester

Hole size required	2.125 in
Type of shear plate inserts	Tungsten carbide
Number of inserts	2 per plate
Number of plates	2 (diametrically opposite)
Spacing between the inserts	0.8 in
Depth of the inserts	0.04 in
Shear area per plate	0.7 in^2
Maximum shear stress	6000 psig
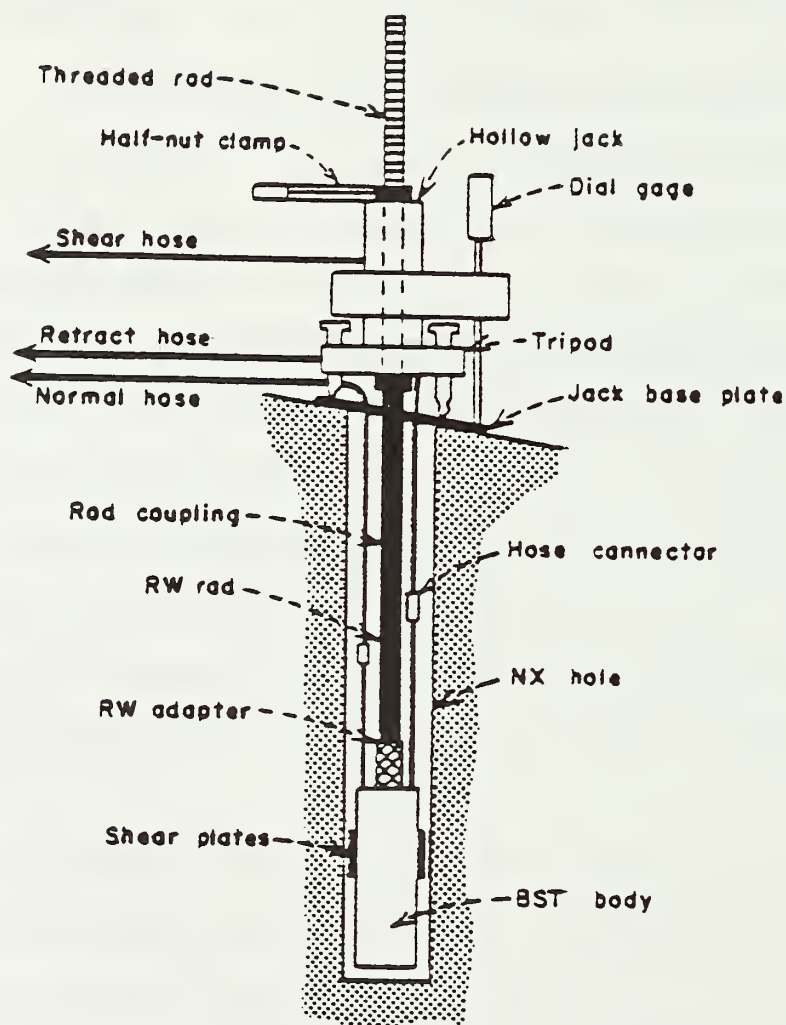
FIGURE 3.2   Schematic of Bore Hole Shear Tester in a Hole.   (Haramy, 1981)

different normal stresses by rotating the shear head of the RBST
through 45°. The normal stresses utilized in the study varied from
200-800 psi, depending upon the nature of the rock encountered; lower
normal stresses were applied in weaker rocks. Wherever possible, the
peak as well as residual values of shear strength were recorded at
each applied normal stress.

Borehole shear tests were also conducted in the immediate roof
strata and coal pillar at one site in each of the two mines. This was
done to determine in-situ strength characteristics of the roof strata
and coal seam.

3.7 Data Analysis

Borehole shear test data were analyzed by plotting peak or residual
shear strength at different normal stresses. Linear regression was
utilized to determine S_0, ϕ, and the equation of the best fit line.
Best fit lines were plotted only if the correlation coefficient was
high enough to represent a 90% confidence level. The values of S_0 and
ϕ for immediate floor strata determined from RBST tests were compared
with those estimated from confined compression tests conducted on
cores in the laboratory.

In a recent study, Chugh (1986) developed the concepts of axial
deformation modulus and lateral strain ratio for a discontinuous rock
mass which correspond to the modulus of elasticity and Poisson's ratio
for an elastic continuum. These concepts are described in Appendix C
and are included here because some laboratory tests were conducted
during the study.

3.8 Moisture Gain Studies

Immediate floor strata in Illinois generally consist of underclays and shale. Strength-deformation characteristics of these rocks significantly change on moisture absorption. Chugh et al. (1981), Bauer (1984), and Aughenbaugh et al. (1976) have conducted studies on moisture gain and changes in strength-deformation characteristics of roof shales from Illinois Basin coal mines. To the best of the author's knowledge, similar studies for immediate floor underclays have not been conducted in the past.

In this study, moisture gain studies were conducted on immediate floor rock cores in the 0-12 in depth range obtained in the vicinity of areas where plate bearing tests were conducted. Four samples of about 25 gm each were oven-dried at 105°C for a period of 24 hr and one sample was placed in each of four humidity chambers maintained at 70%, 80%, 90% and 100% constant relative humidity (R.H.). Samples were weighed to within 0.001 gm at intervals varying from 15 min to 8 hr, and these measurements were made until the samples acheived a constant weight. It normally took about 72 hr to attain equilibrium moisture content at 70% R.H.

Four 10 gallon glass tanks with dimensions of about 20 in x 10 in x 12 in (L_c x W_c x H_c) were used as humidity chambers. These were provided with aluminium lids and were made air tight by using silicone sealant. Each tank was provided with a 3 in diameter Muffin fan suspended from the underside of the aluminium lid with its speed controlled with a variac. The fan was used to circulate air inside the chamber to maintain relatively constant humidity at all points in the chamber.

Saturated salt solutions were utilized for humidities less than 100%. These saturated solutions, when accompanied by an excess of salt in solid phase, can liberate large volumes of water vapor without a significant change in relative humidity. With a careful selection of a salt or a mixture of salts, a relatively constant R.H. can be maintained over a long period of time.

Saturated salt solutions in glass jars were placed in the tanks. Depending upon the number of the samples placed in each humidity chamber, two or three salt solution containers were placed in each tank to minimize fluctuations in R.H. during weight gain measurements. Relative humidities of 70 %, 80 %, and 90 % were obtained using the following salt solutions.

Salt	Relative Humidity
NH_4CL & KNO_3	70%
$(NH_4)_2SO_4$	80%
$NH_4H_2PO_4$	90%

The 100% R.H. was achieved by sprinkling water constantly over a 'wicking' material suspended from the lid of the chamber. Sprinkling was acheived with a small submersible pump placed in the chamber. A small fan was placed directly behind the suspended wicking material so that it circulated air through the water-soaked wick. The author has used this technique previously to study moisture gain in Illinois Basin roof shales.

CHAPTER 4

RESULTS AND DISCUSSION

4.1 Pillar Design in the Illinois Coal Basin - State of the Art

Two types of geological settings are generally observed in Illinois Basin coal mines:

1) Coal seam associated with competent immediate roof and floor strata,

2) Coal seam associated with competent roof strata but underlain by weak floor strata - usually underclays of varying thickness.

Pillar design procedures currently being used are briefly discussed below. A considerable portion of this discussion is based on Chugh and Prasad (1983).

Coal Seam Associated with Competent Roof and Floor Strata

Design procedures for this case have been discussed by Bieniawski (1982) and Chugh et al. (1983), and general guidelines have been recommended. The procedure usually involves determination of the average vertical stress on pillars due to overburden by the tributary area method; determination of pillar strength by one of the several pillar strength formulas such as Holland and Gaddy (1973), Holland (1964), Obert and Duvall/Wang (1975), and Bieniawski/PSU (1981); estimation of the factor of safety; and adjustment of pillar dimensions, if necessary, until an adequate factor of safety (1.2-1.5) consistent with a reasonable percentage of extraction is achieved. The most commonly utilized pillar strength formulas are given below.

Holland-Gaddy Formula (1973):

$$\sigma_p = K_c \frac{(W_p)^{0.5}}{h} \, , \qquad (4.1)$$

where σ_p = in-situ pillar strength, psi

W_p = pillar width, in

h = mined height of the coal seam, in

K_c = a constant characteristic of the seam.

The value of K_c is given by the famous Gaddy formula:

$$\sigma_c = K_c/(d_s)^{0.5}, \qquad (4.2)$$

where σ_c is the unconfined compressive strength of a coal cube of size "d_s".

The formula gives valid results for W_p/h ratios up to eight (8). For $W_p/h > 8$, the formula underestimates pillar strength.

Obert-Duvall/Wang's Formula (1975):

$$\sigma_p = \sigma_{cc}(0.778 + 0.222 \, W_p/h). \qquad (4.3)$$

σ_{cc} represents the strength of the critical size specimen (36 in for U. S. conditions, Hustrulid, 1975) and is determined from the Gaddy formula above. Based on field tests, this equation is considered to be valid for W_p/h ratios from 0.25 - 8.

Bieniawski/PSU Formula (1981):

$$\sigma_p = \sigma_{cc}[(0.64 + 0.36 \, W_p/h)]^{\alpha}. \qquad (4.4)$$

where α is equal to 1.4 for $W_p/h > 5$.

This formula (α=1.0) is valid for W_p/h ratios of up to five. Beyond this value, confinement tends to increase pillar strength very rapidly.

Holland (1964) Formula:

$$\sigma_p = \sigma_{cc} \cdot (W_p/h)^{0.5}. \tag{4.5}$$

These formulas were developed based primarily on data from Appalachian coal fields. Validation of these formulas in Illinois has not been attempted, although pillar designs are based on them.

Using the laboratory strength data for the Herrin (No. 6) coal seam, Chugh et al. (1983) compared the above formulas for width/height ratios larger than one (Figure 4.1) and concluded the following:

1) The Holland-Gaddy and Holland formulas predict a non-linear increase in pillar strength with increasing W_p/h. The Holland-Gaddy formula predicts the lowest pillar strength and becomes more conservative for higher W_p/h ratios. The Holland formula also tends to become conservative for $W_p/h > 13$. The Holland-Gaddy formula was most commonly utilized for pillar design in Illinois Basin mines until about 1980.

2) The Bieniawski/PSU formula for $\alpha = 1.0$ as well as Obert-Duvall/Wang formulas predict a linear increase in pillar strength with increasing W_p/h. The Bieniawski/PSU formula, however, predicts a larger pillar strength than the Obert-Duvall/Wang formula, except for $W_p/h = 1$.
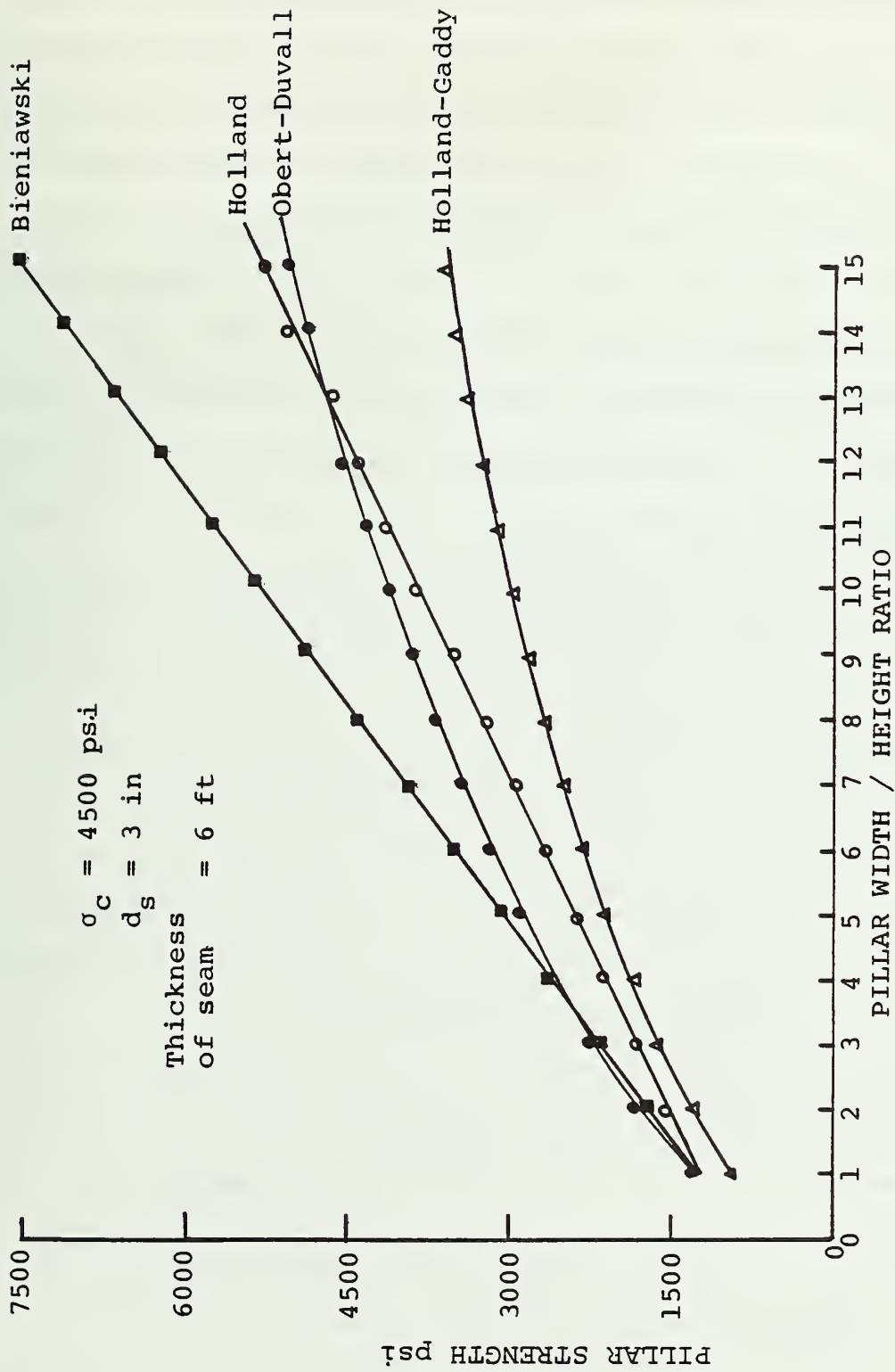
FIGURE 4.1 A comparison of commonly utilized pillar strength formulas.

Recently, Bieniawski (1982) has made a strong case for the use of Bieniawski/PSU formula with $\alpha = 1.0$ for pillar design under U.S. conditions. Since "critical size" may in itself significantly overestimate pillar strength, and since Bieniawski's formula further predicts the highest pillar strength amongst the four formulas presented above, Chugh et al. (1983) recommended the following guidelines for Illinois Basin coal mines until additional field data had been obtained to substantiate the Bieniawski/PSU formula:

1) For $W_p/h < 5$, any of the formulas discussed above may be utilized.

2) For $W_p/h > 5$, use the Obert-Duvall/Wang or Holland formulas. The reasons for these recommendations are:

   o The Obert-Duvall/Wang formula has been shown to hold true in assessing in-situ strength of coal pillars for W_p/h up to 8 in West Virginia.

   o Most of the pillars in the past have been designed on the basis of the Holland-Gaddy Formula, which is very conservative. Mine operators can significantly improve extraction by designing on the basis of the Obert-Duvall/Wang or Holland formulas without undue risk.

Chugh et al. (1983) emphasized that most of the field data on coal pillars was obtained in the Appalachian coal fields. Very little data are available for Illinois Basin coals. They recommended using these formulas in conjunction with a close investigation of the behavior of these pillars under field conditions. Most mine operators in Illinois have used these guidelines for design since 1983.

Wilson's (1981) approach to coal pillar design involving yielding of the outer portions of the pillar have not been extensively used to date in Illinois Basin coal mines because their validity in the area has not been demonstrated. The author thinks that the approach has merit and should be evaluated.

Coal Seam Associated With Competent Roof Strata But Underlain by Weak Floor Strata

In several areas, actively mined coal seams are underlain by weak underclay of varying thickness. For such a case, pillars must be designed on the basis of the load carrying capacity of the floor rather than the coal pillars. Inadequate design may lead to bearing capacity failure of the floor, collapse of the roof, and/or failure of the pillar either in a localized manner or over extensive areas, depending on actual field conditions. Even if pillar collapse does not occur, the problem of floor heave in mine entries may assume serious enough proportions to warrant discontinuation of mining.

Rockaway and Stephenson (1979) and Chugh et al. (1983) have recommended the use of Eq. 2.14 and 2.15 to estimate the UBC of immediate floor strata for Illinois Basin coal mines. Several pillar designs in Illinois are based on these equations. Chugh and Bandopadhay (1982) utilized these formulas to design coal pillars in a western Kentucky mine and developed graphs to predict floor heave in different areas of the mine.

Based on several pillar design studies involving soft floor in Illinois over the last five years, the author has recommended the following to mine operators:

1) Prediction of the bearing capacity of immediate floor strata based on Eq. 2.18 developed by Speck (1981) may lead to a very conservative design, and in some cases may prohibit mining. The primary reason for this is that the equation predicts a linear decrease in strength with increasing natural moisture content. Bauer (1984) and the author have found the decrease to be non-linear.

2) The natural moisture content of the top 8-12 in of immediate floor strata should not be used to predict C_o and UBC for floor strata underneath pillars. The author recommends obtaining the natural moisture content on cores from floor strata at 6 in intervals to a depth involving all soft floor strata and 2-3 ft of competent strata below it. The data obtained can then be utilized to define the thickness of weak floor and its strength under pillars. The depth below the coal seam where the natural moisture content markedly decreases defines the thickness of the weak floor and should be used in Eq. 2.16 for the calculation of the UBC.

3) A safety factor of 1.2 for pillars requiring short-term stability and 1.5 for pillars requiring long-term stability should be used until more experience is gained in field conditions.

4.2 Design Considerations for Pillars Under Weak Floor Conditions

The design should incorporate the assessment of: 1) bearing capacity of floor, 2) pillar settlement, and 3) mode of floor failure.

The UBC of immediate floor strata represents the load carrying capacity of the foundation and is a prerequisite for design of coal

pillars. Theoretical and field determination techniques for the UBC
and their limitations have been discussed in sections 2.2-2.4.

Pillar settlement is a function of the average stress on the pillar
and deformability of immediate floor strata. The nature and extent of
absolute and differential pillar settlements determine the effective
use of a mine opening and the redistribution of stresses in the roof,
pillar, and floor. For example: 1) differential settlement and
stress concentrations at the roof-pillar and pillar-floor interface
may cause tensile and shear stresses in the mine opening and pillar
and result in pillar sloughing, fracture development, or collapse of
the opening; 2) differential settlement of adjacent pillars may
transfer load to adjoining pillars or pillars in an entire section
which may become overloaded; 3) floor heave may occur in openings as
weak floor strata underneath pillars is pushed sideways and upwards
into mine openings.

Total as well as differential settlements of pillars are important.
The latter are more critical because these lead to tensile and
compressive strains. Both are important, however, since a high value
of total settlement typically leads to high differential settlement.
No data are available in the literature on the amount of total or
differential settlement which can be allowed in a particular mining
operation.

Estimation of pillar settlement requires a knowledge of the
different lithologic units in the immediate floor, their lateral
extent and their strength-deformation characteristics. An average
value of the deformation modulus of floor strata in the 0-18 in depth
range below the coal seam may be determined from plate load tests by

using Eq. 2.22. Techniques need to be developed to estimate deformability of floor strata underneath pillars.

Failure of the pillar foundation may occur as punching shear, local shear or general shear (Figure 2.3). Each type will have a different effect on the floor heave and stability of pillars. The mode of failure depends on a number of factors that have not been fully explored so far, even in soils. Relative compressibility of floor strata and the rate of loading may be two important factors. Depth of foundation and/or rate of loading may change the mode of failure from general shear to punching shear. A punching failure mode may also result if a relatively rigid layer is underlain by a compressible layer. All these factors should be considered at a specific location in assessing the likely mode of failure. Some of the other factors to be considered include seam inclination, ground water table, and width of pillar to height ratio.

Design procedures and limiting values of the different variables above must be established based on research if effective design of coal pillars under weak floor conditions is to be achieved. Currently, design is based on the UBC determined from plate load tests which may or may not represent the bearing capacity of immediate floor strata underneath pillars.

4.3 Field Geotechnical Studies

Ultimate Bearing Capacity Tests

A total of 20 tests were conducted at Mine 1; eleven (11)under as-mined conditions and nine (9) under soaked-wet condition. Twenty-three (23) plate load tests were performed in Mine 2; fifteen (15) under as-mined condition and eight (8) under soaked-wet condition.

The UBC, DM_{50}, and DM_{90} data for different plate sizes under as-mined and soaked-wet conditions for Mine 1 are summarized in Tables 4.1 and 4.2. Similar data for Mine 2 are summarized in Tables 4.3 and 4.4. Typical stress-deformation plots from selected sites in two mines are shown in Figures 4.2-4.5; similar plots from other sites are included in Appendix A. Reduction in the UBC, DM_{50}, and DM_{90} values for Mine 1 and Mine 2 due to water wetting are presented in Tables 4.5 and 4.6.

The effect of plate size on the UBC and DM_{50} under as-mined and soaked-wet conditions for Mine 1 and Mine 2 are presented in Tables 4.7 and 4.8 and in Figures 4.6 and 4.7. Linear regression analysis between the UBC and DM_{50} were attempted for the two mines and the results are summarized in Table 4.9 and Figure 4.8 Pertinent observations for each mine are given below.

Mine 1

1) The UBC and DM_{50} appear to be unaffected by plate size under as-mined and soaked-wet conditions. This observation is consistent with results reported by others (Secs.2.2-2.4).

2) Neglecting the effect of plate size, the $\bar{X}$ and σ values for UBC and DM_{50} under as-mined condition are 1000 psi (mean), 177.9 psi (σ) and 2.68 x 10^4 psi (mean), 1.11 x 10^4 psi (σ). Similar values under soaked-wet condition are 670.0 psi, 82.65 psi and 1.58 x

TABLE 4.1 Ultimate bearing capacity and deformation modulus data
for Mine No. 1

As-Mined Condition

Site No.	Plate Size in	Natural Moisture Content (%)	Ultimate Bearing Capacity psi	Axial Deformation Modulus[1] 10^4 psi	
				50% UBC	90% UBC
1	6	2.66	Hyd. Jack Capacity Exceeded	ND	ND
	8		Hyd. Jack Capacity Exceeded	ND	ND
2	6	1.48	Hyd. Jack Capacity Exceeded	ND	ND
3	8	4.48	1,110	2.24	1.54
	12		834	1.74	1.11
4	6	3.02	1,268	4.61	2.86
	8		1,100	2.76	1.88
	12		805	137.47	73.42
5	6	5.83	800	1.51	1.10
	8		1,138	ND	5.74
	12		945	3.07	3.19

[1]From Eq. 2.22
ND: Not determined

TABLE 4.2 Ultimate bearing capacity and deformation modulus data
for Mine No. 1

Soaked-Wet Condition

Site No.	Plate Size in	Natural Moisture Content (%)	Ultimate Bearing Capacity psi	Axial Deformation Modulus[1] 10^4 psi	
				50% UBC	90% UBC
1	6	2.66	Hyd. Jack Capacity Exceeded	ND	ND
	8		Hyd. Jack Capacity Exceeded	ND	ND
2	6	1.48	Hyd. Jack Capacity Exceeded	ND	ND
3	8	4.48	572	0.87	0.56
	12		636	0.63	0.61
4	8	3.02	772	1.15	1.60
	12		634	3.32	2.32
5	8	5.82	772	2.32	2.77
	12		634	1.21	1.04

[1]From Eq. 2.22
ND: Not determined

TABLE 4.3 Ultimate bearing capacity and deformation modulus data
for Mine No. 2

Site No.	Plate Size in	Natural Moisture Content (%)	Ultimate Bearing Capacity psi	Axial Deformation Modulus[1] 10^4 psi	
				50% UBC	90% UBC
1	6		658	0.66	0.47
	8		1,119	1.71	1.04
	8	4.19	1,375	3.65	1.95
	12		1,370	11.25	9.81
	12		1,333	4.94	4.84
2	6	2.25	5,470	27.42	32.41
3	6		1,272	4.16	2.12
	6		2,259	9.00	6.15
	8.75	3.14	1,470	4.03	1.46
	8.75		824	2.87	1.76
4	6		1,880	7.00	5.08
	8	5.78	1,340	5.17	5.01
5	6		853	3.75	3.30
	8	5.34	1,147	2.85	2.76
	12		676	1.54	0.94

[1]From Eq. 2.22

81

TABLE 4.4 Ultimate bearing capacity and deformation modulus data
for Mine No. 2

Soaked-Wet Condition

Site No.	Plate Size in	Natural Moisture Content (%)	Ultimate Bearing Capacity psi	Axial Deformation Modulus[1] 10^4 psi	
				50% UBC	90% UBC
1	8	4.19	676	1.00	0.65
	12		345	0.90	0.70
2	6	2.25	5,000	7.20	7.20
3	6	3.14	617	1.18	0.69
4	8	5.78	406	0.24	0.23
	12		510	0.50	0.44
5	8	5.34	808	1.87	1.76
	12		647	2.17	1.98

[1]From Eq. 2.22
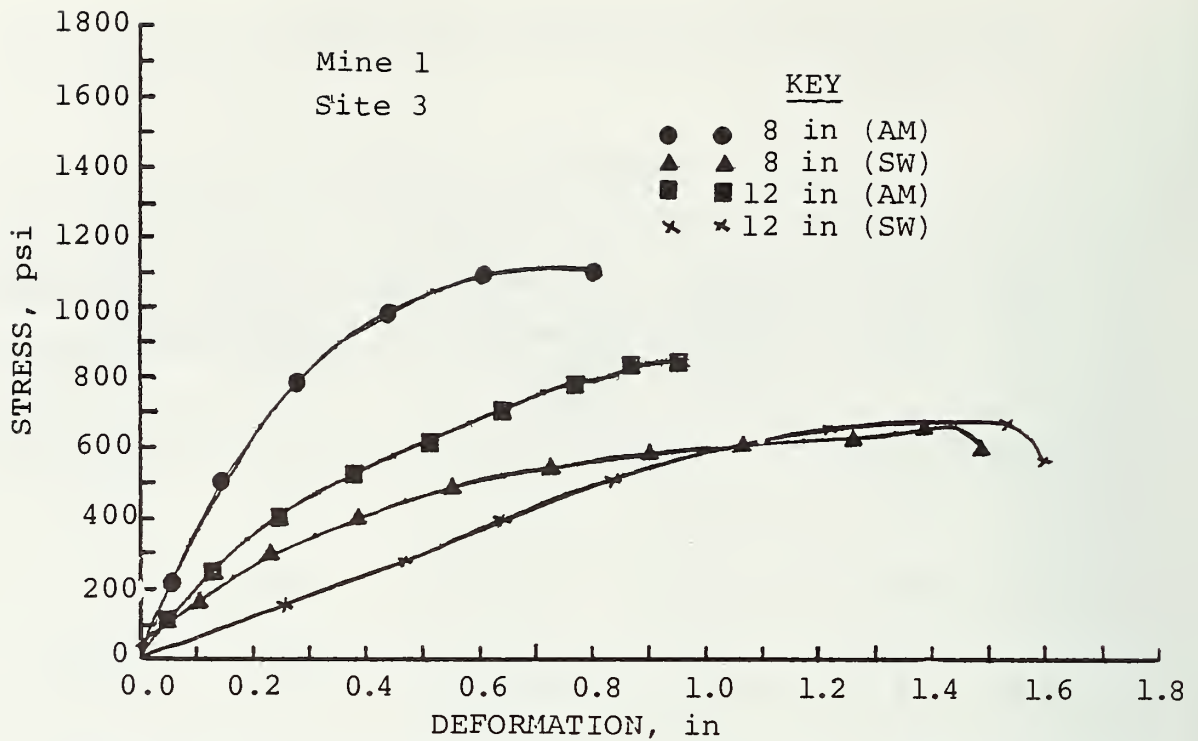
FIGURE 4.2 Stress-deformation curves for immediate floor strata based on plate load tests.
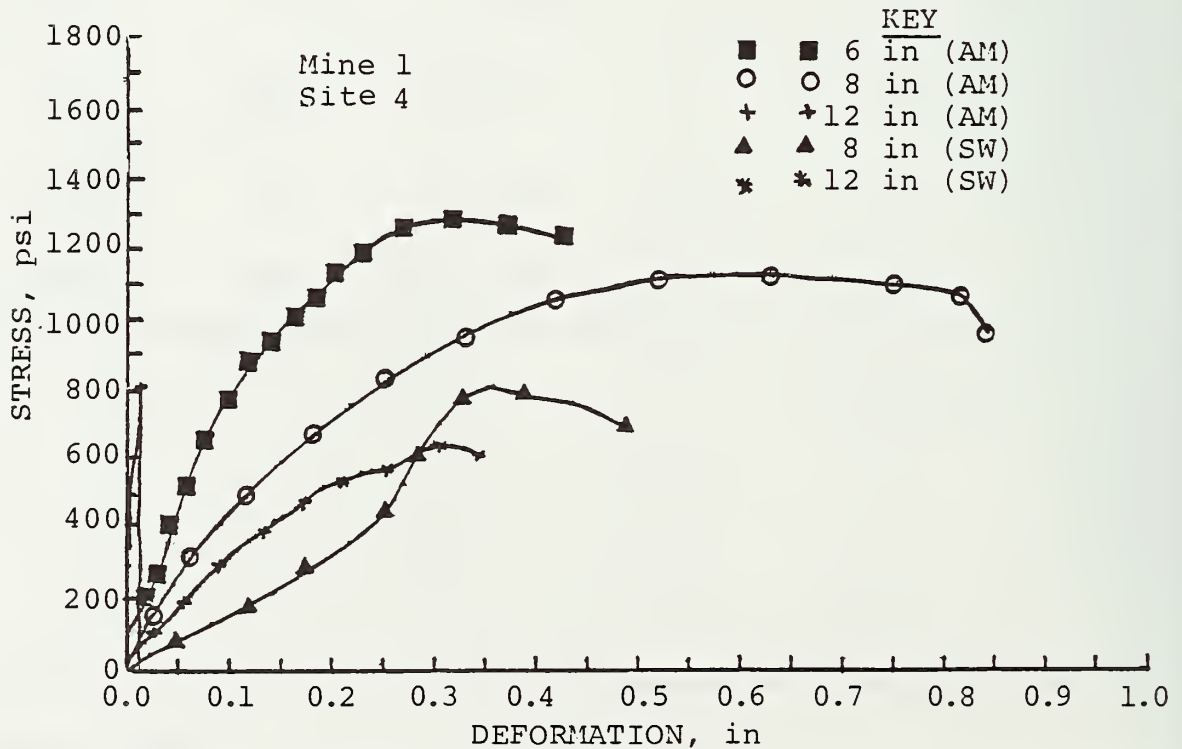
FIGURE 4.3 Stress-deformation curves for immediate floor strata based on plate load tests.
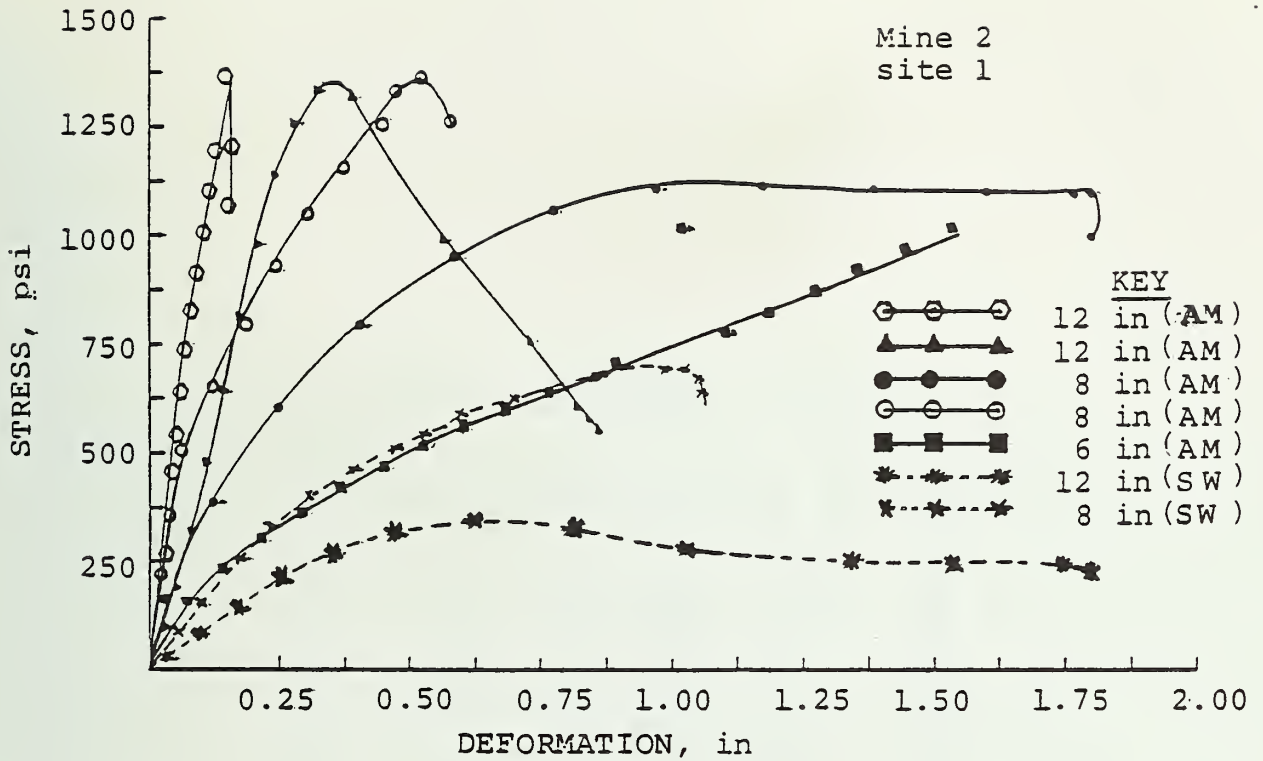
FIGURE 4.4   Stress - deformation curves for immediate
floor strata based on plate load tests.
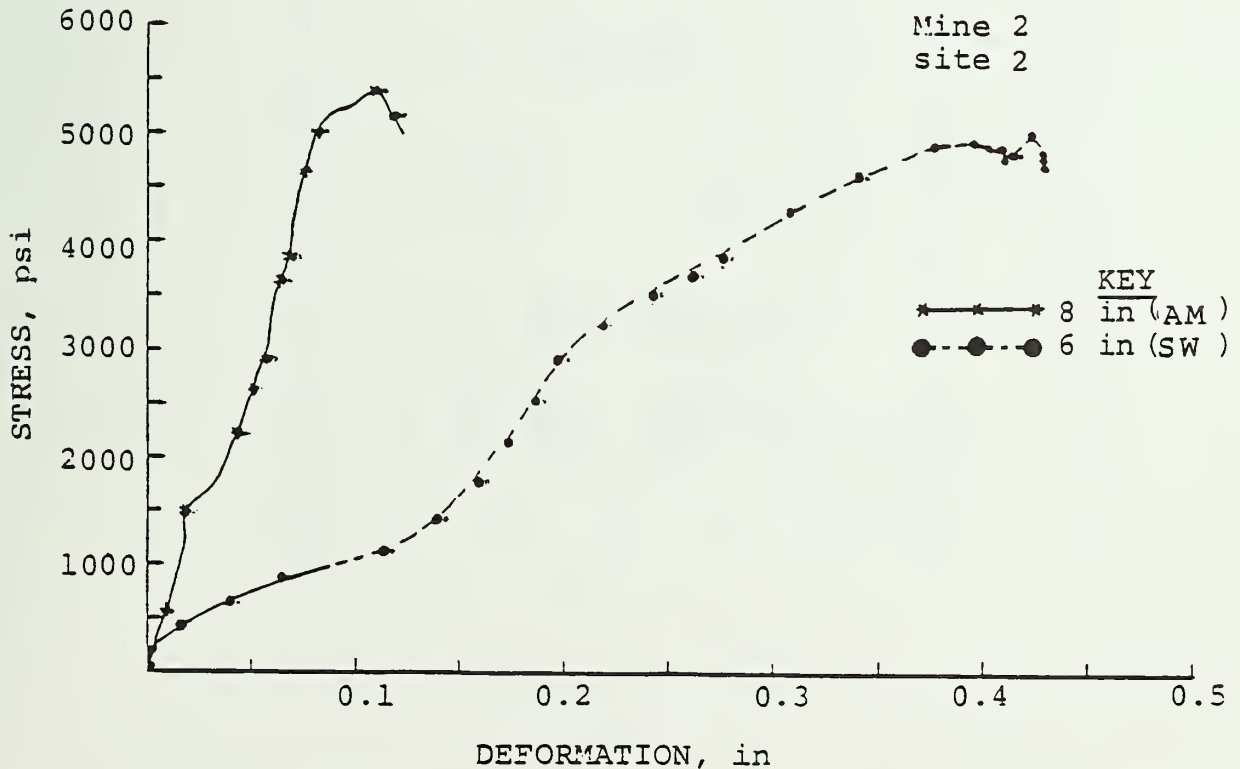
FIGURE 4.5   Stress - deformation curves for immediate
floor strata based on plate load tests.

TABLE 4.5 Effect of Wetting on ultimate bearing capacity and axial deformation moduli[1] for Mine No. 1.

Site No.	Ultimate Bearing Capacity (psi)[1]			Axial Deformation Modulus (10^4 psi)					
				50% UBC			90% UBC		
	As-Mined (AM)	Soaked-Wet (SW)	Ratio SW/AM	As-Mined (AM)	Soaked-Wet (SW)	Ratio SW/AM	As-Mined (AM)	Soaked-Wet (SW)	Ratio SW/AM
3	972	604	0.62	2.09	0.75	0.35	1.32	0.58	0.44
4	1,057	703	0.66	3.68	2.23	0.60	2.37	1.96	0.82
5	961	703	0.73	2.29	1.76	0.77	3.34	1.90	0.56

[1]Mean value based on all plate load tests at a particular site.

TABLE 4.6 Effect of Wetting on ultimate bearing capacity and axial deformation moduli for Mine No. 2.

| Site No. | Ultimate Bearing Capacity (psi)[1] | | | Axial Deformation Modulus (10^4 psi) | | | | | |
| | | | | 50% UBC | | | 90% UBC | | |
	As-Mined (AM)	Soaked-Wet (SW)	Ratio SW/AM	As-Mined (AM)	Soaked-Wet (SW)	Ratio SW/AM	As-Mined (AM)	Soaked-Wet (SW)	Ratio SW/AM
1	1,171	510	0.44	2.74	0.95	0.35	2.07	0.67	0.32
2	5,470	5,000	0.91	27.42	7.20	0.26	32.41	7.20	0.22
3	1,188	617	0.52	3.68	1.18	0.32	1.78	0.69	0.39
4	1,610	458	0.28	6.08	0.37	0.06	5.04	0.33	0.06
5	892	727	0.79	2.71	2.02	0.74	2.33	1.87	0.80

[1]Mean value based on all plate load tests at a particular site.

TABLE 4.7 Effects of plate area on ultimate bearing capacity under as-mined and soaked-wet conditions.

Mine	Linear Regression Parameters					Sample Statistics[1]	
	No. of Tests[2]	Intercept 10^4 psi	Slope psi/in^2	Correlation Coefficient (r)	Test value of r for 90% Confidence	Mean Y 10^4 psi	Standard Deviation σ 10^4 psi
As-Mined							
1	8	1,185.11	-2.130	-0.58	0.62	1,000.0	177.90
2	14	1,221.27	-0.568	-0.07	0.46	1,178.2	350.07
1 and 2 (combined)	22	1,230.24	-1.497	-0.21	0.36	1,110.3	304.09
Soaked-Wet							
1	6	761.90	-0.880	-0.47	0.73	670.0	82.65
2	7	701.53	-1.366	-0.40	0.67	572.7	161.81
1 and 2 (combined)	13	718.45	-1.021	-0.33	0.48	617.6	135.96

[1] Sample statistics are provided where correlation coefficient for linear regression is not significant at 90% confidence level.

[2] Number of tests in this table may not match with numbers in successive tables depending upon the number of outlier data.

TABLE 4.8 Effect of plate area on axial deformation modulus under as-mined and soaked-wet conditions.

Mine	No. of Tests[2]	Linear Regression Parameters				Sample Statistics[1]	
		Intercept 10^4 psi	Slope psi/in^2	Correlation Coefficient (r)	Test value of r for 90% Confidence	Mean Y 10^4 psi	Standard Deviation σ 10^4 psi
As-Mined							
1	6	3.116	-0.005	-0.237	0.73	2.68	1.11
2	12	3.921	-0.005	-0.121	0.48	3.53	1.75
1 and 2 (combined)	18	3.740	-0.006	-0.173	0.39	3.25	1.58
Soaked-Wet							
1	6	1.228	0.003	0.145	0.73	1.58	1.03
2	7	1.022	0.001	0.073	0.67	1.12	0.69
1 and 2 (combined)	13	1.075	0.002	0.135	0.47	1.33	0.86

[1]Sample statistics are provided where correlation coefficient for linear regression is not significant at 90% confidence level.

[2]Number of test in this table may not match with numbers in successive tables depending upon the number of outlier data.
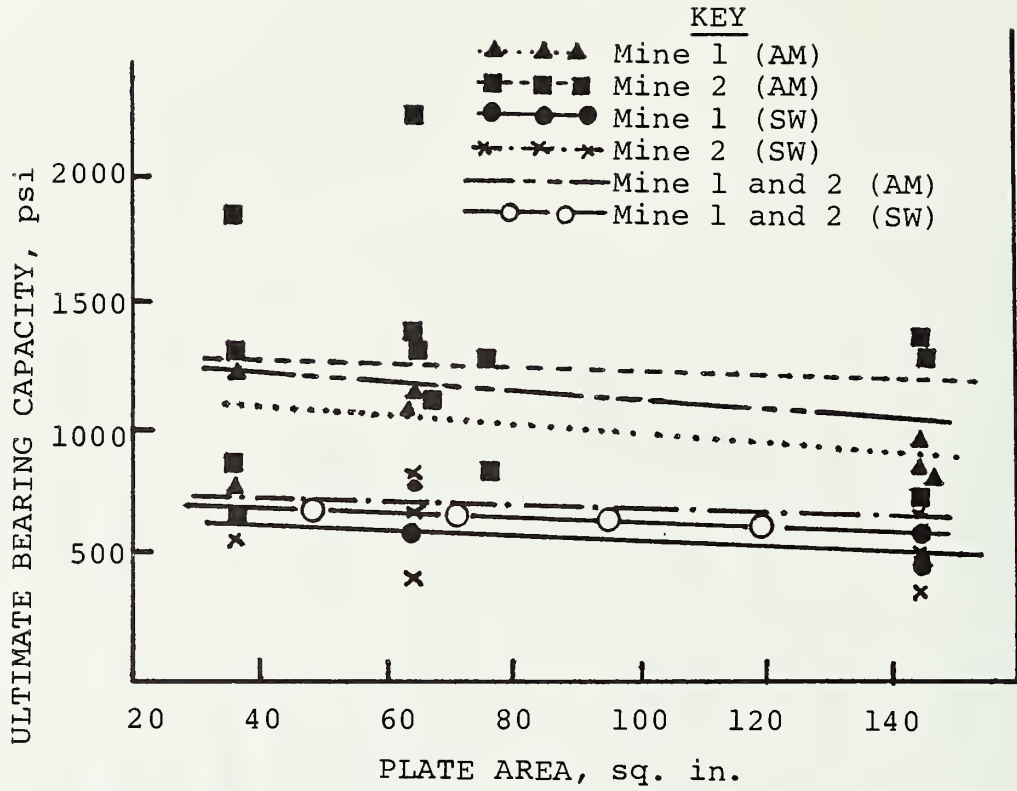
FIGURE 4.6   Effect of plate size on ultimate
bearing capacity.
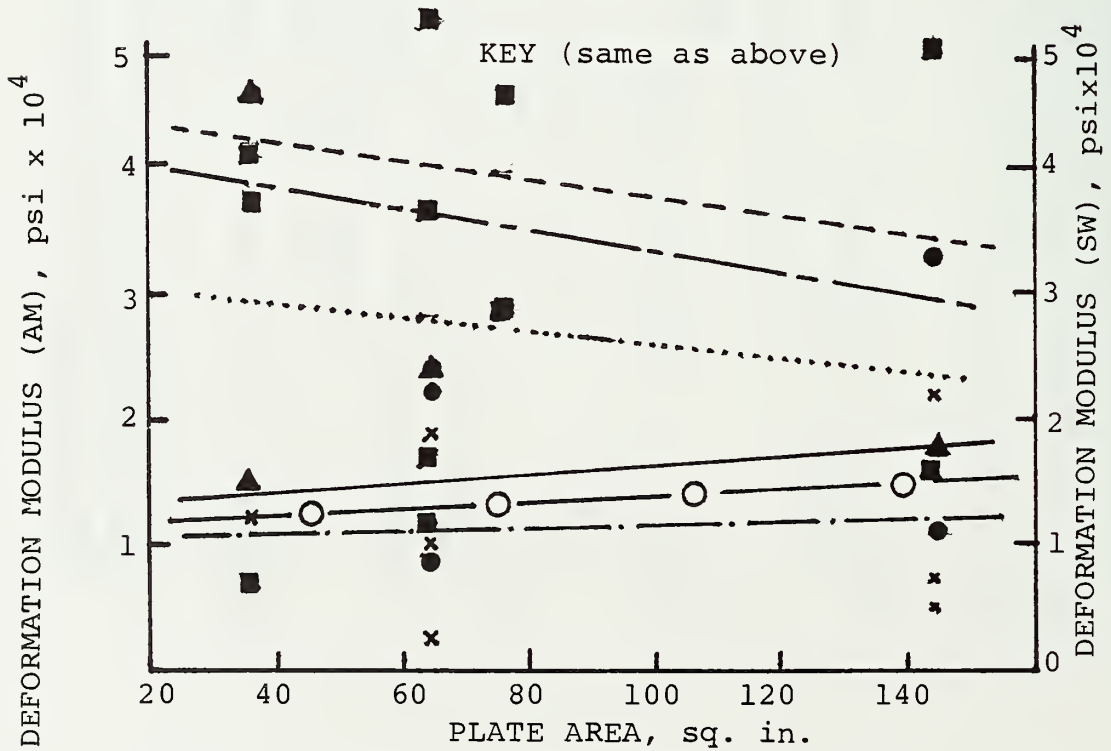
FIGURE 4.7   Effect of plate size on axial
deformation modulus.

TABLE 4.9 Corelation results for variation of UBC with DM_{50}.

Mine	Linear Regression Parameters					Sample Statistics[1]	
	No. of Tests[2]	Intercept 10^4 psi	Slope	Correlation Coefficient (r)	Test value of r for 90% Confidence	Mean Y 10^4 psi	Standard Deviation σ 10^4 psi
As-Mined							
1	6	633.16	139.98	0.86	0.73	1,009.50	181.08
2	12	545.96	175.27	0.85	0.48	1,162.25	360.65
1 and 2 (combined)	18	557.20	170.60	0.86	0.39	1,111.33	315.21
Soaked-Wet							
1	6	644.25	15.87	0.19	0.73	670.00	82.65
2	7	386.06	166.23	0.71	0.67	572.71	161.81
1 and 2 (combined)	13	510.93	79.82	0.50	0.48	617.61	135.96

[1]Sample statistics are provided where correlation coefficient for linear regression is not significant at 90% confidence level.

[2]Number of tests in this table may not match with numbers in successive tables depending upon the number of outlier data.

FIGURE 4.8 Correlation of deformation modulus with ultimate bearing capacity.
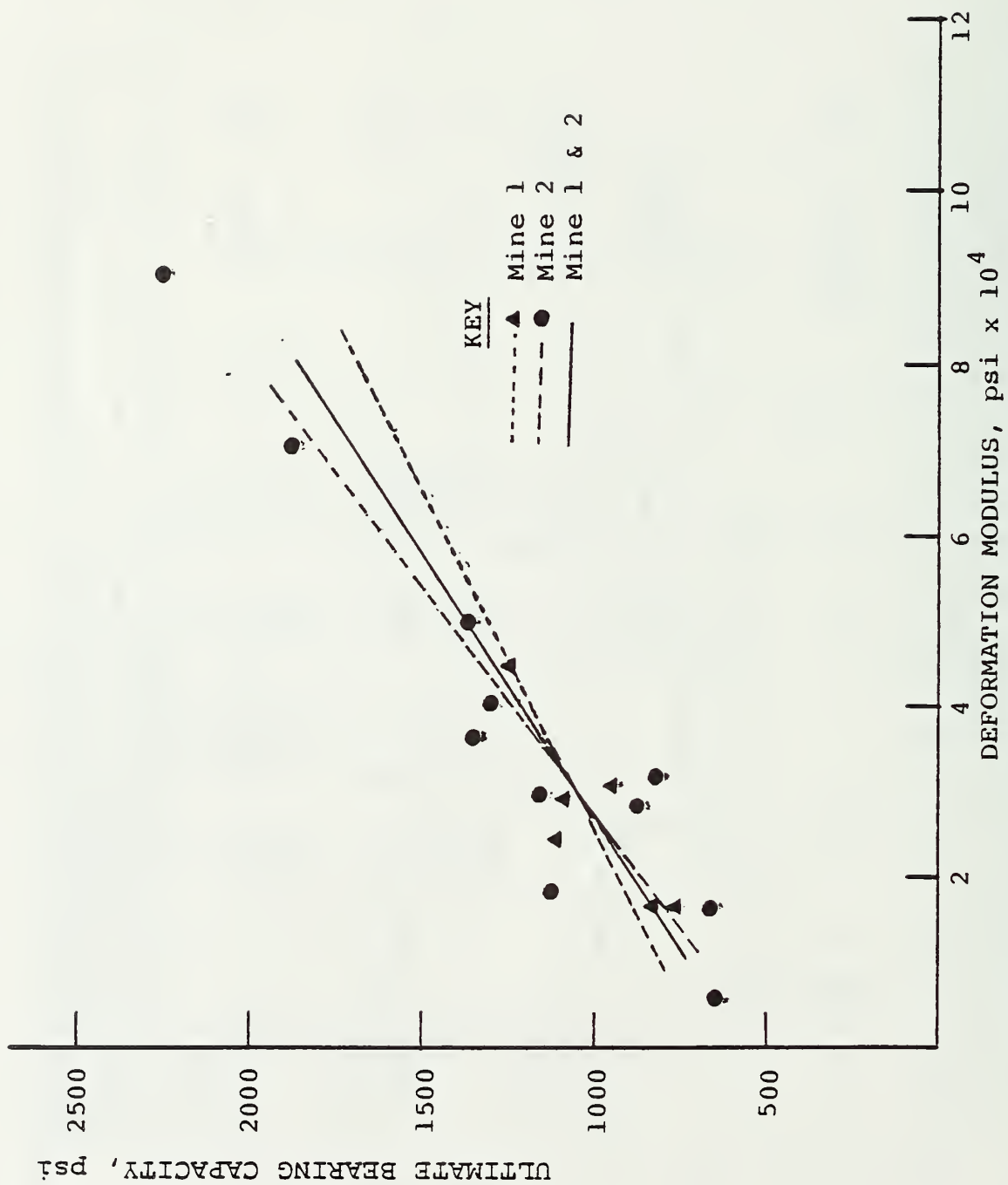
10^4 and 1.03×10^4 psi. Wetting reduces the DM_{50} by about 40% and the UBC by about 30%.

3) Stress-deformation plots under as-mined and soaked-wet conditions show two typical behaviors.

    (i) Significant load drop at initial failure and negative slope in the post-failure region (Figure 4.3). Slopes of the curves until initial failure were relatively constant. This behavior was mostly observed under as-mined conditions and where the UBC was larger than 1000 psi. This is considered to represent general shear type of failure (Figure 2.3),

    (ii) Slope of stress-deformation plot is non-linear until a constant minimum or zero slope is attained (Figure 4.2). This was generally observed under the soaked-wet condition and where the UBC was generally less than 1000 psi. Deformation moduli for these cases were significantly lower than observed under (i) above. This is considered to represent local shear and/or punching type of failure (Vesic, 1963; Figure 2.3).

4) Assuming $\phi = 0$, $q = 0$, the $\bar{X}$ and σ values for S_o under as-mined condition are 162.1 psi and 28.8 psi. Similar values under soaked-wet condition are 108.6 psi and 13.4 psi.

5) Average natural moisture content for immediate floor strata in the 0-12 in depth range below the coal seam under as-mined condition is 4.44 %.

6) There is no evidence of inelastic deformations occurring in immediate floor strata due to excavation of mine openings or due to the excavation being open for a period of time before bearing capacity tests areconducted. This observation is based on the fact that slopes of the stress-deformation plot above and below the premining vertical stress are very similar.

7) There appears to be a significant correlation ($r = 0.87$) between the UBC and the DM_{50} (Table 4.9), considering a 90% confidence level. The equation of the significant line is given by:

$$UBC = 633.2 + 139.5 \; DM_{50}, \hspace{3cm} (4.6)$$

8) The DM_{90} is generally lower than the DM_{50}, but there is much larger variability in the DM_{90} values than for the DM_{50} values (Table 4.1).

Mine 2

1) Although the UBC and DM_{50} values under as mined and soaked-wet conditions appear to decrease somewhat with increasing plate area, the effect is not statistically significant for a 90% confidence level (Table 4.7).

2) Assuming the UBC and DM_{50} values to be independent of the plate area, $\bar{X}$ and σ values for UBC and DM_{50} under as-mined conditions are 1255.4 psi (mean), 443.3 psi (σ) and 3.53×10^{4} psi (mean), 1.75×10^{4} psi (σ). Similar values under soaked-wet condition are 572.7 psi, 161.8 psi and 1.12×10^{4} psi, 0.69×10^{4} psi.

3) Stress-deformation plots, under as-mined and soaked-wet conditions, show behavior similar to that observed at Mine 1.

4) Average natural moisture content for immediate floor strata in the 0-12 in depth range below the coal seam under as-mined condition is 4.14%.

5) As in the case of Mine 1, there is no evidence of inelastic deformations having occurred due to excavation of the mine opening at the sites where plate load tests are conducted.

6) Linear regression between the UBC and DM_{50} variables (Table 4.8) show significant correlation (r = 0.92) under as-mined condition. The relationship may be described as:

$$UBC = 545.9 + 175.3 \ DM_{50} \qquad (4.7)$$

7) The observation on comparison of DM_{50} and DM_{90} values for Mine 1 is valid for this mine also. Since UBC and DM_{50} values for Mine 1 and Mine 2 are similar, the plate load test data for the two mines were combined and analyzed as above. As for each mine, the combined data also show UBC and DM_{50} to be unaffected by plate area and a significant correlation (r = 0.91) between the UBC and DM_{50}. The equation of the significant line is given by:

$$UBC = 557.2 + 170.6 \ DM_{50} \qquad (4.8)$$

Borehole Shear Tests

Immidiate Floor Strata: At Mine 1, RBST data could be obtained at only four (4) of the five (5) sites and only peak strength data were obtained. At site 1, water was encountered in the hole and it caved in soon after drilling. Immediate floor strata at site

2 was generally fractured and gave large variability in data. For Mine 2, peak as well as residual strength data were obtained for five (5) sites. A linear failure envelope based on mean values of S_o and ϕ has been determined for each site. In addition, failure envelopes have been determined for each site for immediate floor strata (0-34 in below the coal seam) and lower strata (34 in or more below the coal seam), where these are meaningful. Pertinent observations from the data for the two mines are presented below.

Mine 1

Normal stress-shear stress data and peak shear strength parameters (S_o and ϕ) at different depths from the four sites are presented in Tables 4.10 and 4.11. Typical failure envelopes from two sites are shown in Figures 4.9 and 4.10; additional similar plots are included in Appendix B.

1) The S_o values vary considerably and are generally less than 500 psi except at site 5 below a depth of 48 in where the values are larger than 800 psi (Table 4.11). Core descriptions indicate increased density of limestone nodules in this zone. $\bar{\bar{X}}$ and σ values for S_o based on all available data are 306.4 psi and 273.7 psi. S_o values generally appear to correlate well with the type of rock, and they do not seem to increase generally with depth.

TABLE 4.10 Normal stress-shear stress data for different
sites for Mine 1.

Depth Below Coal Seam in	Lithologic Description	Normal Stress psi	Shear Strength	
			Peak psi	Residual
Site 2				
20	Limestone with slickensides	235.5	430.28	N.D
		624.9	771.89	N.D
		1,014.3	1,455.10	N.D
32	Shale	235.5	468.10	N.D
		624.9	638.90	N.D
		1,014.3	468.10	N.D
44	Shale	235.5	581.90	N.D
		624.9	923.60	N.D
		1,014.3	1,113.40	N.D
54	Shale	235.5	544.00	N.D
		624.9	733.80	N.D
		1,014.3	961.60	N.D
Site 3				
60	Shale	235.5	619.90	N.D
		624.9	923.60	N.D
		1,014.3	1,398.10	N.D
		1,403.7	1,493.00	N.D
Site 4				
12		235.5	240.40	N.D
		624.9	619.90	N.D
		1,014.3	1,398.10	N.D
22	Dark Grey Shale Crumbled	235.5	259.30	N.D
		624.9	695.90	N.D
		1,014.3	1,189.40	N.D
34	Sandy Shale	235.5	202.40	N.D
		624.9	619.90	N.D
		1,014.3	942.60	N.D
50	Sandy Shale	235.5	354.20	N.D
		624.9	1,113.40	N.D
		1,014.3	1,417.10	N.D

N.D - Not Determined

TABLE 4.10 (cont.)

Depth Below Coal Seam in	Lithologic Description	Normal Stress psi	Shear Strength	
			Peak psi	Residual

Site 4

62	Sandy Shale	235.5	354.20	N.D
		624.9	885.70	N.D
		1,014.3	1,341.20	N.D

Site 5

24	Underclay	235.5	164.40	N.D
		624.9	240.40	N.D
		1,014.3	392.20	N.D
36	Grey Shale with Limestone Nodules	235.5	430.20	N.D
		624.9	1,037.50	N.D
		1,014.3	1,075.50	N.D
		1,403.7	1,151.40	N.D
48	Grey Shale with Limestone Nodules	624.9	1,189.40	N.D
		1,014.3	1,398.10	N.D
		1,403.7	1,606.90	N.D

N.D - Not Determined

TABLE 4.11 Summary of peak strength characteristics of immediate floor strata based on borehole shear tests for Mine 1.

Depth Below Coal Seam in	Lithology	Natural Moisture Content %	Cohesive Strength S_o psi	Angle of Internal Friction φ deg	Corr. Coeff. r	Test value[1] of Corr. Coeff.
Site 2						
20	Limestone with slickensides	0.93	63.3	52.8	0.98	0.98
32	Shale	3.68	525.1	0.0	0.00	0.98
44	Shale	2.81	446.6	34.3	0.99	0.98
54	Shale	2.88	411.4	28.2	1.00	0.98
Site 3						
60		ND	457.5	38.5	0.97	0.90
Site 4						
22	Dark Grey Shale	2.18	ND	ND	ND	ND
34	Sandy Shale	1.60	ND	ND	ND	ND
50	Sandy Shale	2.04	108.7	53.8	0.97	0.98
62	Sandy Shale	2.11	68.4	51.7	1.00	0.98
Site 5						
24	Underclay	2.88	82.9	16.3	0.98	0.98
36	Grey Shale with Lime	1.89	460.2	29.5	0.86	0.98
48	Grey Shale with Lime	1.99	854.3	28.2	1.00	0.98

[1]Test Value for Corr. Coeff. for 90% significance. (Ref. sec 3.7)
ND - Not determined.
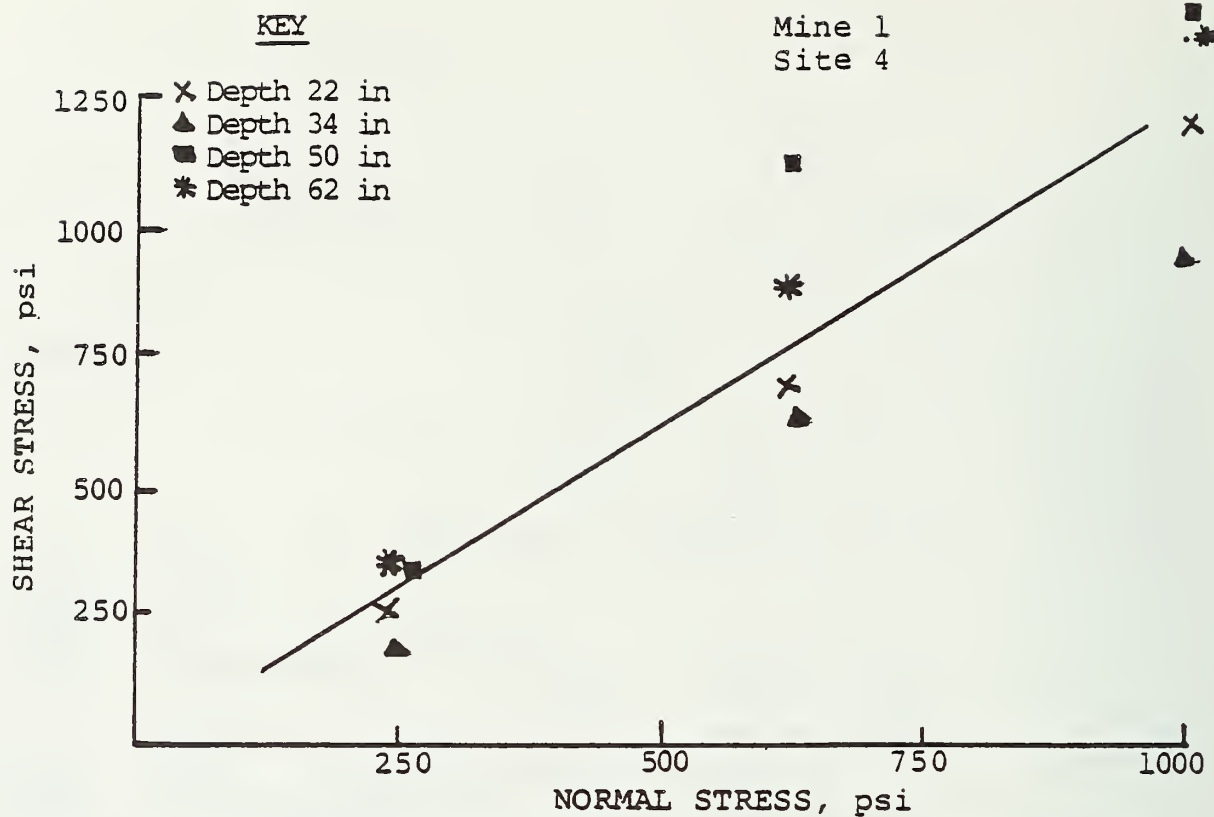
FIGURE 4.9 Shear strength - normal stress relationships
for immediate floor strata.
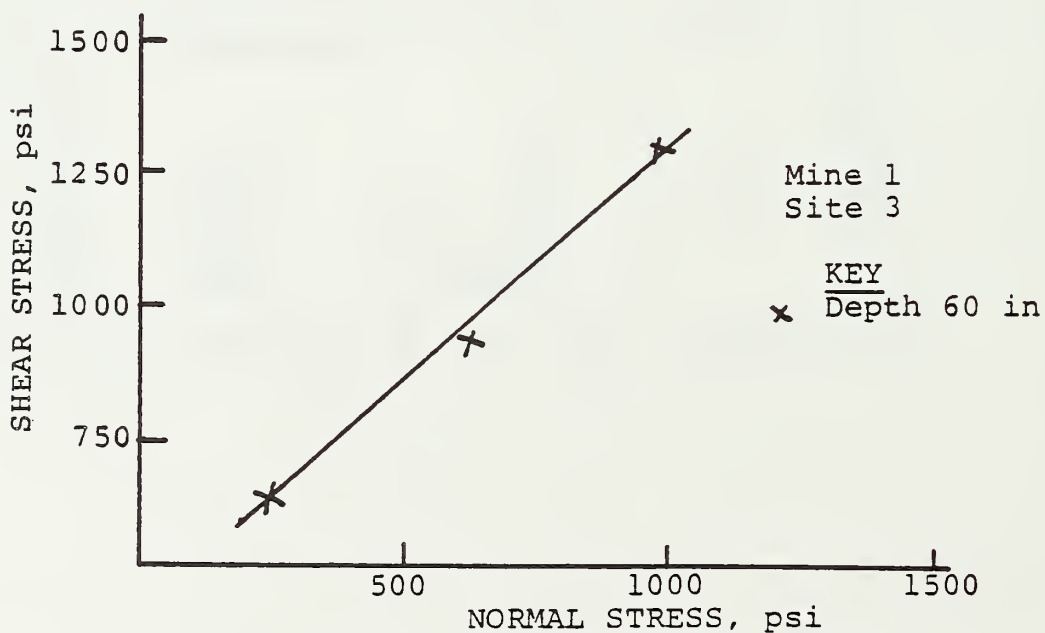
FIGURE 4.10. Shear strength - normal stress relationships
for immediate floor strata.

2) The angle of internal friction (ϕ) ranges from 0-56.1; $\bar{X}$ and σ values for this parameter are 37.1° and 16.7°. Angle ϕ values do not seem to vary significantly with depth at a particular site.

3) A linear failure envelope appears to be a good representation of immediate floor strata behavior at different depths based on observed correlation coefficients of 0.80 to 1.00 in all cases except one.

4) An analysis of the depths of tests with lithologic logs indicates that all tests at sites 2, 3, and 5 are conducted in different lithologies. Therefore, S_o and ϕ values for a particular depth presented in Table 4.11 represent properties of that lithologic unit. At site 4, all tests were conducted in one lithologic unit. Therfore, normal stress-shear stress data at different depths were combined and the failure envelope in Figure 4.9 represents average properties of that lithologic unit.

Mine 2

Data on peak and residual shear strength parameters are presented in Tables 4.12-4.14. Typical failure envelopes from two sites are shown in Figures 4.11 and 4.12; other similar plots are included in Appendix B.

1) S_o values based on peak shear strength range from 0-517.2 psi; $\bar{X}$ and σ values for the data are 279.4 psi and 116.6 psi. Angle ϕ values range between 17.8°-60.3°; $\bar{X}$ and σ values for this parameter are 41.4° and 12.2°. S_o values appear to depend upon the nature of rock and do not necesszarily increase with depth.

100

TABLE 4.12 Normal stress-shear stress data for different sites
for Mine 2

Depth Below Coal Seam in	Lithologic Description	Normal Stress psi	Shear Strength	
			Peak psi	Residual psi
Site 1				
13	Dark Underclay Relatively hard	235.5 624.9 1,014.3 1,403.7	430.2 506.1 999.6 1,189.4	335.1 278.3 847.7 999.6
23	Sandy Shale/ Sandstone	235.5 624.9 1,014.3 1,403.7	354.2 581.9 581.9 771.8	202.4 430.2 468.1 619.9
33	Sandy Shale/ Sandstone	235.5 624.9 1,014.3 1,403.7	354.2 771.8 1,530.9 1,341.2	202.4 619.9 1,303.2 1,151.4
49	Sandy Shale/ Sandstone	235.5 624.9 1,014.3 1,403.7	581.9 809.8 1,530.9 1,834.7	430.2 657.9 1,379.2 1,720.8
61	Sandy Shale/ Sandstone	235.5 624.9 1,014.3	554.0 999.6 1,341.2	430.2 847.7 1,189.4
Site 2				
18	Medium Grey Sandy Shale	235.5 624.9 1,014.3 1,403.7	430.2 885.7 999.6 1,758.8	278.3 733.8 619.9 1,568.9
30	Medium Grey Shale with Limestone Nodules	235.5 624.9 1,014.3 1,403.7	619.9 961.6 999.6 1,341.2	468.1 619.9 695.9 961.6

TABLE 4.12 (Cont.)

Depth Below Coal Seam in	Lithologic Description	Normal Stress psi	Shear Strength	
			Peak psi	Residual
Site 2				
47	Silty Medium Grey Shale	235.5	430.2	316.3
		624.9	923.6	771.8
		1014.3	999.6	847.7
		1403.7	1189.4	999.6
55	Silty Medium Grey Shale	235.5	430.2	278.3
		624.9	923.6	733.8
		1014.3	999.6	847.7
		1403.7	1379.2	1208.3
67	Silty Medium Grey Shale	235.5	392.2	259.3
		624.9	961.6	771.8
		1014.3	1530.9	1303.2
		1403.7	1379.2	999.6
Site 3				
14	Dark Underclay	235.5	430.2	278.3
		624.9	847.7	620.0
		1014.3	999.6	809.8
		1403.7	1075.5	923.6
21	Light Grey Shale	235.5	468.1	316.3
		624.9	468.1	316.3
		1014.3	733.8	582.0
		1403.7	999.6	620.0
31	Grey Sandy Shale	235.5	392.2	278.3
		624.9	961.6	809.8
		1014.3	1341.2	1151.4
		1403.7	1569.0	1379.2
45	Grey Sandy Shale	235.5	506.1	278.3
		624.9	961.6	771.8
		1014.3	_7.3	999.6
		1403.7	1948.6	1569.0

TABLE 4.12 (Cont.)

Depth Below Coal Seam in	Lithologic Description	Normal Stress psi	Shear Strength	
			Peak psi	Residual
Site 3				
56	Grey Sandy Shale	235.5	430.2	297.3
		624.9	999.6	885.7
		1014.3	999.6	695.9
		1403.7	1948.6	1758.6
68	Grey Sandy Shale	235.5	620.0	449.1
		624.9	999.6	847.7
		1014.3	1227.3	1037.5
		1403.7	1493.0	1265.3
Site 4				
8.5	Underclay Slickensided	235.5	525.1	430.2
		624.9	762.3	667.4
		1014.3	952.1	857.2
		1403.7	1284.3	1141.9
19	Underclay Slickensided	235.5	525.1	430.2
		624.9	999.6	857.2
		1014.3	1948.6	1758.8
		1403.7	2233.3	1758.8
31	Limey Shale	235.5	572.5	477.6
		624.9	1094.5	999.6
		1014.3	1948.6	1758.8
		1403.7	2565.4	2328.2
44	Grey Shale Changing to Black Shale with depth, grain size increases with depth.	235.5	430.2	430.2
		624.9	1948.6	1711.3
		1014.3	952.1	809.8
		1403.7	1474.1	1379.2
55	Grey Shale Changing to Black Shale with depth, grain size increases with depth	235.5	525.1	430.2
		624.9	1331.7	1094.6
		1014.3	1948.6	1569.0
		1403.7	1948.6	1569.0

TABLE 4.12 (Cont.)

Depth Below Coal Seam in	Lithologic Description	Normal Stress psi	Shear Strength	
			Peak psi	Residual
Site 4				
67	Grey Shale Changing to Black Shale with depth, grain size increases with depth	235.5 624.9 1014.3 1403.7	287.8 999.6 1569.0 2233.3	192.9 857.2 1379.2 1948.6
82	Grey Shale, Competent and Limey	235.5 624.9 1014.3 1403.7	335.3 857.2 1047.0 1569.0	192.9 714.9 809.8 1284.3
92	Grey Shale, Competent and Limey	235.5 624.9 1014.3 1403.7	809.8 1474.1 1853.7 2897.6	620.0 1379.2 1663.9 2707.8
Site 5				
12	Underclay Massive, Limey	235.5 624.9 1014.3 1403.7	544.0 771.8 847.7 999.6	335.3 657.9 582.0 809.8
18	Underclay Massive, Limey	235.5 624.9 1014.3 1403.7	354.2 468.1 1075.5 809.8	297.3 240.4 999.6 695.9
29	Underclay Massive	235.5 624.9 1014.3 1403.7	354.2 430.2 657.9 961.6	240.4 297.3 544.0 809.8
43	Limey Shale	235.5 624.9 1014.3 1403.7	430.2 923.6 1682.8 1569.0	316.3 752.8 1455.1 1436.1

TABLE 4.12 (Cont.)

Depth Below Coal Seam in	Lithologic Description	Normal Stress psi	Shear Strength	
			Peak psi	Residual psi
Site 5				
53	Limey Shale	235.5	468.1	373.2
		624.9	1075.5	961.6
		1014.3	1720.8	1531.0
		1403.7	2100.4	1948.6
64	Limey Shale	235.5	582.0	430.2
		624.9	809.8	695.9
		1014.3	999.6	847.7
		1403.7	1493.0	1379.2

TABLE 4.13 Summary of peak strength characteristics of immediate floor strata based on borehole shear tests for Mine 2.

Depth Below Coal Seam in	Lithology	Natural Moisture Content %	Cohesive Strength S_o psi	Angle of Internal Friction ϕ deg	Corr. Coeff. r	Test Value of Corr. Coeff. [1]
Site 1						
13	Dark underclay relatively hard	4.50	198.0	35.4	0.96	0.90
23	Sandy Shale/ Sandstone	1.78	308.8	17.8	0.95	0.90
33	Sandy Shale/ Sandstone	1.25	216.5	43.7	0.89	0.90
49	Sandy Shale/ Sandstone	1.41	246.5	49.0	0.98	0.90
61	Sandy Shale/ Sandstone	1.34	321.9	45.7	1.00	0.98
Site 2						
18	Medium Gray Shale (Sandy)	4.26	155.6	46.5	0.96	0.90
30	Medium Grey Shale with limestone nodules	1.58	517.2	29.5	0.96	0.90
47	Silty Medium Grey Shale	1.98	390.3	31.1	0.94	0.90
55	Silty Medium Grey Shale	2.12	317.9	36.9	0.97	0.90
67	Silty Medium Grey Shale	1.00	322.9	42.2	0.89	0.90

[1] Test Value for Corr. Coeff. for 90% significance. (Ref. sec 3.7)

TABLE 4.13 (cont.)

Depth Below Coal Seam in	Lithology	Natural Moisture Content %	Cohesive Strength S_o psi	Angle of Internal Friction ϕ deg	Corr. Coeff. r	Test Value of Corr. Coeff.[1]
Site 3						
14	Dark Underclay	3.08	398.8	28.2	0.94	0.90
21	Light Grey Shale	2.30	275.9	25.5	0.94	0.90
31	Grey Sandy Shale	0.99	243.0	42.8	0.98	0.90
45	Grey Sandy Shale	1.80	194.1	49.7	0.98	0.90
56	Grey Sandy Shale	1.14	135.7	49.5	0.93	0.90
68	Grey Sandy Shale	1.27	485.7	36.2	0.99	0.90
Site 4						
8.5	Underclay Slickensided	5.56	361.6	32.4	0.99	0.90
19	Underclay Slickensided	1.01	148.2	57.3	0.98	0.90
31	Limey Shale	1.53	107.0	60.3	1.00	0.90
44	Grey Shale changing to Black Shale	2.48	132.6	52.5	1.00	0.90
55	Grey Shale changing to Black Shale	1.56	409.8	51.5	0.94	0.90
67	Grey Shale changing to Black Shale	2.16	-75.9	58.7	1.00	0.90

[1]Test Value for Corr. Coeff. for 90% significance. (Ref. sec 3.7)

TABLE 4.13 (cont.)

Depth Below Coal Seam in	Lithology	Natural Moisture Content %	Cohesive Strength S_o psi	Angle of Internal Friction ϕ deg	Corr. Coeff. r	Test Value of Corr. Coeff. [1]
Site 4						
82	Grey Shale Competent and Limey	2.61	133.1	45.0	0.99	0.90
92	Grey Shale Competent and Limey	1.53	360.5	59.6	0.98	0.90
Site 5						
12	Underclay, Massive Limey	5.92	487.2	20.3	0.98	0.90
18	Underclay, Massive Limey	5.63	261.4	26.9	0.78	0.90
19	Underclay, Massive Limey	6.36	169.5	27.8	0.97	0.90
43	Limey Shale	0.57	272.5	47.0	0.92	0.90
53	Limey Shale	0.94	174.7	54.9	0.99	0.90
64	Limey Shale	1.13	355.9	36.9	0.97	0.90

[1]Test Value for Corr. Coeff. for 90% significance. (Ref. sec 3.7)

TABLE 4.14 Summary of residual strength characteristics of immediate floor strata based on borehole shear tests for Mine 2.

Depth Below Coal Seam in	Lithology	Natural Moisture Content %	Cohesive Strength S_o psi	Angle of Internal Friction ϕ deg	Corr. Coeff. r	Test Value[1] of Corr. Coeff.
Site 1						
13	Dark Underclay relatively hard	4.50	75.9	33.3	0.91	0.90
23	Sandy Shale/Sandstone	1.78	158.5	18.3	0.97	0.90
33	Sandy Shale/Sandstone	1.25	76.2	42.2	0.90	0.90
49	Sandy Shale/Sandstone	1.41	80.2	49.7	0.98	0.90
61	Sandy Shale/Sandstone	1.34	213.2	44.3	1.00	0.90
Site 2						
18	Medium Grey Shale (Sandy)	4.26	9.3	44.0	0.89	0.90
30	Medium Grey Shale with Limestone Nodules	1.58	358.8	21.8	0.97	0.90
47	Silty Medium Grey Shale	1.98	286.4	28.6	0.95	0.90
55	Silty Medium Grey Shale	2.12	155.8	36.7	0.98	0.90
67	Silty Medium Grey Shale	1.00	254.2	35.3	0.81	0.90

[1]Test Value for Corr. Coeff. for 90% significance. (Ref. sec 3.7)

TABLE 4.14 (Cont.)

Depth Below Coal Seam in	Lithology	Natural Moisture Content %	Cohesive Strength S_o psi	Angle of Internal Friction ϕ deg	Corr. Coeff. r	Test Value[1] of Corr. Coeff.
Site 3						
14	Dark Underclay	3.08	210.5	28.6	0.97	0.90
21	Light Grey Shale	2.30	210.9	16.8	0.92	0.90
31	Grey Sandy Shale	0.99	137.6	43.1	0.98	0.90
45	Grey Sandy Shale	1.80	41.7	46.5	0.99	0.90
56	Grey Sandy Shale	1.14	26.5	47.1	0.88	0.90
68	Grey Sandy Shale	1.27	344.6	34.1	0.99	0.90
Site 4						
8.5	Underclay Slickensided	5.56	284.8	30.8	1.00	0.90
19	Underclay Slickensided	1.01	172.5	51.5	0.95	0.90
31	Limey Shale	1.53	62.7	58.3	1.00	0.90
44	Grey Shale changing to Black Shale	2.48	153.8	48.6	1.00	0.90
55	Grey Shale changing to Black Shale	1.56	346.7	45.0	0.93	0.90
67	Grey Shale changing to Black Shale	2.16	-124.0	56.1	1.00	0.90
82	Grey Shale Competent and Limey	2.61	41.3	40.9	0.97	0.90

[1]Test Value for Corr. Coeff. for 90% significance. (Ref. sec 3.7)

TABLE 4.14 (Cont.)

Depth Below Coal Seam in	Lithology	Natural Moisture Content %	Cohesive Strength S_o psi	Angle of Internal Friction ϕ deg	Corr. Coeff. r	Test Value[1] of Corr. Coeff.
Site 4						
92	Grey Shale Competent and Limey	1.53	214.4	59.3	0.98	0.90
Site 5						
12	Limey Underclay	5.92	312.6	19.1	0.88	0.90
18	Limey underclay	5.63	146.8	26.7	0.71	0.90
29	Limey underclay	6.36	61.4	26.7	0.97	0.90
43	Limey Shale	0.57	135.1	46.2	0.94	0.9u
53	Limey shale	0.94	89.0	53.7	1.00	0.90
64	Limey Shale	1.13	207.0	37.6	0.97	0.90

[1]Test Value for Corr. Coeff. for 90% significance. (Ref. sec 3.7)
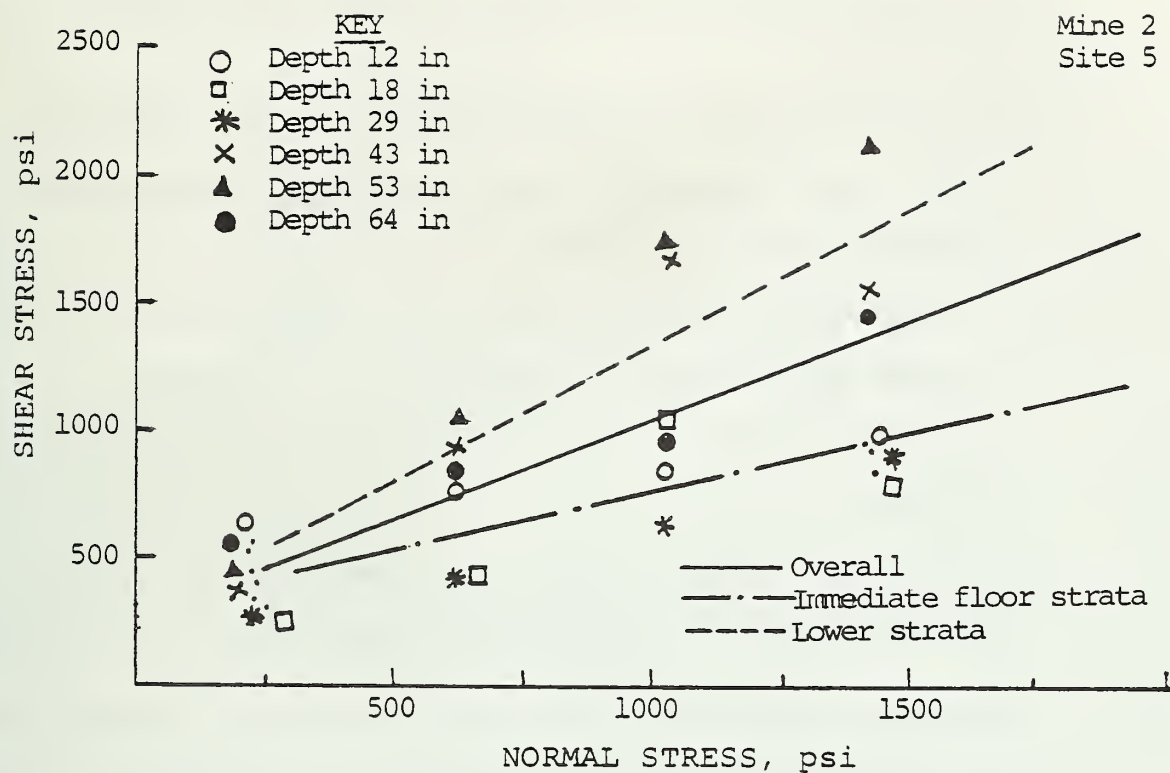
FIGURE 4-11 Shear strength - normal stress relationships for immediate floor strata.
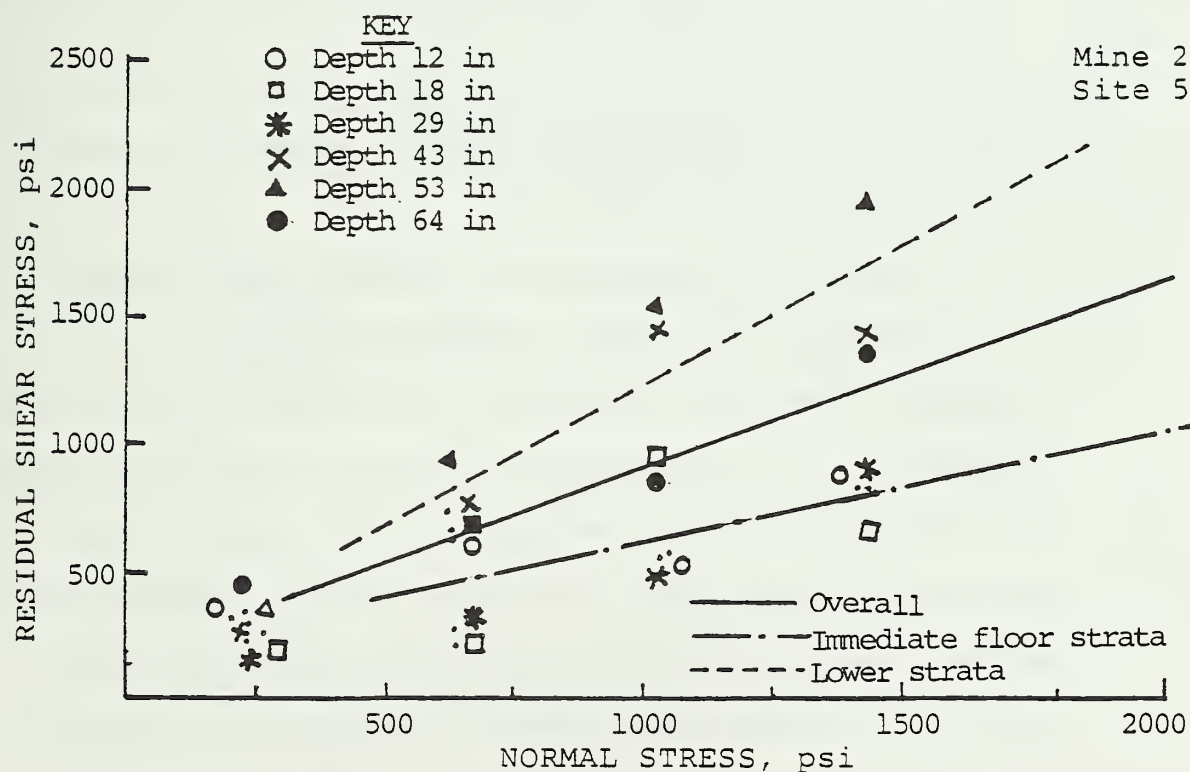
FIGURE 4-12 Shear strength - normal stress relationships for immediate floor strata.

2) S_o values based on residual shear strength range between 0.0-358.8 psi; $\bar{X}$ and σ values are 167.9 psi and 103.2 psi. Residual ϕ values range between 16.8°- 59.3°, and $\bar{X}$ and σ values for this parameter are 38.4° and 11.8°.

3) A linear failure envelope seems to fit the peak as well as residual shear strength parameters well as indicated by correlation coefficients which are generally in the range of 0.85 to 0.99.

4) RBST data at different depths in the same lithologic unit was grouped together for regression to estimate its S_o and ϕ values and their standard deviations. The results for different sites are summarized in Table 4.15 and some pertinent comments are given below.

   (i) Although S_o values for immediate floor strata (0-30 in below the coal seam) are about the same as for the lower strata (30 in or more below the coal seam), ϕ values are generally higher for the lower strata.

   (ii) Variability in test data for immediate floor strata are generally much higher than for lower strata.

Analysis of the shear stress-normal stress data for the two mines (Figures 4.9 - 4.12) show some non-linearity at high normal stresses. The author thinks that this may be due to two reasons: 1) the floor material is characterized by a non-linear failure envelope, and 2) it may have failed during normal stress application causing shear strength to be reduced and resultant non-linearity in the failure

TABLE 4.15 Analysis of borehole shear test data by lithologic units.

Site No.	Grouped Data Depths Below Coal Seam in	Lithologic Description	Cohesive Strength S_o psi Mean	Standard Deviation	Angle of Internal Friction ϕ deg Mean	Standard Deviation
1	13, 23	Dark underclay/Silty shale	253.4	78.3	26.6	12.4
	33, 49, 61	Light grey shale grading into sandstone	261.6	54.3	46.1	2.7
2	18, 30	Medium grey sandy shale. Lime present	336.4	255.7	38.0	12.0
	47, 55, 67	Grey shale with limestone nodulus	343.7	40.4	36.7	5.5
3	14, 21, 31	Dark grey underclay/shale	305.9	82.1	32.9	10.6
	45, 56, 68	Sandy shale with limestone nodules	271.8	187.5	45.1	7.7
4	8, 19, 31	Broken underclay/limey shale	205.7	136.5	50.0	15.4
	44, 55	Limey grey shale with large limestone nodules	271.2	196.0	52.0	0.8
	67, 82, 92	Dense grey shale with limestone nodules	139.2	218.3	54.4	8.2
	12, 18, 29	Broken dark underclay	306.0	163.5	25.0	4.1
5	43, 53, 64	Limey shale with limestone nodules	267.7	90.7	46.3	9.0

envelope. Therefore, it is extremely important to limit the applied
normal stress to a value which.is about 70-80 % of the failure stress
of the floor material. Above these percentage values, time dependent
deformations may become significant and it may be difficult to
maintain the normal stress constant throughout the period of the test.

It is also important to consider the state of stress in the
immediate floor strata after an opening is excavated and how it may
affect material behavior during borehole shear tests. Three-
dimensional states of stress in elements prior to and after mining an
opening are shown in Figure 4.13. Additional stress redistribution
occurs due to drilling of the borehole. Stress relief in the vertical
and horizontal directions, due to excavation of the mine opening, may
cause the material to fail and alter its strength characteristics. S_o
values obtained from RBST tests underneath an opening may be lower
than those underneath a pillar. Angle of internal friction, ϕ,
values, however, may be larger underneath an opening than those
underneath a pillar because the material is under have normal stress
and may even be fractured.

Immediate Roof Strata: Borehole shear tests were conducted at one
site in each of the two mines and pertinent observations are given
below.

Mine 1

Shear strength characteristics of immediate roof strata to a height
of 60 in above the coal seam are summarized in Table 4.16 and Figure
4.14. S_o and ϕ values based on peak shear strength are 346.5 psi and
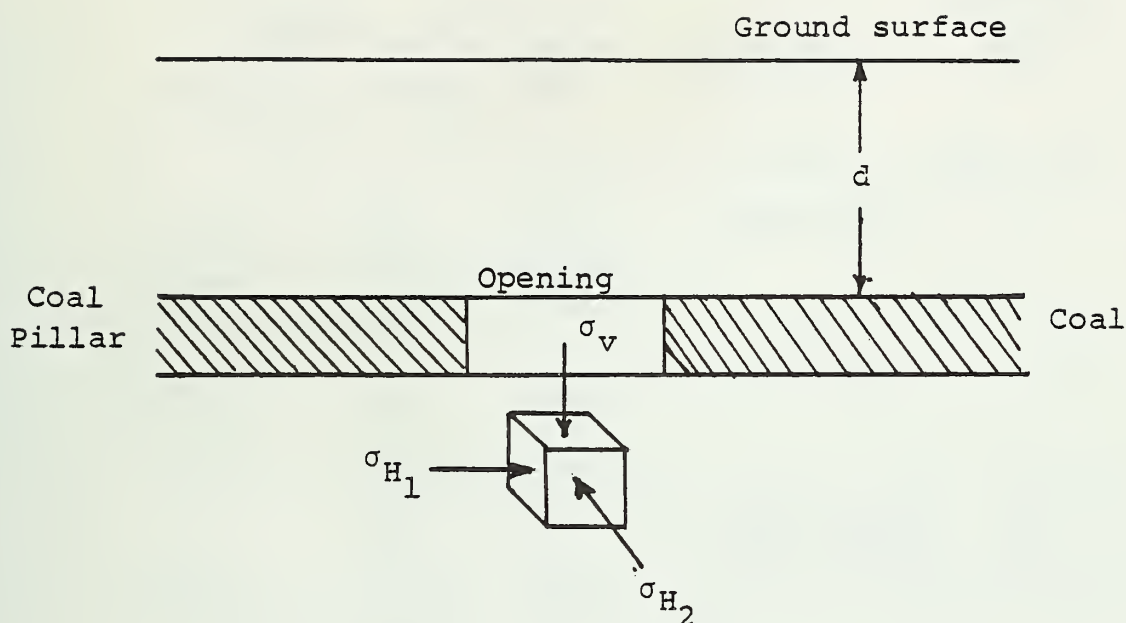
Prior to mining

$$\sigma_v = \gamma \cdot d$$

$$\sigma_{H_1} = \left(\frac{\mu}{1-\mu}\right)\sigma_v + \sigma_t$$

$$\sigma_{H_2} = \left(\frac{\mu}{1-\mu}\right)\sigma_v + \sigma_t$$

After mining

$$\sigma_v = 0$$

$$\sigma_{H_1} \leqslant \sigma_t$$

$$\sigma_{H_2} \leqslant \left(\frac{\mu}{1-\mu}\right)\sigma_v + \sigma_t$$

where σ_t represents the value of the tectonic stress

FIGURE 4.13 State of stress on an element below a mine opening prior to and after mining

TABLE 4.16 Shear strength characteristics of immediate roof
strata based on borehole shear tests for Mine 1

| Depth Below Coal Seam in	Lithologic Description	Normal Stress psi	Shear Strength	
			Peak psi	Residual
17	Grey Shale	1,014.3	999.6	923.6
		1,403.7	1,151.4	999.6
		1,793.1	1,303.2	1,227.3
		2,182.5	1,569.0	1,493.0
31	Grey Shale	1,014.3	809.8	657.9
		1,403.7	961.6	847.7
		1,793.1	1,341.2	1,303.2
		2,182.5	1,606.9	1,569.0
47	Silty Shale	624.9	430.2	392.2
		1,014.3	923.6	809.8
		1,403.7	1,151.4	1,075.5
		2,182.5	1,379.2	1,265.3
59	Silty Shale	624.9	961.6	809.8
		1,014.3	809.8	771.8
		1,403.7	1,189.4	1,113.4
		1,793.1	1,417.1	1,341.2
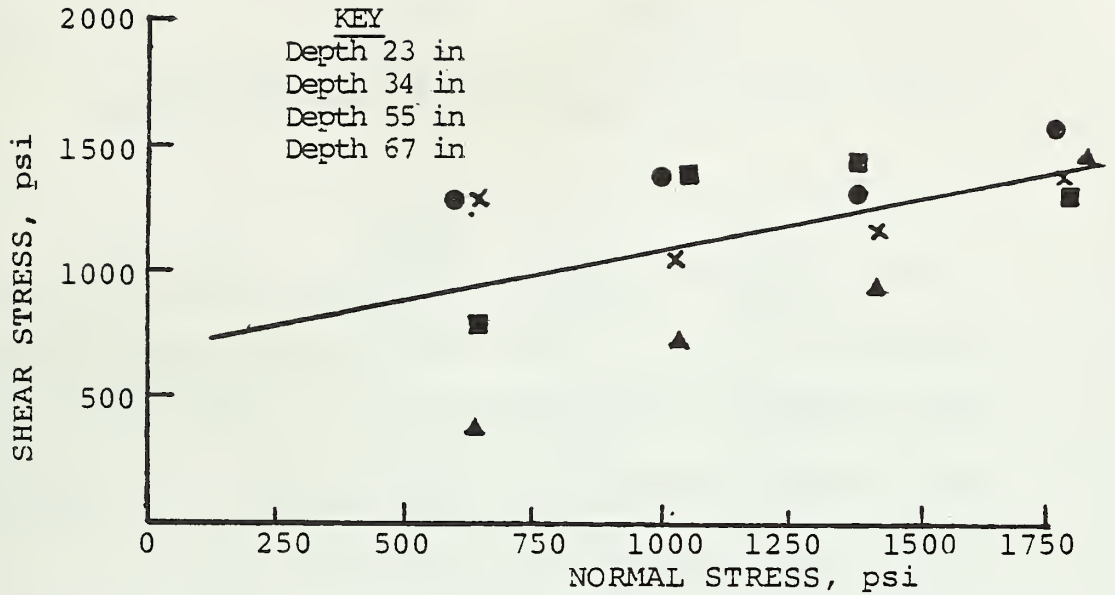
FIGURE 4.14   Shear strength - normal stress relationship for immediate roof strata - Mine 1.
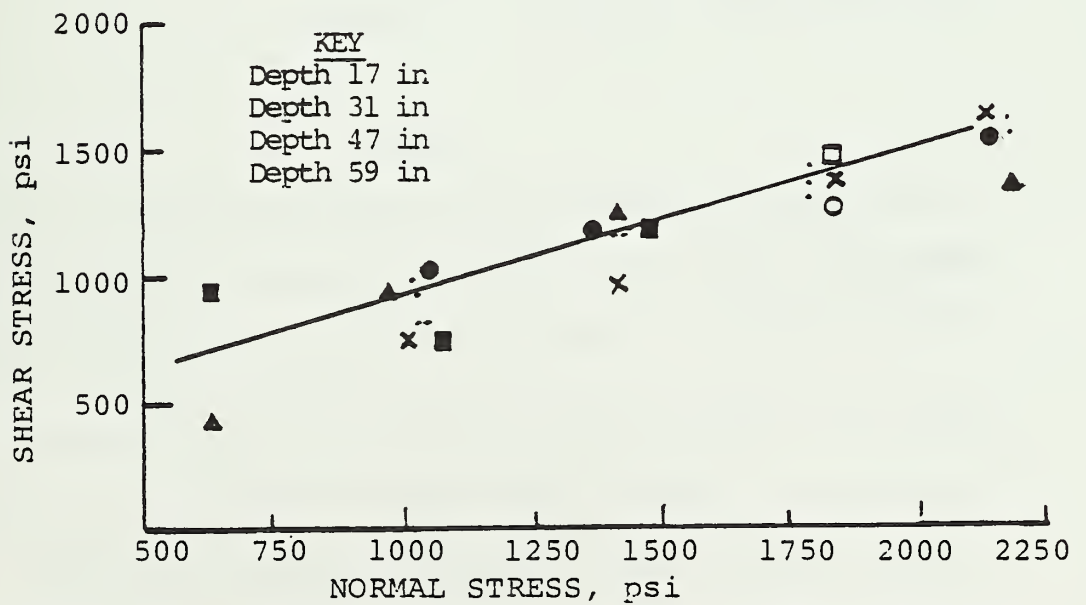
FIGURE 4.15   Shear strength - normal stress relationship for immediate roof strata - Mine 2.

28.6°; similar values based on residual shear strength are 231.3 psi and 29.5°. Recently, Hanna et al. (1986) also conducted borehole shear tests at this mine to a height of 60 in and reported S_o and ϕ values of 250 psi and 27.0° based on peak shear strength.

Mine 2

Data on peak and residual shear strength parameters at this mine are summarized in Table 4.17. The failure envelope based on the peak shear strength is shown in Figure 4.15. S_o and ϕ values based on peak shear strength are 656.2 psi and 22.8°;similar values based on residual shear strength are 421.9 psi and 19.9°.

Coal seam: Borehole Shear tests were attempted at one site in each mine. However, data could be successfully obtained in mine 2 only.

Mine 1

Two holes drilled for borehole shear tests caved immediately after drilling and tests could not be conducted.

Mine 2

Data on peak and residual shear strength parameters for coal are summarized in Table 4.18. The failure envelope based on peak shear strength is shown in Figure 4.16 & 4.17. S_o and ϕ values based on peak shear strength are 61.5 psi and 41.1° with a significant correlation (r = 0.90), similar values for residual shear strength are -37.7 psi and 39.1° with a correlation coefficient of 0.90.

TABLE 4.17 Shear strength characteristics of immediate roof
strata based on borehole shear tests for Mine 2.

Depth Below Coal Seam in	Lithologic Description	Normal Stress psi	Shear Strength	
			Peak psi	Residual
23	Grey Shale	624.9	1236.8	1047.0
		1014.3	1331.7	1047.0
		1403.7	1331.7	1047.0
		1793.1	1521.5	1094.5
34	Grey Shale	624.9	1236.8	1047.0
		1014.3	1047.0	714.9
		1403.7	1189.4	961.6
		1793.1	1379.2	1141.9
55	Grey Shale	624.9	382.7	164.4
		1014.3	714.9	335.3
		1403.7	923.6	572.5
		1793.1	1512.0	1265.3
67	Grey Shale	624.9	809.8	496.6
		1014.3	1331.7	1047.0
		1403.7	1379.2	686 4
		1793.1	1303.2	1094.5

TABLE 4.18   Shear strength characteristics of coal based on
borehole shear tests for Mine 2.

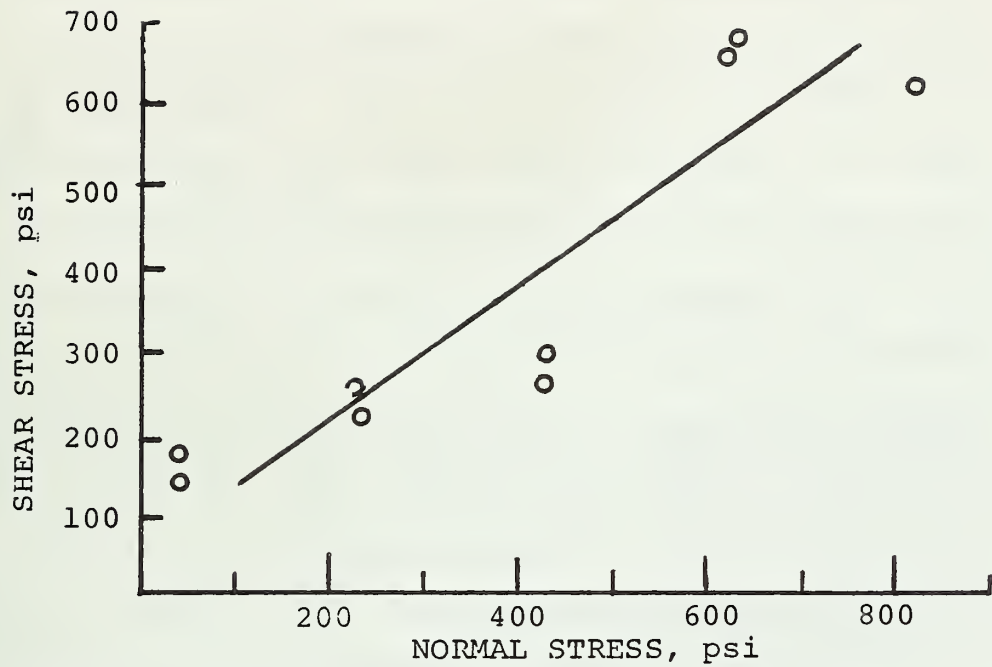| Depth	Normal Stress psi	Shear Stress psi	Residual Stress psi
30"	40.8	164.4	69.5
	235.5	221.4	107.5
27"	430.2	316.3	202.4
	624.9	695.9	563.0
24"	819.6	657.9	525.0
	624.9	714.9	563.0
21"	430.2	278.3	183.4
	235.5	278.3	126.5
16"	40.8	145.5	50.6

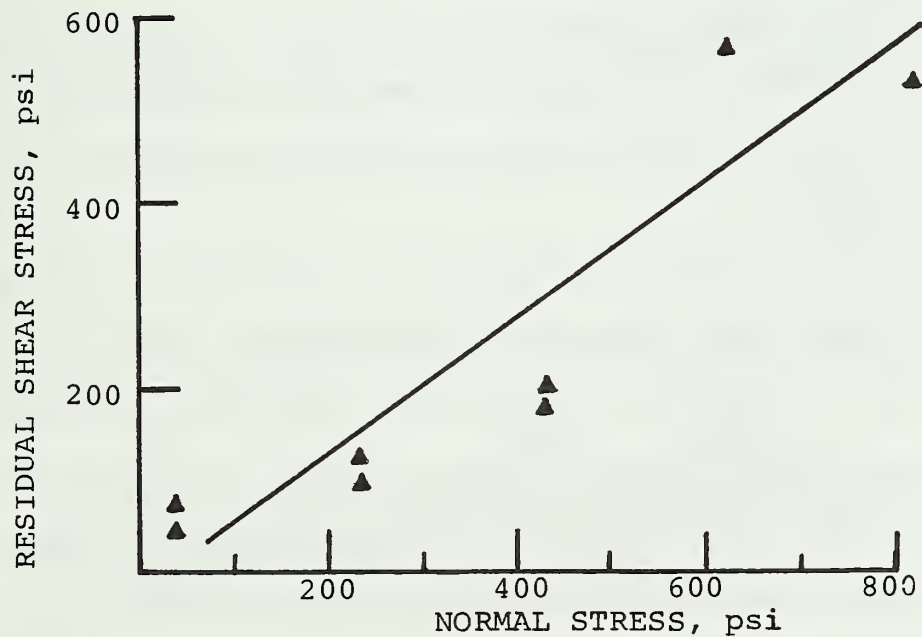FIGURE 4.16 Peak shear strength-normal stress relationship for coal at Mine 2.

FIGURE 4.17 Residual shear strength-normal stress relationship for coal at Mine 2.

4.4   Laboratory Geotechnical Studies

Strength Deformation Studies: The data for immediate floor strata
under unconfined and confined compressive stress for Mine 1 and Mine 2
are summarized in Tables 4.19 and 4.20. A limited number of block
samples of immediate roof stratum and coal from the two mines were
also studied for their strength-deformation characteristics under
unconfined compressive stress conditions. The data obtained are
summarized in Tables 4.21-4.22.

Moisture Gain Studies: Percent moisture gain data for Mine 1 and Mine
2 are shown in Figure 4.18 and Figure 4.19. The curves are not
statistical fit lines. Pertinent comments are given below.

1) All samples show an exponential increase in moisture gain, and
    most attain the equilibrium moisture content within 72 hr.

2) Most of the moisture gain is achieved within 20 hr after the
    samples are placed in a specific R.H. chamber.

3) Maximum moisture content is attained 24-30 hr after initiation of
    the test. After this period, the moisture content drops somewhat
    to the equilibrium moisture content level and remains relatively
    constant.

4) Moisture gain data for 70%, 80%, and 90% R.H. could be reproduced
    and the author considers the data meaningful. Similar data at
    100% R.H. could not be replicated because of the precipitation of
    water vapor on samples. Samples at this R.H. showed very high
    moisture gain and equilibrium moisture content was never attained.

5) An equilibrium moisture content of 3% at 90 % R.H. may be
    expected. Since the natural moisture content of in-place
    underclay is about 1.5%, a moisture gain of 1.5% may be expected

TABLE 4.19 Compressive strength – deformation properties of immediate floor strata for Mine 1

Site No.	Depth Below Coal Seam (inch)	Rock Type	Moisture Content (%)	Confining Stress (σ_3, psi)	Axial Stress (σ_1, psi)	Axial Deformation Modulus ($\times 10^6$ psi) At 50% of σ_1	At 100% of σ_1	Lateral Deformation Ratio * ($\dot{\varepsilon}_x/\dot{\varepsilon}_z$)	Cohesion (C, psi)	Friction Angle (ϕ, Degree)	Remarks
1	12 – 16	Grey Shale	2.73	0	4178.0	0.62	0.44	0.68			
2	13 – 18	Grey Shale	2.30	0	5633.1	0.82	0.53	0.45	1000	45.0	
	24 – 28	Grey Shale	2.31	100	5025.4	0.68	0.28	0.26			
	28 – 34	Grey Shale	2.21	300	7450.0						
3	33 – 36	Grey Shale	2.88	0	4653	0.52	0.12	0.46	900	45.0	
	43 – 58	Grey Shale		300	6244.6						
4	37.5 – 41	Grey Shale	3.54	100	4808.2	0.65	0.56	1.19	900	54.0	
	58.5 – 63	Sandy Shale	2.75	0	5272.0	0.70	0.69	0.40			
	65.5 – 70	Sandy Shale	2.20	300	8361.2	0.90	0.61	0.21			
	78 – 83	Sandy Shale	2.63	500	10230.0						
5	23 – 26	Grey Shale	4.98	0	6836.0	0.42	0.44	0.27	1025	49.0	
	38 – 43	Grey Shale	3.05	100	4855.1	0.75	0.92	0.54			
	47 – 51	Grey Shale	1.80	300	7935.9	1.12	0.89	0.92			
6	54 – 58	Sandy grey shale	2.32	0	7387.0	1.04	0.79	0.19	1075	58.0	
	62 – 66	Sandy grey shale		100	8289.1	1.26	1.06	0.45			
	68 – 72	Sandy grey shale		0	8029.0						
7	4.5 – 8.5	Grey shale	2.12	0	7876.0	1.06	1.20	0.78	1100	57.5	
	9 – 13	Grey Shale	2.21	100	10759.2	1.20	0.88	0.42			
	14 – 18	Sandy Shale	2.21	0	6528.0	1.14	0.68	0.71			
	22 – 26.5	Sandy grey shale	2.18	300	11786.2	1.53	1.24	0.99			
	48 – 53	Sandy grey shale	2.04	500	13304.3	1.32	1.15		1300	48.0	
	56 – 60	Sandy grey shale	2.11	0	9926	0.96	1.00				
	62.5 – 66	Sandy grey shale	2.11	100	11671.9	1.16	1.00				
8	63 – 67	Sandy Shale	2.19	0	9136.0	1.33	0.72	0.48	1375	47.0	
	70.5 – 75	Sandy Shale	2.13	100	9980.9						
	79.5 – 84	Sandy shale	1.84	300	10669.4	0.89	0.66	0.51			
	89 – 93.5	Sandy shale	2.25	500	12391.6	1.10	0.89	0.15			
9	42 – 46.5	Grey shale	1.97	100	8407.5	0.94	0.44	0.13	1200	52.0	
10	43.5 – 47	Grey shale	2.45	0	7835.0	0.76	0.67	0.34			
9	54 – 58.5	Grey shale	1.66	300	10331.8	1.36	1.09	0.68			

* 50% of failure stress

TABLE 4.20 Compressive strength – deformation characteristics of immediate floor strata for Mine 2

Site No.	Depth Below Coal Seam (in)	Rock Type	Moisture Content pct	Confining Stress (σ_1, psi)	Axial Stress (σ_3, psi)	Axial Deformation Modulus (x 10^6 psi)		Lateral Deformation Ratio ($\varepsilon_x/\varepsilon_t$)	Cohesion (S_o, psi)	Friction Angle (ϕ, Deg)	Remarks
						At 50 pct of σ_3	At 90 pct of σ_3				
1	3.0 - 6.0	Underclay/ Silty Shale	3.95	0	5,809	0.37	0.44	0.26	900	55.10	
	3.5 - 7.5	Underclay/	3.95	100	5,339	0.55	0.61	1.59			
1	15.0 -18.0	Dark Silty Gray Shale	3.49	300	5,391	0.69	0.58	0.49	ND	ND	
	6.0 -10.0	Dark Silty Gray Shale	3.95	500	5,387	0.66	0.59	0.38			
2	0.0 - 3.0	Gray Shale	3.57	0	4,392	ND	ND	ND	800	52.00	
	12.0 -17.0	Medium Gray Sandy Shale	3.58	100	8,056	1.50	1.38	1.24			
2	6.0 -10.0	Medium Gray Shale	2.95	500	8,408	1.28	1.14	0.53	ND	ND	
3	6.0 - 9.0	Dark Gray Shale	2.95	0	5,998	0.36	0.41	0.51	2550	9.00	
	8.0 -12.0	Medium Gray Shale	4.92	500	6,685	0.68	0.56	0.54			
3	25.0 -29.0	Light Gray Silty Shale	0.99	100	10,770	1.53	1.46	1.84	2350	38.50	
	23.0 -27.0	Light Gray Sandy Shale	0.34	300	10,546	0.96		0.11			

TABLE 4.20 (Continued)

Site No.	Depth Below Coal Seam (in)	Rock Type	Moisture Content pct	Confining Stress (σ_1, psi)	Axial Stress (σ_3, psi)	Axial Deformation Modulus (x 10^6 psi)		Lateral Deformation Ratio (ϵ_x/ϵ_z)	Cohesion (S_d, psi)	Friction Angle (ϕ, Deg)	Remarks
						At 50 pct of σ_3	At 90 pct of σ_3				
4	15	Underclay	5.85	0	2,663.00	0.27	0.21	0.88	ND	ND	
4	23	Limey Gray Shale	1.78	100	6,920.00	1.21	1.05	0.44	ND	ND	
	51 - 55	Limey Gray Shale	1.49	300	9,366.00	1.03	0.88	0.26			
	17 - 21	Dark Gray Shale	0.70	500	15,357.00	2.07	1.94	3.64			
5	53 - 58	Limey Gray Shale	1.30	0	8,691.00	0.97	0.28	7.58	1150	70.50	
	57 - 56	Limey Gray Shale	0.76	100	21,169.00	1.15	2.14	0.78			
	46 - 50	Limey Gray Shale	0.76	300	20,414.00	2.14	1.58	20.6			
5	12 - 16	Underclay	5.92	500	4,889.37	0.65	0.58	0.48	ND	ND	

TABLE 4.21 Strength-deformation properties of immediate roof stratum for Mine 1 and Mine 2

Site Number	Unconfined Compressive Strength C_o psi	Axial[1] Deformation Modulus at 50% of C_o 10^6 psi	Lateral[1] Deformation Ratio $\varepsilon_x/\varepsilon_z$
Mine 1			
1	6,005	0.387	0.07
2	9,815	0.714	0.10
3	9,804	0.900	0.06
4	7,489	0.557	0.08
5	10,957	0.68	0.10
Mine 2			
1	9,454	0.536	0.12
	10,356	0.582	0.22
2	9,917	0.542	0.07
	6,363	0.280	0.22
3	7,750	0.487	0.22
	8,157	0.644	0.07

[1] See Appeniix C

TABLE 4.22   Strength-deformation properties of coal stratum
for Mine 1 and 2

Site Number	Unconfined Compressive Strength C_o psi	Axial[1] Deformation Modulus at 50% of C_o 10^6 psi	Axial[1] Deformation Modulus at 90% of C_o 10^6 psi	Lateral[1] Deformation Ratio $\varepsilon_x/\varepsilon_z$
Mine 1				
1	4,833	0.301	0.368	0.48
2	3,796	0.206	0.219	0.37
Mine 2				
1	2,423	0.178	0.193	0.55
2	5,316	0.286	0.327	0.07
3	5,247	0.25	0.307	0.15
4	5,331	0.321	0.316	0.68

[1]See Appendix C
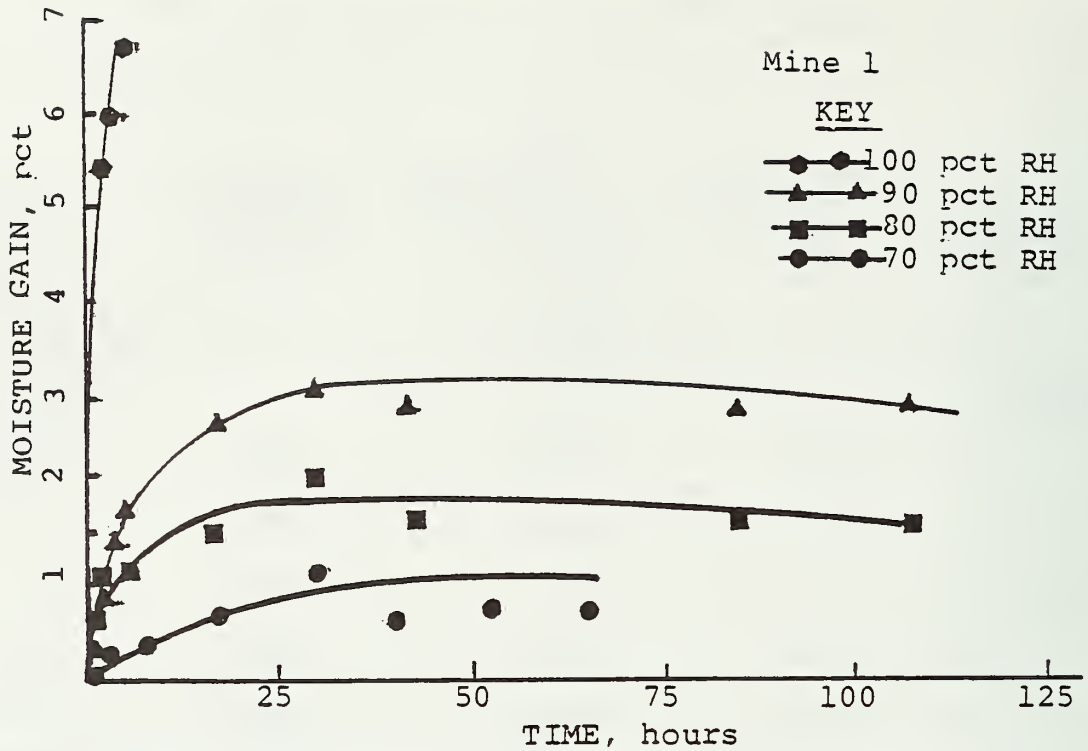
FIGURE 4.18 Moisture gain data for immediate floor strata at mine 1 at different relative humidities
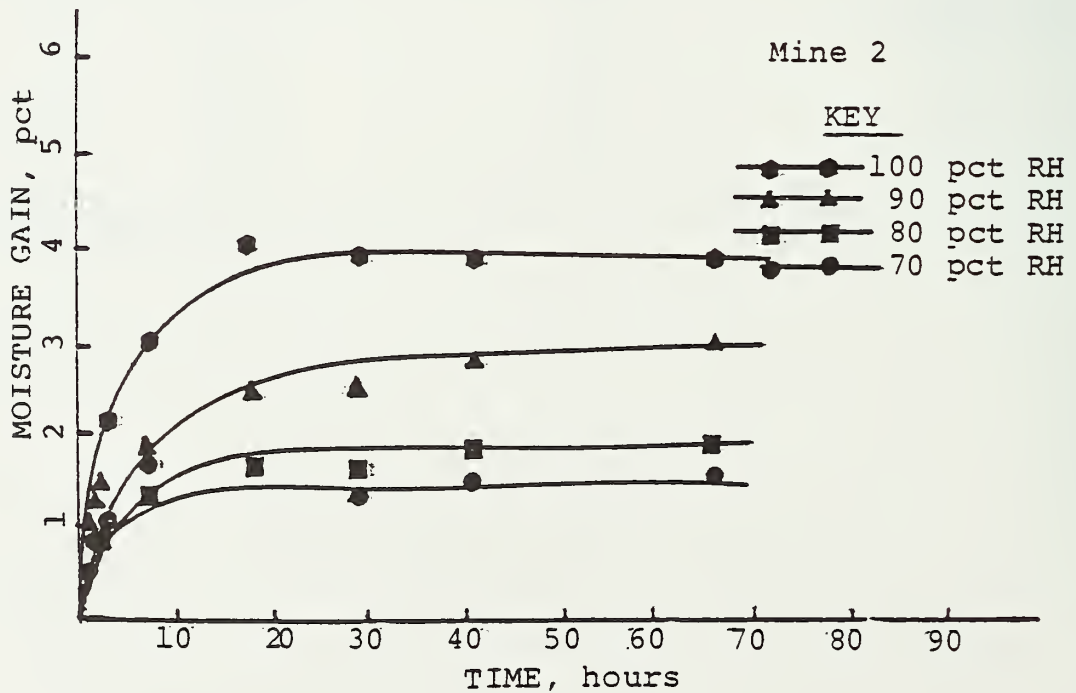

FIGURE 4.19 Moisture gain data for immediate floor strata at mine 2 at different relative humidities

in freshly mined areas. This amount of moisture gain may result in some reduction of the strength-deformation properties of underclay.

4.5 Correlation Between Laboratory and Field Determined Geotechnical Data

The following correlations were attempted for each mine individually and for the two mines combined:

1) UBC and S_o from borehole shear tests in the 0-12 in depth range below the coal seam.

2) DM_{50} from plate load tests vs DM_{50} from confined compression tests.

3) Natural moisture content of immediate floor strata in the 0-12 in depth range below the coal seam and UBC.

4) S_o at a particular depth from borehole shear tests and S_o from confined compression tests at about the same depth.

Only correlation (3) above was found to be statistically significant at the 90 % confidence level. Correlation between the UBC and natural moisture content is shown in Figure 4.20. Each data point represents the mean value of the UBC based on all plate load tests at a site. The following comments are pertinent for attempted correlations:

1) UBC and, hence, DM_{50} may be estimated with confidence from the natural moisture content of immediate floor strata for the two mines. These two mines extract different seams but are only 30 miles apart. The data from a third mine about 160 miles away from these mines was also plotted on Figure 4.20 to determine if the correlation may have application throughout Illinois. It is
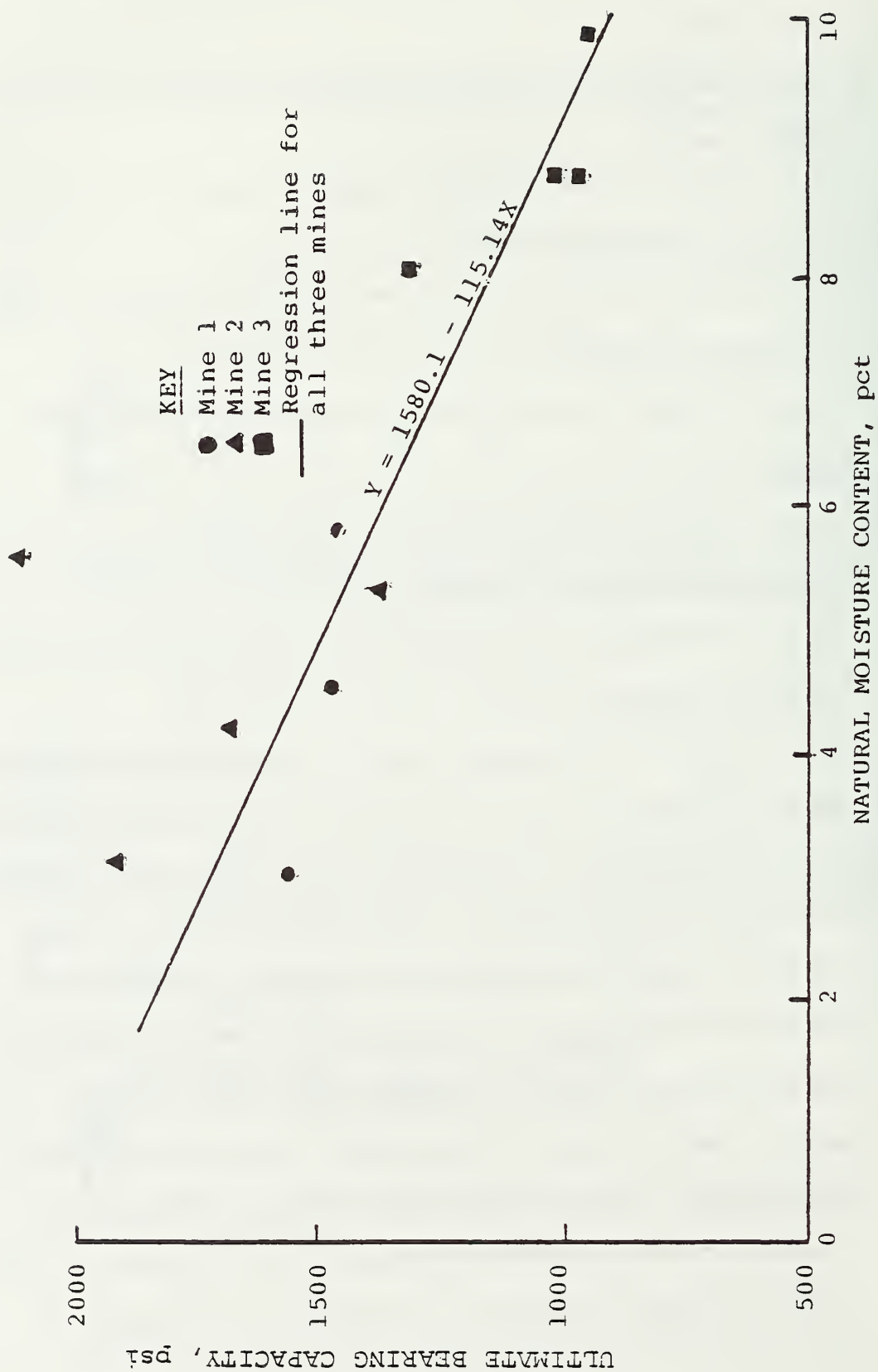
FIGURE 4.20 Correlation of ultimate bearing capacity with natural moisture content of immediate floor strata in 0-12 in range.

interesting to note that the correlation seems to be valid for the third mine also. The data available are, however, too limited to make any general conclusions or observations at this time.

2) Correlations between DM_{50} from plate bearing tests and DM_{50} from confined compression tests were only marginally significant for Mine 1 and Mine 2. Furthermore, for Mine 1 the intercept was negative but the slope was positive. The reverse was true for Mine 2. The correlation was significant for the combined data from the two mines, but this is not considered meaningful from a physical point of view. Correlations between DM_{50} from plate bearing tests and DM_{50} from confined compression tests are shown in Figure 4.21 and the linear regression parameters for the same are given in Table 4.23.

3) A very poor correlation ($r = 0.22$) was observed between the UBC and S_o obtained from borehole shear tests in the 0-12 in depth range below the coal seam for the case of the two mines combined. Analysis of the data showed a larger variability in S_o values ($\bar{X}$ = 305.7 psi, σ = 162.7 psi) as compared to UBC values ($\bar{X}$ = 1209.2 psi, σ = 302.3 psi).

4) While a good correlation between S_o from borehole shear tests and S_o from confined compression tests was observed for Mine 2 ($r=0.92$), a similar analysis for Mine 1 and combined data showed very poor correlations ($r<0.22$). S_o values from borehole shear test were generally lower and showed a larger variability as
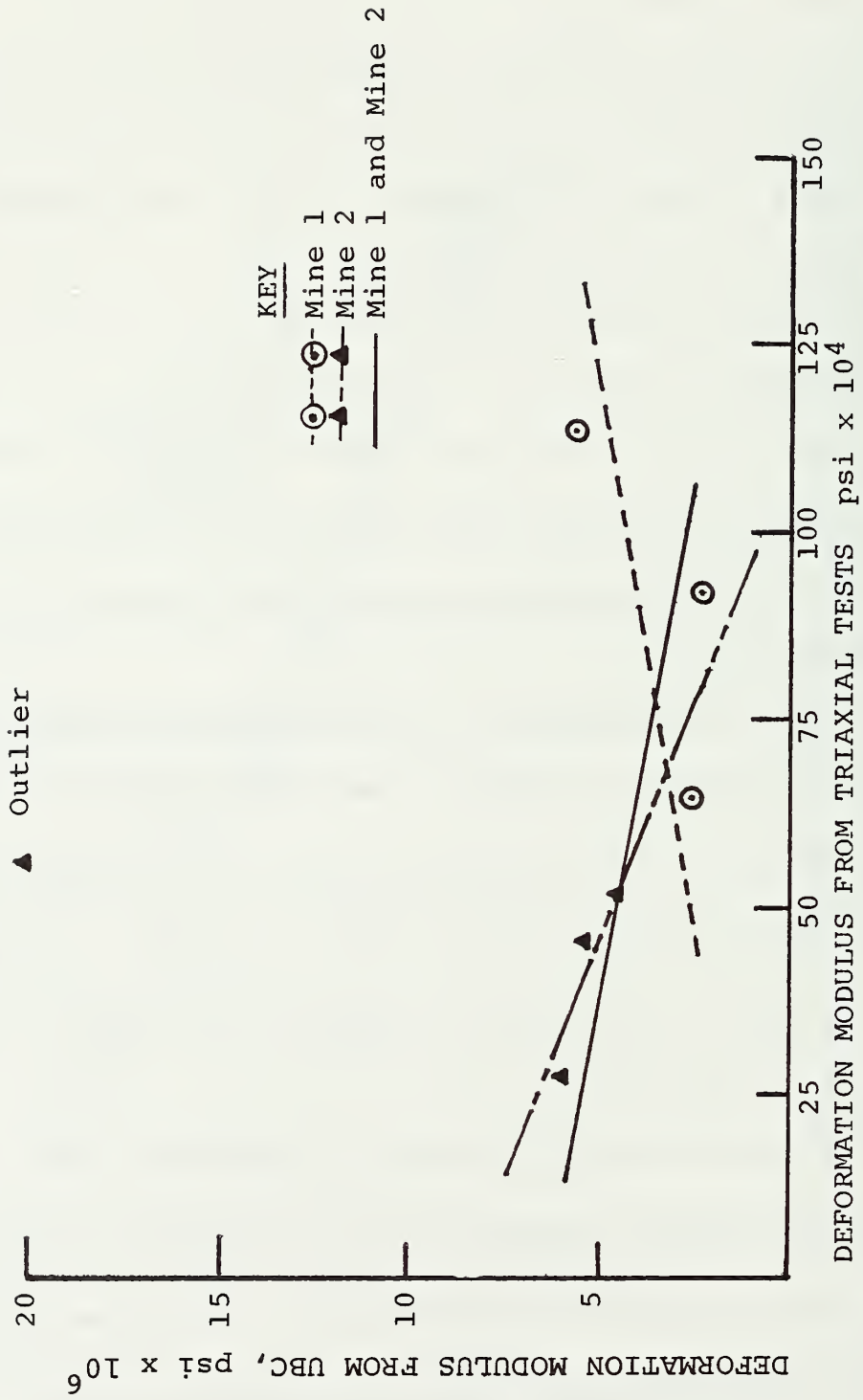
FIGURE 4.21 Correlation of deformation modulus as obtained from triaxial test with that obtained from bearing capacity tests.

TABLE 4.23 Correlation results for variation of DM_{50} from TCT and DM_{50} from UBC test.

| Mine | No. of Tests[2] | Linear Regression Parameters | | | | Sample Statistics[1] | |
		Intercept 10^4 psi	Slope	Correlation Coefficient r	Test value of r for '90% Confidence	Mean Y 10^4 psi	Standard Deviation σ 10^4 psi
As-Mined							
1	3	-4.10	0.065	0.96	0.99	2.68	0.86
2	4	8.49	-0.077	-0.89	0.90	4.59	1.42
1 and 2 (combined)	7	6.40	-0.036	-0.75	0.67	ND	ND

[1] x axis -- Deformation modulus at 50% of TCT strength.
[2] y axis -- Deformation modulus at 50% of UBC.

compared to confined compression test values. This observation is similar to the one made by Panek (1979) after considerable research with the RBST in several coal and non-coal mines. He thought that only competent samples were selected for confined compression tests, thus giving high values. Strengths determined by the RBST are representative of a very small (1 in^2) in-place area whose characteristics could change widely and rapidly depending upon the nature of rock encountered. This is particularly true for immediate floor strata where slickensides and limestone nodules are randomly distributed.

4.6 Development of a Floor Stability Criterion

Floor stability criteria should be based on two factors: 1) UBC of immediate floor strata, and 2) pillar settlement. UBC, a stress based criterion, would be applicable where general shear type failure associated with relatively low settlement or deformation and rapid load loss in the post-failure region is observed, such as in Figure 4.4 (12 in, as-mined). Immediate floor strata at both mines showed this type of behavior under as-mined condition at several sites. The rapid load-loss in the post-failure region would imply quick redistribution of stresses in adjoining pillars if one of the pillars were to fail due to the UBC failure. This may lead to pillar punching, coal outbursts, and/or floor heave. At present, pillar designs in Illinois under weak floor conditions are based on this criterion but do not account for dynamic loading imposed on adjacent pillars in case of a pillar failure. Where load loss in the post-failure region is not rapid, redistribution of stresses on adjoining

pillars and floor heave will occur over a long period of time and the likelihood of coal bursts would be significantly reduced.

The failure criterion based on this parameter should incorporate both the UBC and the slope of the post-failure part of the stress-deformation curve. The critical slope of the stress-deformation curve would depend upon the stiffness of the mining system, involving the overburden, coal seam, and floor strata.

Pillar settlement, total as well as differential, are important parameters in assessing floor stability, but have not been considered in design. This is primarily because critical values of these parameters have not been determined in the laboratory or under field conditions. These parameters should be considered not only at the coal seam level currently being mined, but their impact on overlying and underlying coal seams, aquifers, and surface movements should also be considered. For example, total pillar settlement at the coal seam level may be acceptable, but resultant effects on an overlying seam, aquifer, or on a surface structure may not be acceptable. Thus, the failure criterion based on these parameters will require establishment of damage criteria for mine openings and coal pillars at the coal seam level, as well as at the surface and/or subsurface levels.

Development of a failure criterion based on pillar settlement will also require a knowledge of the deformation properties of immediate floor strata, which are generally not determined during plate loading tests.

Chapter 5

SUMMARY AND CONCLUSIONS

This study has involved measurement of the ultimate bearing capacity (UBC) and in-place shear strength characteristics of immediate floor strata below the Illinois No. 6 and No. 5 coal seams in two underground coal mines in Illinois. The UBC was measured using plate load tests under as-mined and soaked-wet conditions. An automated system for conducting plate load tests was designed and fabricated during the study. Plate deformations under applied load were measured using linear variable differential transformers and were utilized to compute the deformation modulus of the immediate floor strata based on the theory of elasticity.

In-place shear strength characteristics were measured at various depths in a 3 in diameter borehole with a Rock Borehole Shear Tester (RBST). Cohesive strength (S_o), angle of internal friction (ϕ) and parameters of a best-fit line for the failure envelope were determined based on linear regression analysis. Borehole shear tests were conducted in the vicinity of the sites where plate load tests were conducted so that correlations between shear strength characteristics, ultimate bearing capacity, and deformation modulus of the immediate floor strata could be attempted. Borehole shear tests were also conducted in the immediate roof stratum and coal seam at one site in each seam to determine their failure envelopes.

Additional correlations were attempted between field determined strength characteristics in this study and laboratory determined strength characteristics from confined compression tests from ongoing studies under a grant from the State of Illinois. Sensitivity of

immediate floor strata to relative humidity changes in the mine were studied by conducting a limited number of moisture gain studies.

Some of the main results of the study are given below:

1) The UBC determined from plate load tests appears to be relatively unaffected by the size of plates used. However, it is not known whether this value can be used to represent the ultimate bearing capacity of the immediate floor strata underneath coal pillars.

2) Wetting reduces the UBC as well as the deformation modulus at 50% UBC (DM_{50}) of the immediate floor strata. The effect may, however, be much larger on DM_{50} than on the UBC (Table 4.6).

3) UBC as well as DM_{50} may be estimated from the natural moisture content of immediate floor strata in the 0-12 in depth range below the coal seam (Figure 4.18).

4) Some stress-deformation plots from plate load tests under as-mined conditions show general shear type failure and are accompanied by a significant load drop in the post-failure region. Under soaked-wet conditions, a typical plot shows localized shear or punching shear type failure. In both conditions, elastic-plastic rather than rigid plastic behavior may be a better representation of the material behavior.

5) Deformation modulus at 50% of the UBC (DM_{50}) determined from plate loading tests may be used in finite element modeling to predict field displacements. This observation is based on previous work (Chugh et al., 1983).

6) No statistically significant correlation was observed between S_o and ϕ values determined from the RBST and those determined from laboratory confined compression tests.

7) UBC and S_o determined from the RBST could not be significantly correlated.

8) S_o and ϕ values determined from the RBST are generally lower and much more variable than those obtained from laboratory confined compression tests.

9) Design of coal pillars under weak floor conditions in Illinois is presently based on the UBC of the immediate floor strata. The UBC is either determined from in-mine plate loading tests or estimated from Brown and Meyerhoff or Vesic's equations (Sec. 2.2). Pillar settlements are not generally considered in design.

10) Residual S_o values are approximately 75-80% of the peak S_o values; ϕ values are approximately the same for both cases.

11) Immediate floor strata in face areas, where relative humidity is 90% or more, may gain 1-2% moisture in 2-3 days, which may reduce its strength-deformation characteristics. The same may also occur in intake entries during the summer months when relative humidity and moisture content of surface air is high.

12) The floor stability criteria should include the UBC and total as well as differential pillar settlements at the coal seam level being mined and their effcts on surface and subsurface structures (aquifers, coal seams, buildings, etc.).

13) The most important parameters of immediate floor strata required for estimation of the UBC under weak floor conditions are the cohesive strengths of immediate floor and substrata, angle of

internal friction, thickness of weak floor and natural moisture content.

14) Measurement of the deformability of the immediate floor strata should be an integral part of conducting plate load tests.

Results summarized above are based on limited studies at two mines. Similar studies need to be conducted at several additional mines. All data should be then analyzed together to develop meaningful correlations which may be valid for portions of the coal basin or for the entire coal basin.

REFERENCES

1. Afrouz, A., 1975. "Yield and Bearing Capacity of Coal Mine Floors", Int. J. of Rock Mechanics and Min. Sci. Vol 12, pp. 241-253.

2. Aughenbaugh, N. B. and Bruzewski, R. F., 1976, "Humidity Effects on Mine Roof Stability," Final Report, U.S. Bureau of Mines, Contract No. H0232057, 164 pp.

3. Barry, A. J., and Nair, O. B., 1970, "In-Situ Tests of Bearing Capacity of Roof and Floor in Selected Bituminous Coal Mines--A Progress Report, Longwall Mining," U.S. Bureau of Mines, RI 7406, 20 pp.

4. Bandopadhay, C., 1982, "Analysis of Soft Floor Interaction on Underground Mining at a Western Kentucky Mine, M.S. Thesis, Southern Illinois University at Carbondale.

5. Bauer, R.A., 1984, "Relationship of Uniaxial Compressive Strength to Point Load and Moisture Content Indices of Highly Anisotropic Sediments of Illinois Basin", Proceedings of the 25th U.S. Symposium on Rock Mechanics, pp. 398-405, Society of Mining Engineers, New York, N.Y.

6. Bieniawski, Z. T., 1982, "Improved Design of Room-and-Pillar Mining Systems" Final Report to U.S. Department of Energy, June, pp.

7. Brown E. T., Ed., 1978, "Commission on Standardization of Laboratory and Field Tests", International Society of Rock Mechanics, September.

8. Brown, J. D. and Meyerhof, G. G., 1969, "Experimental Study of Bearing Capacity in Layered Clays," Proceedings Seventh Intern. Conf. Soil Mech. Found. Engrg., Mexico City, Vol 2, pp. 45-51.

9. Buisman, A. S. K., 1940, "Grondmechanica", Waltman, Delft. pp. 190.

10. Chugh, Y. P., Chandrashekhar K., and Caudle R. D., 1986, "A Geotechnical Study of the Effects of Soft Floor on Room-and-Pillar Coal Mining in Central Illinois", Paper to be Published in the Annual Generic Mineral Institute (Mine Systems and Ground Control) Proceedings, Moscow, Idaho, November.

11. Chugh, Y. P., Bandopadhay, C., Caudle, R. D., (1984), "Analysis of Soft Floor Interaction in Underground Mining at an Illinois Basin Coal Mine", ISRM Symposium on Design and Performance of Underground Excavations, Cambridge, U.K., Brown, E. T., and Hudson, J. A., Editors, September, 1984.

12. Chugh, Y. P. et al., 1986, "Laboratory Characterization of Immediate Floor Strata Assiciated with Coal Seams in Illinois", Final Report to Mine Subsidence Research Program, Illinois State Geological Survey, Champaign, Urbana, Illinois, May, 238 pp.

13. Chugh, Y. P., Okunola, A. and Hall, M., 1981, "Moisture Absorption and Swelling Behavior of the Dykesburg Shale", Transactions Society of Mining Engineers, Vol. 268, pp. 1808-1812.

14. Chugh, Y. P. and Prasad, K. V. K., 1983, "Workshop Design of Coal Pillars in Room-and-Pillar Mining". Unpublished course notes, Southern Illinois University, 50 pp.

15. De Beer, E. E., 1949, "Grondmechanica", Deel II, Funderingen, N.V. Standard Boekhandel, Antwerpen, pp. 41-51.

16. De Beer, E. E., 1965, Bearing Capacity and Settlement of Shallow Foundations on Sand", Bearing Capacity and Settlement of Shallow Foundations, Proceedings of a Symposium held at Duke University, pp. 15-34.

17. De Beer, E. E., 1965, "The Scale Effect on the Phenomenon of Progressive Rupture in Cohesionless Soils", Proceedings Sixth International Conference on Soil Mechanics and Foundation Engineering, Montreal, Vol. II, pp. 13-17.

18. De Beer, E. E., 1967, "Proefondervindelijke Bijdrage Tot de Studie Van Het Gransdraagvermogen Van Zand Onder Funderingen op Staal; Bepaling Von Der Vormfactor s_b, Annales des Travaux

Publics de Belgique, 68, No. 6, pp. 481-506; 69, No. 1, pp. 41-88; No. 4, pp. 321-360; No. 5, pp. 395-442; No. 6, pp. 495-522.

19. Handy, R. L. et al., 1976, "Rock Borehole Shear Test", Proc. 17th U.S. Symposium on Rock Mechanics, Society of Mining Engineers, pp 11.

20. Hanna, K. et al., 1986, "Effect of High Horizontal Stress on Coal Mine Entry Intersection Stability", 5th Conference on Ground Control in Mining, Morgantown, West Virginia.

21. Haramy, K. Y., 1981, "Borehole Shear Tester: Equipment and Technique", Bureau of Mines Information Circular, IC 8867, 16 pp.

22. Haramy, K. Y. and DeMarco., 1983, "Use of the Borehole Shear Tester in Pillar Design", 24th U.S. Symposium on Rock Mechanics, Society of Mining Engineers.

23. Jenkins, J. D., (1958) "Some Investigations into the Bearing Capacities of Floors in the Northcumberland and Dunham Coal Fields", Trans. Inst. Min. Engineers (London) Vol. 117, pp. 726-738.

24. Kennard, W., (1985) Private Communication, Department of Mining Engineering, Southern Illinois University.

25. Kerisel, J., 1967, "Scaling Laws in Soil Mechanics", Proceedings, Third Panamerican Conference on Soil Mechanics and Foundation Engineering, Caracas, Vol. III, pp. 69-92.

26. Kimura, T., Kusakabe, O., and Saitoh, K., 1985, "Geotechnical Model Test of Bearing Capacity Problem in a Centrifuge", Geotechnique Vol. 35, No.1, pp. 33-45.

27. Kraff, L. M. and Helfrich S. C., 1983, "Bearing Capacity of Shallow Footings/Sand over Clay", Canadian Geotechnical Journal, Vol. 20, No.1, pp. 182-185.

28. Lawritzen, R. and Schjetne K., 1976, "Stability Calculations for Offshore Gravity Structures", Proceedings of the Eighth Offshore Technology Conference, Houston, Texas, Paper No. OTC-2431, pp. 75-82.

29. Mandel, J., 1965, Interference Plastique de Semelles Filantes; Proceedings, Sixth Intern. Conf. Soil Mech. Found. Engrg., Montreal, Vol. II, pp. 127-131.

30. Mandel, J. and Salencon, J., 1969, "Force Portante d'un Sol Sur Une Assise Rigide", Proc. Seventh Intern. Conf. Soil Mech. Found. Engrg., Mexico, Vol. 2, pp. 157-164.

31. Panek, L. A., 1979, "Criterion of Failure for Design of Rock Mass Structures as Determined by Borehole Shear Tests", Proceedings. Fourth Congress, International Society for Rock Mechanics, Montreux, Switzerland, Vol. 2, pp. 509-515.

32. Prandtl, L., 1921, "Uber die Eindringungsfestigkeit plastisher Baustoffe unde die Festigekeit von Schneuten - Zeitzchrift fur Argewandte Mathematik und Mechanik", 1, No. 1, pp. 15-20.

33. Rockaway, J. D. and Stephenson, R. W., 1979, "Investigation of the Effects of Weak Floor Conditions on the Stability of Coal Pillars", Report No. BUMINES-OFR-12-81, 227 pp.

34. Speck, C. R., 1981, "The Influence of Certain Geologic and Geotechnical Factors on Coal Mine Floor Stability - A Case Study", Proceedings of First Conference on Ground Control in Mining, Morgantown, WV, pp. 44-49.

35. Stuart, J. G., 1962, "Interference between Foundations with Special Reference to Surface Footings in Sand", Geotechnique, 12, No. 1, pp. 15-22.

36. Terzaghi, K., 1943, "Theoretical Soil Mechanics", J. Wiley & Sons, New York.

37. Schebotarioff, G. P., 1951, "Soil Mechanics, Foundations and Earth Structures", McGraw-Hill, New York, pp. 655.

38. Vesic, A. S., 1964, "Model Investigations of Deep Foundations and Scaling Laws, Panel Discussion, Session II", Proceedings, North American Conference on Deep Foundations, Mexico City, Vol II, pp. 525-533.

39. Vesic, A. S., 1973, "Analysis of Ultimate Loads of Shallow Foundations", Journal Soil Mech. and Found. Div., ASCE, Vol. 99, No. SM1, pp. ??????

40. Vesic, A. S., 1970, "Research on Bearing Capacity of Soils " (unpublished).

41. West, J. M. and Stuart, J. G., 1965, "Oblique Loading Resulting from Interference Between Surface Footings on Sand", Proceedings, Sixth International Conference on Soil Mechanics and Foundation Engineering, Montreal, Vol. II, pp. 214-217.

42. Winterkorn, H.F. and Fang, H.Y., (1975), "Foundation Engineering Handbook," Van Nostrand Reinhold Company, Inc. New York, NY, 751 pp.

43. Whitman, R. V., 1970, "The response of Soil to Dynamic Loadings", Contract Report No. 3-26, U.S. Army Waterways Experiment Station, Vicksburg, Miss, 216 pp. ???.

44. Wilson, A. H., 1981, "Stress and Stability in Coal Ribsides and Pillars", Proceedings of the 1st Annual Conference on Ground Control, West Virginia University, Morgantown, West Virginia.

APPENDIX A

STRESS-DEFORMATION PLOTS FOR PLATE BEARING TESTS FROM

SELECTED SITES IN MINE 1 AND MINE 2
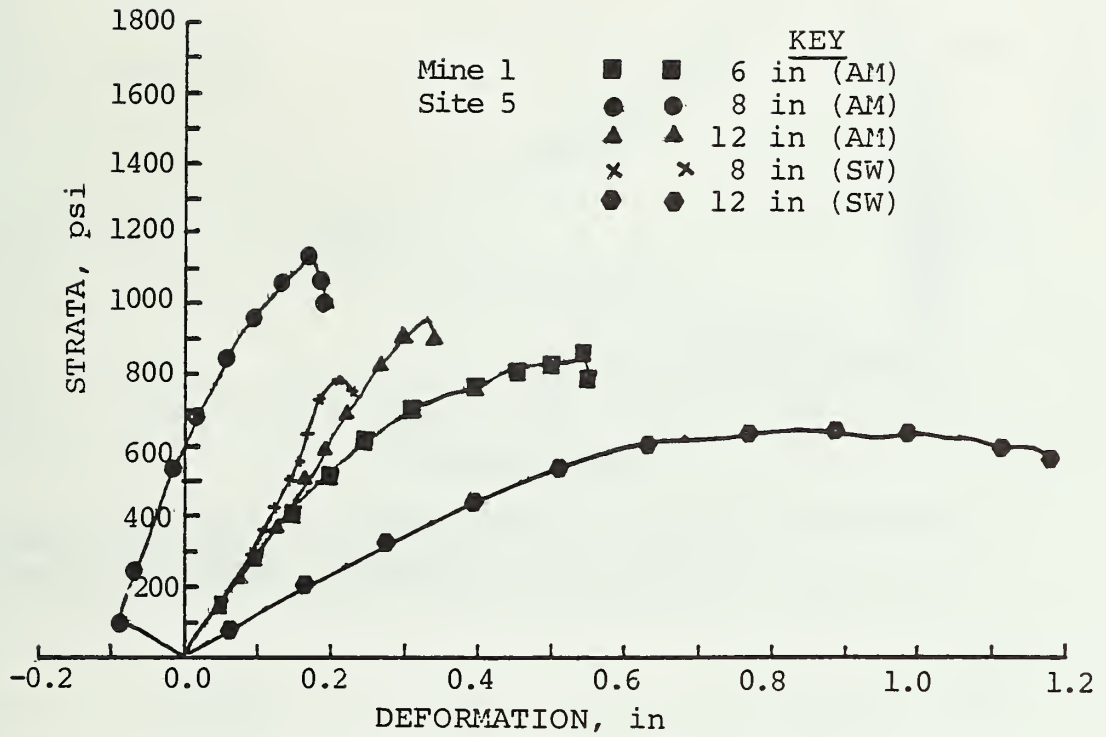
FIGURE A-1 Stress-deformation curves for immediate floor strata based on plate load tests.
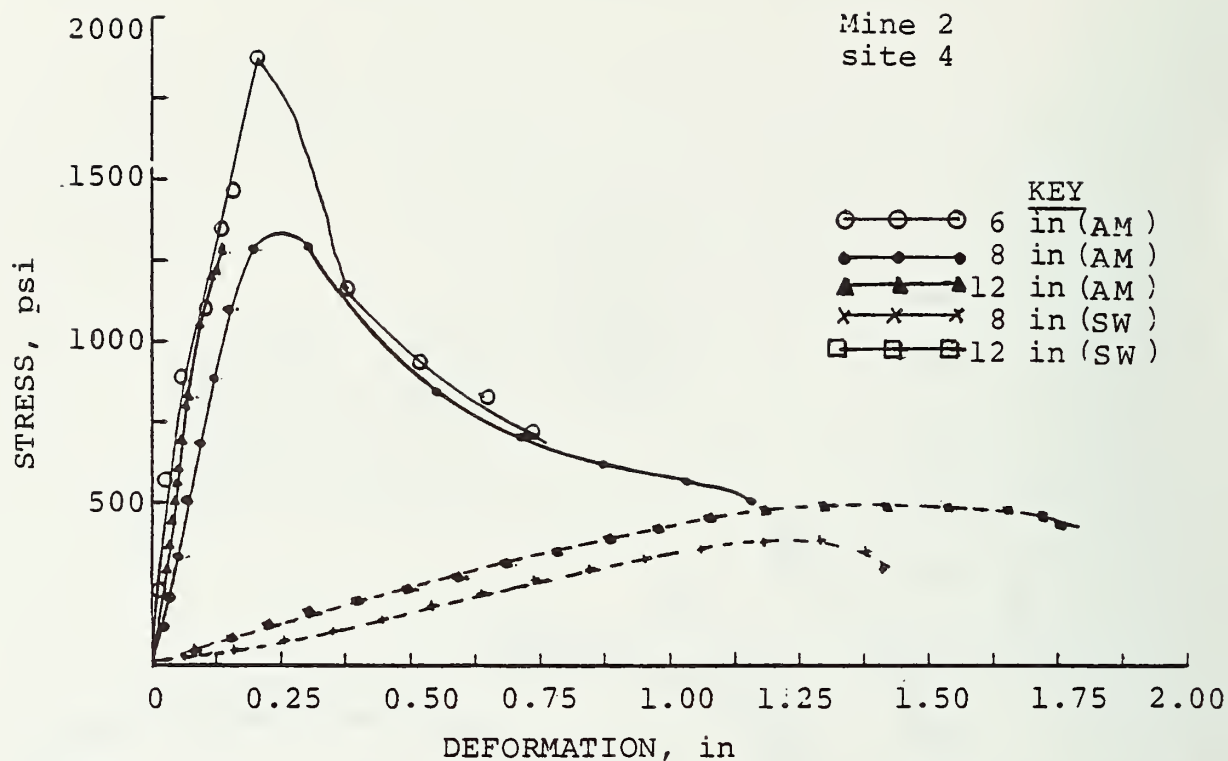
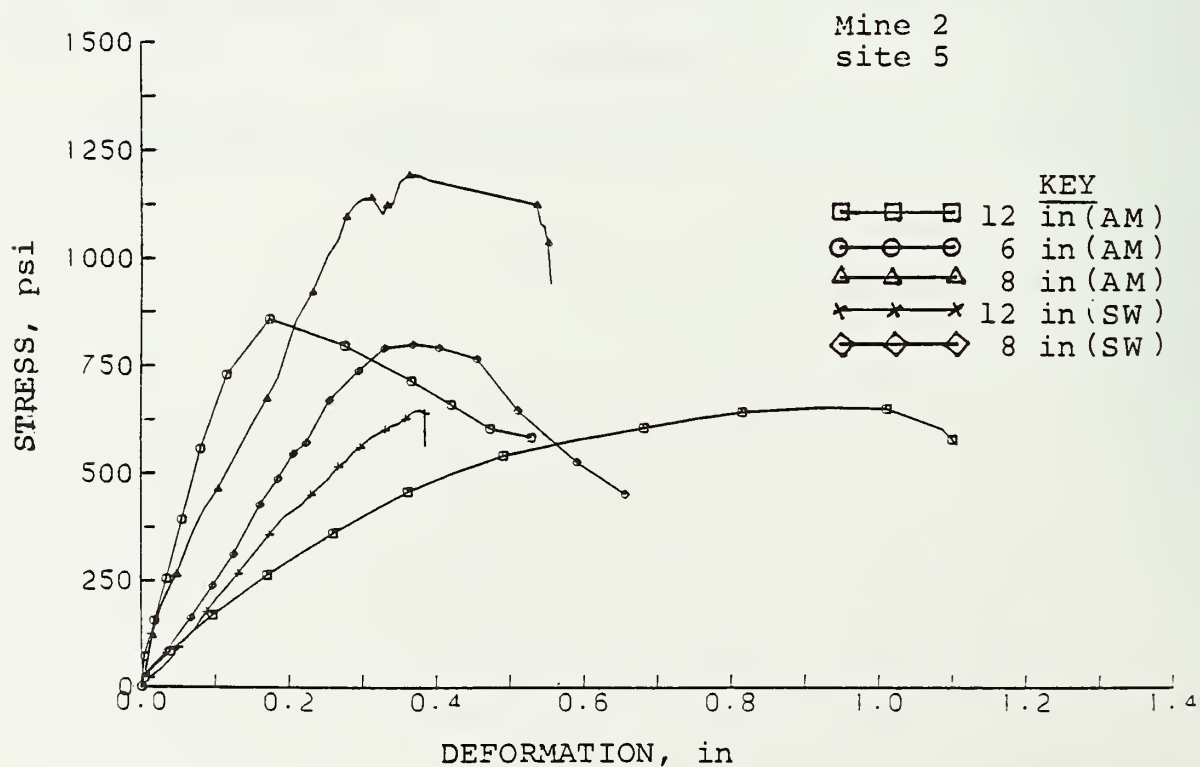FIGURE A-2 Stress - deformation curves for immediate floor strata based on plate load tests.

FIGURE A-3 Stress - deformation curves for immediate floor strata based on plate load tests.

APPENDIX B

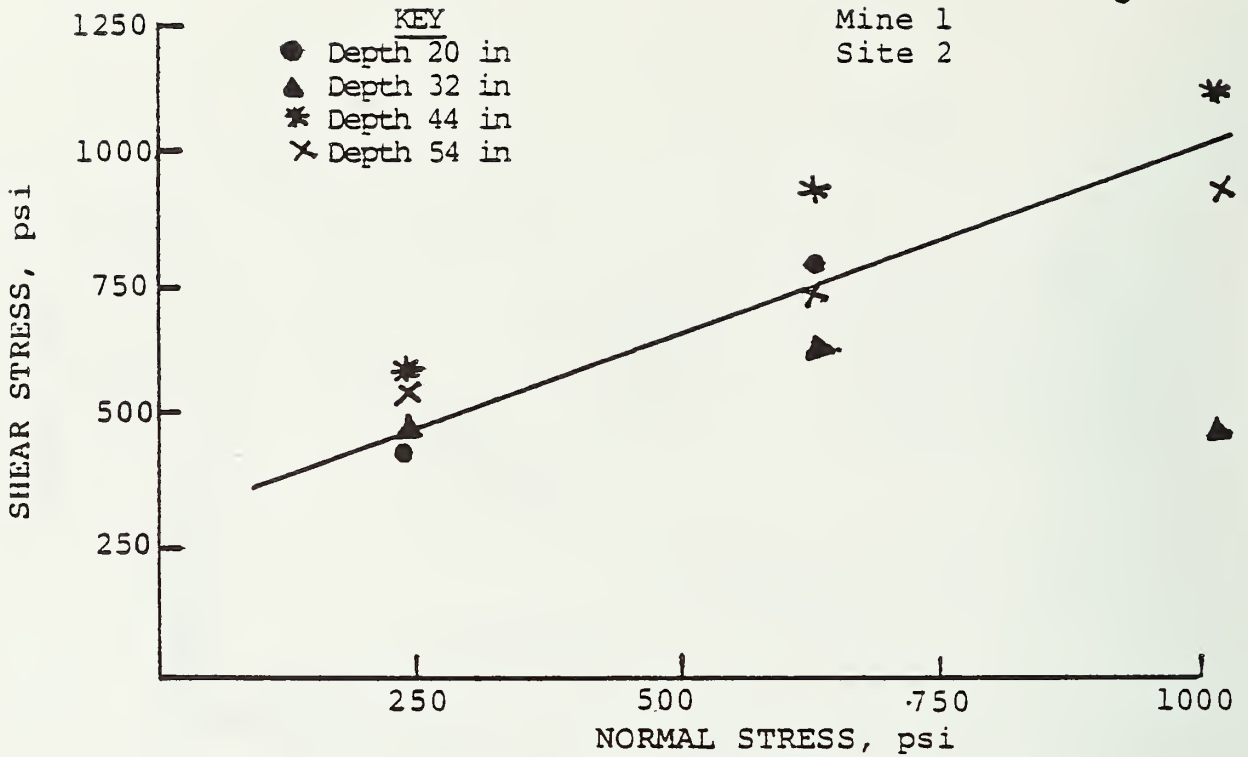SHEAR STRENGTH CHARACTERISTICS OF IMMEDIATE FLOOR

STRATA FOR SELECTED SITES FROM MINE 1 AND MINE 2

FIGURE B-1 Shear strength - normal stress relationships for immediate floor strata.
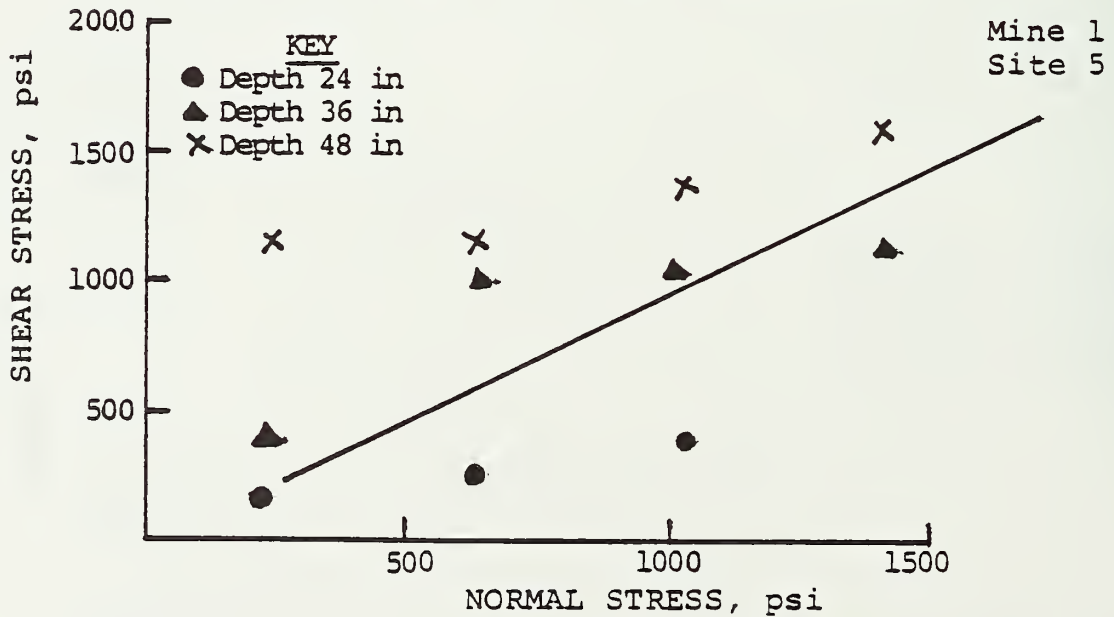
FIGURE B-2 Shear strength - normal stress relationships for immediate floor strata.
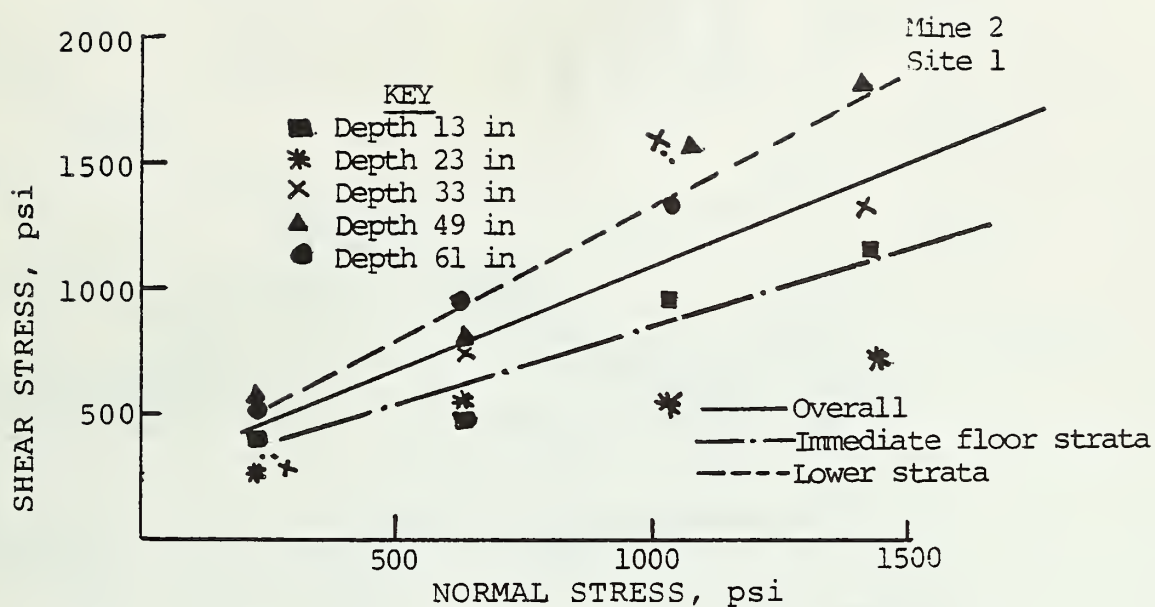
FIGURE B-3 Shear strength - normal stress relationships for immediate floor strata.
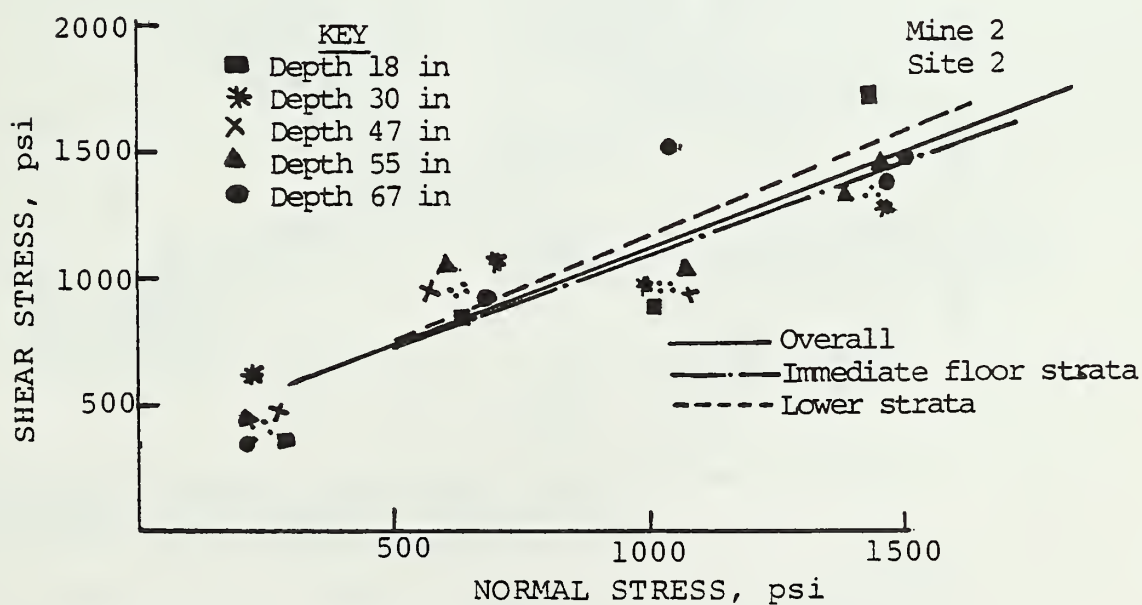
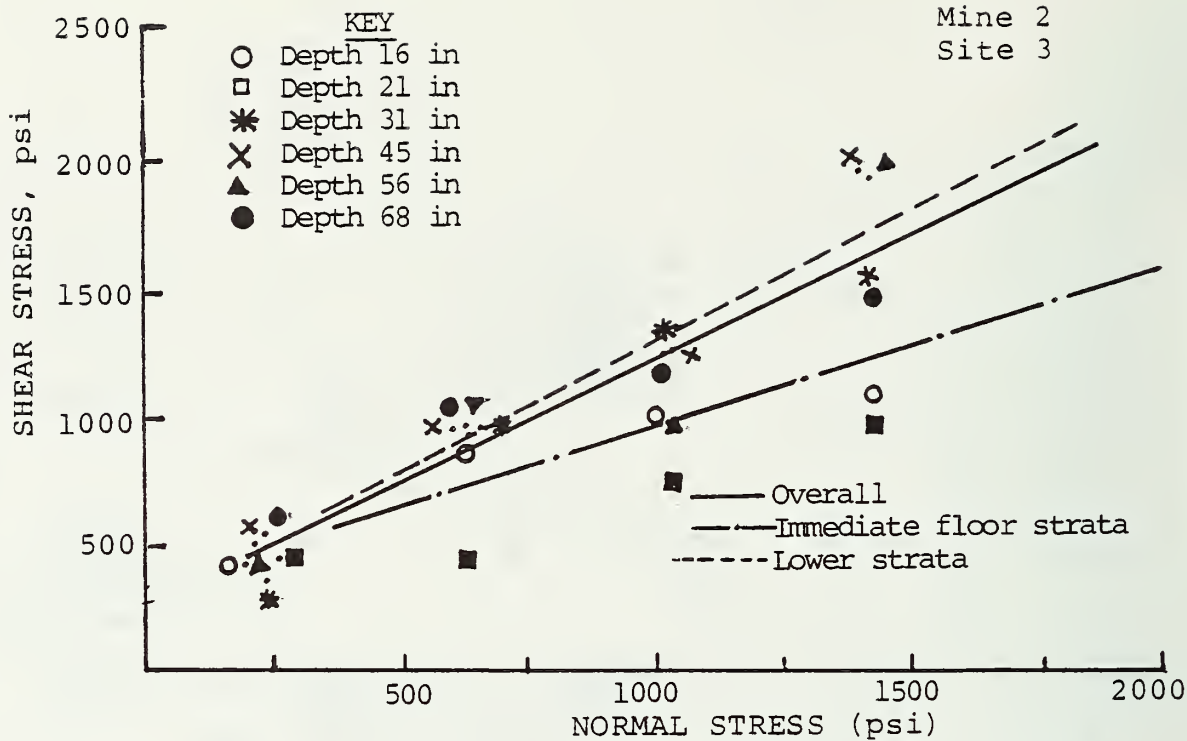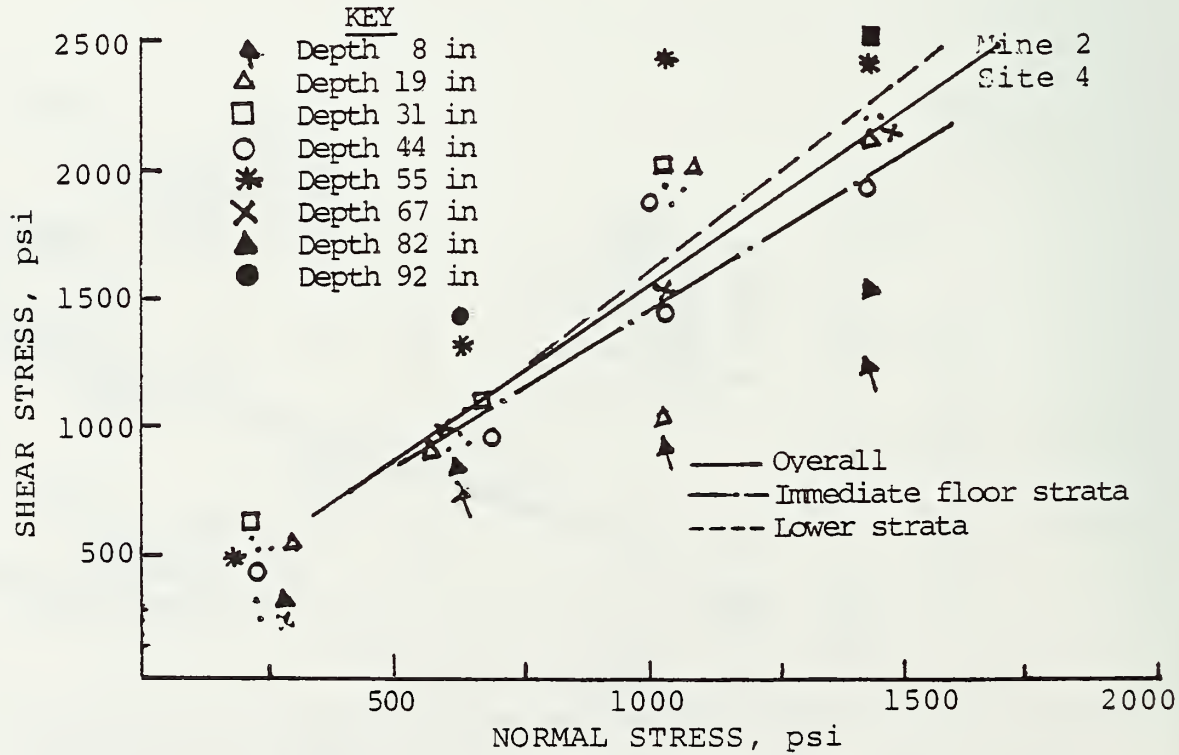FIGURE B-4 Shear strength - normal stress relationships for immediate floor strata.

FIGURE B-5 Shear strength - normal stress relationships for immediate floor strata.

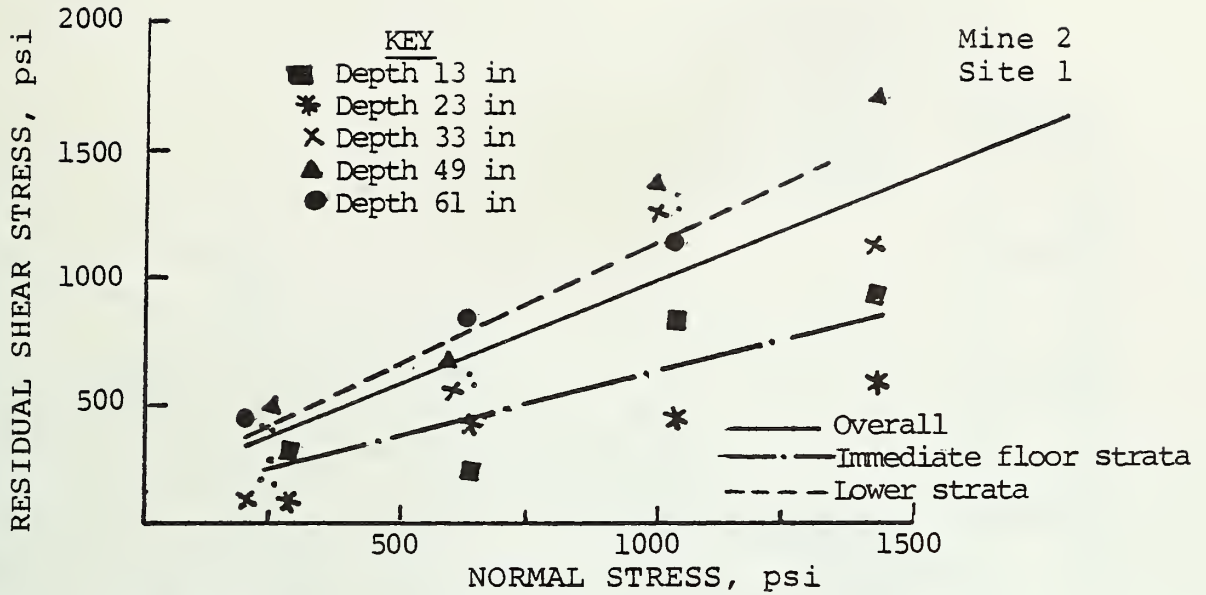FIGURE B-6 Shear strength - normal stress relationships for immediate floor strata.

FIGURE B-7 Shear strength - normal stress relation-
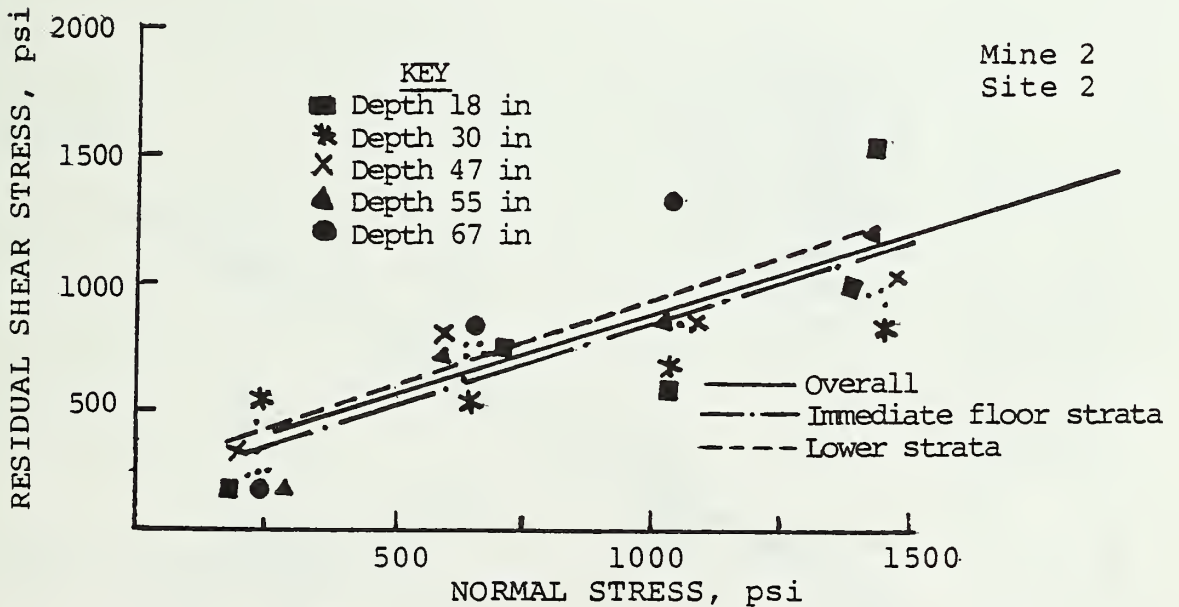ships for immediate floor strata.

FIGURE B-8 Shear strength - normal stress relation-
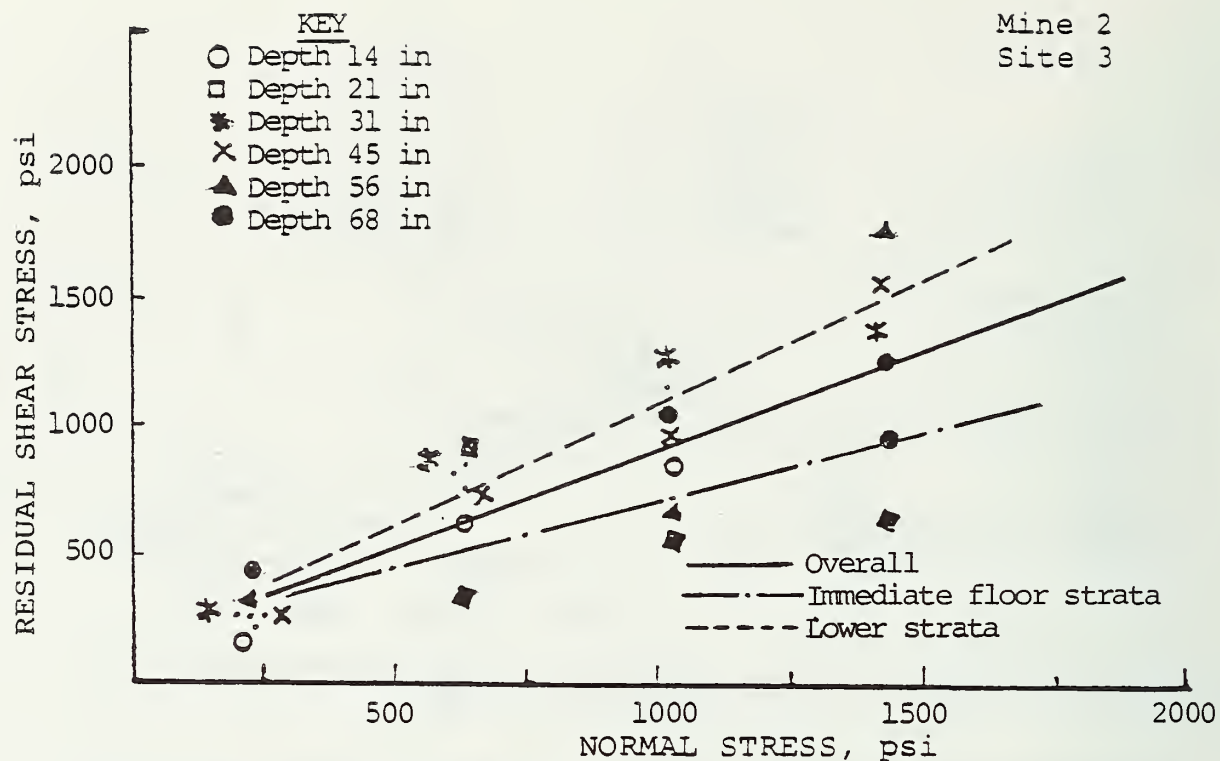ships for immediate floor strata.

FIGURE B-9   Shear strength - normal stress relationships for immediate floor strata.
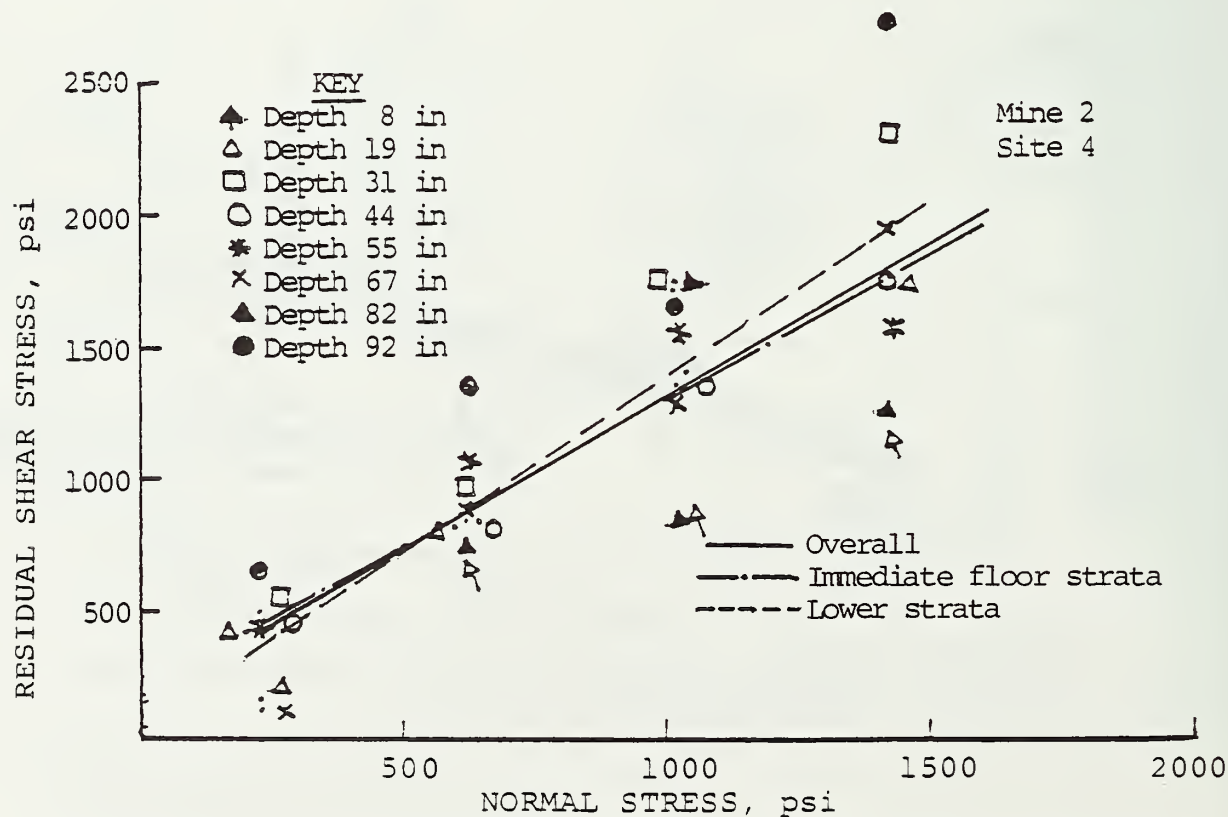

FIGURE B-10 Shear strength - normal stress relationships for immediate floor strata.

APPENDIX C

DEFORMATION MODULI FOR DISCONTINUOUS ROCK MASSES

<u>Deformation Moduli For Discontinuous Rock Masses</u>

Classical definitions of the modulus of elasticity and
Poisson's ratio apply to an elastic continuum only. A
discontinuous rock mass such as an underclay associated with a
coal seam behaves very differently when subjected to stress.
Typical stress-axial strain and stress-lateral strain curves for
such a rock are shown in Figure C.1. The following comments are
pertinent:

1) Both curves are S-shaped and are characterized by
   low values of slope at low and high stresses.
   Linear portions of the curve may or may not exist.

2) None or only a portion of the strains, particularly
   lateral strains, may be recoverable at any stress
   level.

3) The ratio of lateral to axial strains at any point
   along the curve may be larger than 0.5 which
   violates the definition of a continuum.

The above comments make the definition of deformation moduli by
terms Modulus of Elasticity and Poisson's ratio improper.
Therefore, the following terms have been utilized in this report
to define moduli of deformation.

$$\text{Axial Deformation Modulus} = \frac{\text{Axial Stress}}{\text{Axial Strain}}$$
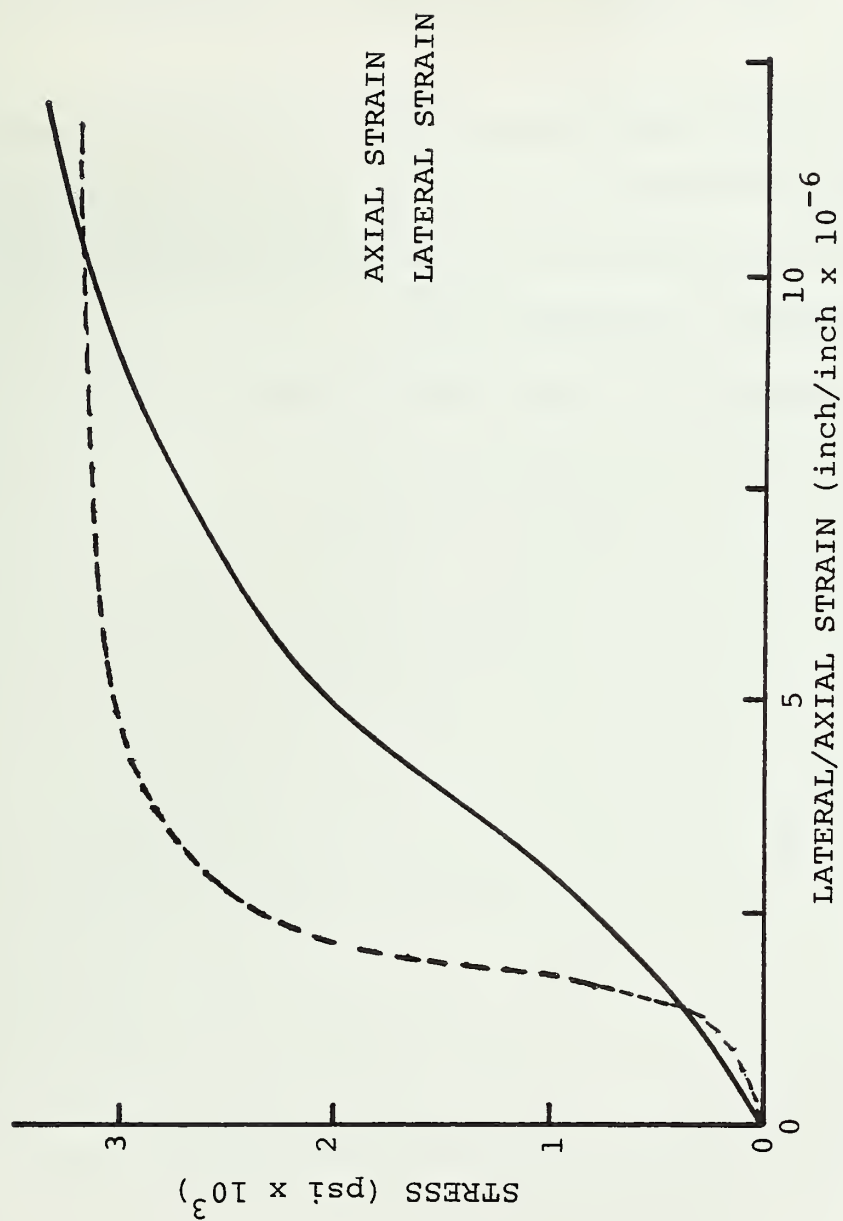
FIGURE C-1. Typical axial stress-axial strain and axial stress-lateral strain curves for a discontinuous rock mass.

$$\text{Lateral Deformation Ratio} = \frac{\text{Lateral Strain}}{\text{Axial Strain}}$$

Tangent or secant values of these moduli of deformation may be calculated.

Although, these terms correspond to definitions of the modulus of elasticity and Poisson's ratio for an elastic continuum, these can be used for continuous and discontinuous rock masses as well as for non-elastic rock masses.

APPENDIX D

LIST OF ABBREVIATIONS USED IN THIS REPORT

LIST OF ABBREVIATIONS USED
IN THE REPORT

A = Area of plate

a_1 = Inner radius of the flat jack or radius of hole

a_2 = Outer diameter of the flat jack

AM = As mined

B = Width of the Footing/test plate

C = Thickness of test plate

C_o = Unconfined compressive strength

d = diameter of plate

d_s = diameter of the sample

DM_{50} = Axial deformation modulus at 50% failure strength

DM_{90} = Axial deformation modulus at 90% failure strength

$\left.\begin{array}{l} E_c = \\ E_q = \\ E_\gamma = \end{array}\right\}$ Shape factors

E = Deformation Modulus

G = Shear Modulus

H = Thickness of weak layer

HF = Heave factor

H_c = Height of Humidity Chamber

h = Height of the coal seam

I_γ = Rigidity index

$I_{\gamma\gamma}$ = Modified Rigidity index

I_c = Depth correction factors

k = Emperical constant used in consistency formula (Pg. 30)

K = Ratio of unconfined shear strength of lower hard layer S_2 to upper weak layer S_1

K_z = constant

K_c = constant characteristic of the coal seam for pillar strength

L = Length of footing

L_c = Length of humidity chamber

m = Empirical constant used in consistency formula

n = Empirical constant used in consistency formula

$\left.\begin{array}{l} N_c = \\ N_q = \\ N_\gamma = \end{array}\right\}$ Bearing capacity factors

N_m = Modified bearing capacity factor

Q = Applied Load

q = Applied stress

q_o = Ultimate Bearing Capacity

q_s = Surcharge stress applied due to the weight of soil above the foundation

RF = Reduction factor

R = Radius

RH = Relative humidity

r = Correlation Coefficient

S_o = Cohesive Strength

S_1 = Unconfined shear strength of upper floor stratum

SW = Soaked wet

TCT = Triaxial compression test

T_0 = Unconfined tensile strength of Rock

UBC = Ultimate Bearing Capacity

uvc = Natural moisture content

W = Actual plate settlement

W_{zi} = Displacement in direction of stress

W_c = Width of Humidity Chamber

W_p = Pillar width

X = Mean Value

z_i = Distance from the loaded surface to the point where displacement is measured

γ = Unit weight of rock

δ_v = constant

Δ = Volumetric strain

$\left.\begin{array}{l} \delta_{qc} = \\ \delta_{cc} = \\ \delta_{\gamma c} = \end{array}\right\}$ Compressibility factors

ϵ_x = Lateral strain

ϵ_y = Vertical strain

ϕ = Angle of internal friction

ρ = Density

σ_{avg} = Average pillar stress

σ_1 = Major Principal Stress

σ_2 = Intermediate Principal stress

σ_3 = Minor Principal Stress

σ = Standard deviation

σ_c = Unconfined compressive strength of a coal cube of size d_s

σ_p = In-situ pillar strength

σ_{cc} = Strength of the critical size specimen (36 in)

σ_{H1} = Horizontal in-situ stress

σ_{H2} = Horizontal in-situ stress

σ_t = In-situ tectonic stress

σ_v = In-situ vertical stress

μ = Poisson's ratio